



ΕΛΛΗΝΙΚΗ  
ΕΠΙΣΤΗΜΟΝΙΚΗ  
ΕΤΑΙΡΕΙΑ  
ΕΔΑΦΟΜΗΧΑΝΙΚΗΣ  
& ΓΕΩΤΕΧΝΙΚΗΣ  
ΜΗΧΑΝΙΚΗΣ

# Τα Νέα

25

## της Ε Ε Ε Ε Γ Μ

### ΠΡΟΓΡΑΜΜΑ ΕΚΔΗΛΩΣΕΩΝ ΠΕΡΙΟΔΟΥ ΔΕΚΕΜΒΡΙΟΥ 2009 – ΙΑΝΟΥΑΡΙΟΥ 2010

Η προετοιμασία της συμμετοχής της Ελληνικής αποστολής στο 17<sup>th</sup> International Conference on Soil Mechanics and Geotechnical Engineering της Αλεξάνδρειας για την προβολή του XV European Conference on Soil Mechanics and Geotechnical Engineering της Αθήνας το 2011 «έρριξε πίσω» τον προγραμματισμό των εκδηλώσεων της εφετεινής περιόδου, παρ' όλο ότι αυτός άρχισε από τον περασμένο Μάιο. Έτσι, σήμερα σας ενημερώνουμε μόνο για τις εκδηλώσεις του προσεχούς διμήνου.

Στα πλαίσια τα προετοιμασίας, όμως, των εφετεινών εκδηλώσεων καταφέραμε κάτι άλλο: μετά από πρόσκληση του Προέδρου της Εκτελεστικής Επιτροπής της ΕΕΕΕΓΜ συναντήθηκαν οι Πρόεδροι των συγγενών επιστημονικών εταιρειών, δηλαδή της ΕΕΕΕΓΜ, της Ελληνικής Επιτροπής Σηράγγων και Υπογείων Έργων (ΕΕΣΥΕ), της Ελληνικής Επιτροπής Μεγάλων Φραγμάτων (ΕΕΜΦ), του Ελληνικού Συνδέσμου Γεωσυνθετικών (ΕΣΓ) και της Επιτροπής Τεχνικής Γεωλογίας της Ελληνικής Γεωλογικής Εταιρείας (είχε προσκληθεί και ο Πρόεδρος του Ελληνικού Τμήματος Αντισεισμικής Μηχανικής / ΕΤΑΜ, ο

(συνέχεια στην σελίδα 4)

Αρ. 25 – ΝΟΕΜΒΡΙΟΣ 2009



Δεν γνωρίζουμε πού είναι η τοποθεσία που εικονίζεται στη φωτογραφία. Εικάζουμε ότι είναι στην περιοχή του Grand Canyon, USA. Την αλιεύσαμε από το «Best pictures on the internet 2007 Awards», όπου πήρε το πρώτο βραβείο στην κατηγορία «Best natural scenery (open spaces)»

## Π Ε Ρ Ι Ε Χ Ο Μ Ε Ν Α

ΣΤΑΥΡΟΣ ΧΡΙΣΤΟΥΛΑΣ (1937 – 2009)	3
Πρόγραμμα Περιόδου Δεκεμβρίου 2009 – Ιανουαρίου 2010	4
Επιστημονικά Άρθρα :	5
- Dimitris Pitilakis <i>"Equivalent Linear Soil-Foundation-Structure Interaction and Performance Based Design"</i>	5
- Asterios Liolios, George Michaltsos, & Konstantinos Liolios <i>"A Numerical Approach to the Seismic Problem of Steel Pile-Soil Interaction under Environmental and Second-Order Geometric Effects"</i>	9
- George Papazafeiropoulos, Prodromos N. Psarropoulos, & Yiannis Tsompanakis <i>"Retaining Wall-Soil-Structure Interaction Effects Due To Seismic Excitation"</i>	11
- Spyros Pavlides, Theodoros Tsapanos, Nikos Zouros, Sotiris Sboras, George Koravos, & Alexandros Chatzipeiros <i>"Using Active Fault Data For Assessing Seismic Hazard: A Case Study From NE Aegean Sea, Greece"</i>	16
- Emiliios Comodromos, Mello Papadopoulou, & Ioannis Rentzeperis <i>"Degradation Of Pile Foundations' Response Due To Cracking: Advanced And Simplified Numerical Approach"</i>	22
- Anastasios Anastasiadis, Kyriazis Pitilakis & Kostas Seneetakis <i>"Dynamic Shear Modulus and Damping Ratio Curves of Sand/Rubber Mixtures"</i>	29
- Varvara Zania, Ioanna Tzavara, Yiannis Tsompanakis, & Prodromos N. Psarropoulos <i>"Geosynthetics As Mitigation Measure For Seismic Hazard on Geostructures"</i>	34
Τιμητικές Διακρίσεις Ελλήνων Γεωτεχνικών – Πάνος Ντακούλας & Γιώργος Γκαζέτας – Πάυλος Μαρίνος	42
Προσεχείς Γεωτεχνικές Εκδηλώσεις:	43
- 1st International Conference on Information Technology in Geo-Engineering	43
- GEO-FRONTIERS 2011 Advances in Geotechnical Engineering	44
- IS-SEOUL 2011 Fifth International Symposium on Deformation Characteristics of Geomaterials	45
- 6 <sup>th</sup> International Symposium on Sprayed Concret	45
Νέα από τις Διεθνείς Γεωτεχνικές Ενώσεις - FedIGS	47
Νέες Εκδόσεις στις Γεωτεχνικές Επιστήμες	48
Ηλεκτρονικά Περιοδικά	52

# ΣΤΑΥΡΟΣ ΧΡΙΣΤΟΥΛΑΣ

## 1937 ÷ 2009

Την Τετάρτη 4 Νοεμβρίου 2009 έφυγε από κοντά μας ο αγαπητός συνάδελφος και φίλος Σταύρος Χριστούλας, μετά από μακροχρόνια ασθένεια. Η κηδεία του έγινε την Παρασκευή 6 Νοεμβρίου 2009 στο κοιμητήριο Παπάγου.



Ο Σταύρος Χριστούλας γεννήθηκε στην Καρδίτσα στις 27 Νοεμβρίου 1937. Έλαβε το δίπλωμα Πολιτικού Μηχανικού από το ΕΜΠ τον Ιούλιο του 1961. Το 1963 διορίστηκε στο Υπουργείο Δημοσίων Έργων (Διεύθυνση Τεχνικών Υπηρεσιών Νομού Καρδίτσας) και το 1965 τοποθετήθηκε Προϊστάμενος Έργων στη Διεύθυνση Τεχνικών Υπηρεσιών Νομού Καρδίτσας.

Από τον Ιανουάριο 1967 έως τον Ιούλιο 1967, με υποτροφία της Γαλλικής Κυβέρνησης και εκπαιδευτική άδεια του ΥΠ.Δ.Ε., παρακολούθησε στη Γαλλία μεταπτυχιακό κύκλο σπουδών Εδαφομηχανικής. Από τον Οκτώβριο 1968 έως τον Ιούλιο 1969, με υποτροφία του Υπουργείου Συντονισμού, παρακολούθησε στη Γαλλία σειρά μαθημάτων στην ECOLE NATIONALE DES PONTS ET CHAUSSEES στην Εδαφομηχανική και στην ASTEF σε θέματα Ηλεκτρονικών Υπολογιστών. Τον Δεκέμβριο του 1969 τοποθετήθηκε Διευθυντής (Νομομηχανικός) στη Διεύθυνση Τεχνικών Υπηρεσιών Νομού Καρδίτσας.

Από τον Οκτώβριο 1973 έως τον Ιούλιο 1975, με υποτροφία του Ι.Κ.Υ. εκπόνησε στο UNIVERSITE LIBRE DE BRUXELLES διδακτορική διατριβή στο αντικείμενο των Θεμελιώσεων σε πασσάλους και του απονεμήθηκε ο τίτλος του Διδάκτορος Μηχανικού.

Με την επιστροφή του στην Ελλάδα, τοποθετήθηκε υπεύθυνος Εδαφοτεχνικών Μελετών Οδοποιίας του ΥΠ.Δ.Ε. και τον Οκτώβριο του 1977 επελέγη και ανέλαβε καθήκοντα ως Διευθυντής Ερευνών Εδαφών του Κέντρου Ερευνών Δημοσίων Έργων (Κ.Ε.Δ.Ε.), όπου και υπηρέτησε μέχρι τον Νοέμβριο του 1987, οπότε εξελέγη στη Σχολή Πολιτικών Μηχανικών του Ε.Μ.Π. σε θέση Επίκουρου Καθηγητή. Στη συνέχεια το 1992 εξελέγη στη βαθμίδα του Αναπληρωτή Καθηγητή και υπηρέτησε μέχρι το 1999, οπότε και συνταξιοδοτήθηκε, λόγω της ασθένειάς του.

Η θητεία του Σταύρου στο ΚΕΔΕ/ΥΠΕΧΩΔΕ σηματοδότησε την ανάπτυξη της Γεωτεχνικής Μηχανικής στο χώρο των Δημοσίων Έργων. Οι άοκνες προσπάθειές του για την προσέλκυση νέων αξιόλογων επιστημόνων στο ΚΕΔΕ, η οργάνωση σύγχρονων και πλήρως εξοπλισμένων εργαστηρίων Εδαφομηχανικής - Βραχομηχανικής - Τεχνικής Γεωλογίας, η προμήθεια εξοπλισμού για την εκτέλεση επιτόπου δοκιμών και γεωτεχνικής διερεύνησης, οι διακρατικές επιστημονικές συνεργασίες, κυρίως με το LCPC Γαλλίας, η οργάνωση σε συνεργασία με το ΤΕΕ σεμιναρίων για την ενημέρωση των μηχανικών των Τεχνικών Υπηρεσιών των

Νομαρχιών σε σύγχρονα θέματα Εδαφομηχανικής, η ανάπτυξη του επιστημονικού Δελτίου του ΚΕΔΕ, η σύνταξη Προτύπων Τεχνικών Προδιαγραφών Εργαστηριακών και Επιτόπου Δοκιμών Γεωτεχνικής ήταν μερικά από τα επιτεύγματα του Σταύρου, που χαρακτήρισαν την περίοδο εκείνη ως «*χρυσή εποχή του ΚΕΔΕ*».

Ως ακαδημαϊκός δάσκαλος, στο σύντομο χρονικό διάστημα που υπηρέτησε στο Ε.Μ.Π., λόγω της ασθένειάς του, ο Σταύρος Χριστούλας, δίδαξε το μάθημα «Θεμελιώσεις - Ειδικά Θέματα» του οποίου δημιούργησε την ύλη διδασκαλίας και τις ασκήσεις του μαθήματος, ενώ παράλληλα εξέδωσε δυο βιβλία βασισμένα στη σύγχρονη διεθνή βιβλιογραφία και στην πολύχρονη εμπειρία του καθώς και οκτώ διδακτικές σημειώσεις.

Την περίοδο 1979 - 1983 διετέλεσε Επιστημονικός Συνεργάτης του UNIVERSITE LIBRE DE BRUXELLES, ενώ κατά την σταδιοδρομία του υπήρξε μέλος διεθνών επιστημονικών-τεχνικών επιτροπών, υπεύθυνος για την οργάνωση ημερίδων, συνεδρίων και σεμιναρίων καθώς και Πρόεδρος επιστημονικών συνεδριάσεων τόσο σε Ελληνικά όσο και Διεθνή Συνέδρια.

Το δημοσιευμένο έργο του (62 επιστημονικές δημοσιεύσεις και 17 κείμενα επιστημονικού περιεχομένου) για θέματα θεμελιώσεων σε πασσάλους, κατασκευής επιχωμάτων με χαλικοπασσάλους, διαστασιολόγησης βαθιών θεμελιώσεων, χρήσης της ιπτάμενης τέφρας στην Οδοποιία, βαθιών εκσκαφών και έργων αντιστήριξης σε αστικό περιβάλλον, μικροζωνικών μελετών κ.ά. αποτελεί ακόμη αξιόλογη πηγή γνώσεων και αναφοράς για τους νέους ερευνητές.

Ο Σταύρος Χριστούλας ήταν ένας καλλιεργημένος άνθρωπος, με γενικότερη παιδεία, ανήσυχο ερευνητικό πνεύμα, εργατικός και συνεργάσιμος, αυτοκριτικός, υποστηρίζοντας με πάθος τις απόψεις του, αλλά αξιολογώντας πάντοτε τις απόψεις και ιδέες των άλλων, πολύ αγαπητός στους συναδέλφους του, αλλά και καταδεκτικός τόσο με τους νεότερους συνεργάτες του όσο και με τους σπουδαστές της Σχολής Πολιτικών Μηχανικών του Ε.Μ.Π. Έτσι θα τον θυμόμαστε πάντοτε, όλοι εμείς που είχαμε την τύχη να συνεργαστούμε μαζί του και να εκτιμήσουμε τον χαρακτήρα του και την προσφορά του.

Ανδρέας Αναγνωστόπουλος  
Γιώργος Τσιαμπάος

# ΠΡΟΓΡΑΜΜΑ ΠΕΡΙΟΔΟΥ ΔΕΚΕΜΒΡΙΟΥ 2009 – ΙΑΝΟΥΑΡΙΟΥ 2010

(συνέχεια από την πρώτη σελίδα)

οποίος, όμως, λόγω ανειλημμένων υποχρεώσεων δεν μπόρεσε να παρασστή) και συζήτησαν τον κοινό προγραμματισμό των εκδηλώσεων της επόμενης περιόδου και την ενημέρωση των μελών όλων των εταιρειών για τις εκδηλώσεις αυτές. Κατ' αυτόν τον τρόπο θα αποφευχθούν συμπτώσεις εκδηλώσεων την ίδια ημέρα, αλλά και ενημέρωση ενός ευρύτερου κοινού για τις διοργανούμενες εκδηλώσεις.

## ΔΕΚΕΜΒΡΙΟΣ 2009

Κυριακή 6 Δεκεμβρίου : Εκδρομή στον Υπόγειο Χώρο Αποθήκευσης Επικίνδυνων Αποβλήτων στο Τεχνολογικό Πάρκο Λαυρίου (η εκδήλωση διοργανώνεται από την ΕΕΣΥΕ και η σχετική ανακοίνωση έχει αποσταλή ήδη στα μέλη της ΕΕ-ΕΕΓΜ)

Δευτέρα 14 Δεκεμβρίου : Διάλεξη του Καθηγητή του University of California, Berkeley Nicholas Sitar με θέμα "On Seismic Design of Retaining Structures", στην Αίθουσα Εκδηλώσεων της Σχολής Πολιτικών Μηχανικών ΕΜΠ, ώρα 19:00.

## ΙΑΝΟΥΑΡΙΟΣ 2010

Τρίτη 12 Ιανουαρίου : Διάλεξη του Dr. Robert THURNER (Keller Grundbau Des.m.b.H) με τίτλο "Compensation grouting for limiting settlements of two railway bridges induced by a twin-tunnel excavation", στην Πολυτεχνική Σχολή του Πανεπιστημίου Πατρών.

Τετάρτη 13 Ιανουαρίου : Διάλεξη του Dr. Robert THURNER (Keller Grundbau Des.m.b.H) με τίτλο "Compensation grouting for limiting settlements of two railway bridges induced by a twin-tunnel excavation", στην Αίθουσα Εκδηλώσεων της Σχολής Πολιτικών Μηχανικών ΕΜΠ, ώρα 19:00.

Δευτέρα 25 Ιανουαρίου : Αθηναϊκή Διάλεξη Γεωτεχνικής Μηχανικής από τον Καθηγητή του Imperial College John Burland με τίτλο "Interaction between geotechnical and structural engineers", στην Αίθουσα Εκδηλώσεων του Κτιρίου Διοίκησης (Πρυτανείας) του ΕΜΠ, ώρα 18:00.

# ΕΠΙΣΤΗΜΟΝΙΚΑ ΑΡΘΡΑ

Το άρθρο που ακολουθούν αποτελούν συμμετοχή συναδέλφων – μελών της ΕΕΕΕΓΜ στο Satellite Conference on Earthquake Geotechnical Engineering, που διοργανώθηκε από την επιτροπή TC 4 της ISSMGE στην Alexandria, Egypt, στις 2 – 3 October 2009. Οι προσκελημένες ομιλίες των Καθηγητών Γιώργου Γκαζέτα κι Κυριαζή Πιτιλάκη πρόκειται να δημοσιευθούν σε ειδικό τόμο πρακτικών που θα εκδοθή από τον εκδοτικό οίκο του SPRINGER στις αρχές του 2010 και, κατά συνέπεια, δεν μπορούν να δημοσιευθούν τώρα στο περιοδικό μας.

## EQUIVALENT LINEAR SOIL-FOUNDATION-STRUCTURE INTERACTION AND PERFORMANCE BASED DESIGN

Dimitris PITILAKIS

Lecturer, Aristotle University of Thessaloniki, Greece

[Dpitolak@civil.auth](mailto:Dpitolak@civil.auth)

### ABSTRACT

*Strong ground motions affect greatly the response of a soil-foundation-structure system. Through the modification of the soil behavior, the structural response is affected. The primer effect of the nonlinear soil behavior is the decrease of the soil stiffness, which in turns might lead to an increase of the soil-foundation displacement. This phenomenon arises practical issues concerning the traditional performance based design. This paper shows that the typically seen demand spectra of structures change, even for moderate earthquake ground motions. The performance based design (PBD) is addressed through an equivalent linear soil-foundation-structure interaction analysis, taking into account simultaneously the primary and secondary nonlinearities in the soil, due to material nonlinearity and radiation respectively. The effects on the system response of the equivalent linear soil characteristics and of the dynamic characteristics of the input ground motion are investigated. The demand spectra of the structural system obtained by the equivalent linear approach are compared with traditional demand spectra, in order to enlighten the effects of the nonlinear soil behavior on the system response. As observed, the nonlinear soil behavior and the interaction with the structure decrease the demand spectral values, evoking rather conservative seismic design if not taken into account.*

Keywords: equivalent linear, soil-foundation-structure interaction, performance based

### INTRODUCTION

It is known in engineering practice that the soil behaves in a nonlinear way even for very small shear strains. Vucetic (Vucetic 1994) showed that a linear soil model is restricted to small shear strain amplitudes, up to  $10^{-5}$ , which suggests that the linear elastic approximation can provide reasonable estimates of the soil response only for small to moderate ground motions. However, the soil exhibits large deformations when subjected to a strong ground motion. This nonlinear behaviour cannot be captured by a linear elastic or viscoelastic model, emerging thus the need for more elaborated constitutive soil models.

In this paper an equivalent linear approximation is implemented in the substructure approach (Gazetas 1983) of soil-foundation-structure interaction (SFSI) in order to ap-

proximate the nonlinear soil behavior (D.Pitilakis 2006). This equivalent linear numerical code was validated through comparisons with other well known software that perform equivalent linear analyses for the soil, such as SHAKE (Schnabel et al. 1972) and CyberQuake (Modaresi and Foerster 2000), as well as with experiments on shaking table (D.Pitilakis 2008). It was shown that the three software produced the same results for the soil response and it was proved theoretically that it is valid to use this approach in a soil-foundation-structure interaction analysis.

To this end, simplified soil-foundation-structure models are used to elucidate the effects of the nonlinear soil behavior on the soil, on the structure and the seismic design of the whole system. The simplified models are subjected to different input ground motions, aiming to excite the nonlinear soil behavior. The effects of the nonlinear soil behavior and the SFSI on the system response are highlighted in the context of the performance based design. Finally, the effect of the vibration of the structural system on the soil is evidenced numerically.

### SIMPLIFIED MODELS

Three different soil-foundation-structure configurations are used to elucidate the effects of the nonlinear soil behavior on the seismic response of the system.

The first configuration consists of a simplified twelve-storey residential building resting on a deep soil profile. Figure 1 shows the schematic representation of the simplified system. The shear modulus reduction and damping curves of the 140m deep soil profile are shown in Figure 2. The soil profile can be classified as type C, according to the EC8. The system is subjected to the San Rocco, 1976 Friuli, Italy earthquake record shown in Figure 3.

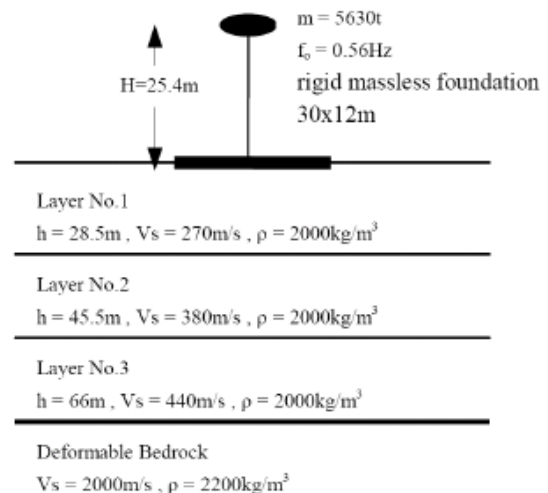


Figure 1. Schematic representation of the first simplified soil-foundation-structure system of the residential structure.

The second simplified structure is a simplified water tower with a lumped mass of 100t fixed at a height of 3.8m over a rigid, surface, square foundation of dimensions  $4\text{m} \times 4\text{m}$ . The fixed base natural frequency of the linear structure is fixed at 3.19Hz and the structural damping at 5%. The soil profile consists of 30m of clayey sand to sandy clay, separated into four layers with different properties, overlying rigid bedrock with significant interface impedance with the soil. The properties for the soil and the structure are shown in Figure 4. The top 6m have shear wave velocity  $V_s=133\text{m/s}$ , suggesting a very soft material. Below lay 6m with  $V_s=206\text{m/s}$ , 8m with  $V_s=237\text{m/s}$  and finally the deeper 10m have  $V_s=284\text{m/s}$ , on top of a rigid halfspace. The soil profile is classified as type C ground according to the EC8 with  $V_{s,30}=209\text{m/s}$ . For linear elastic behavior, the natu-

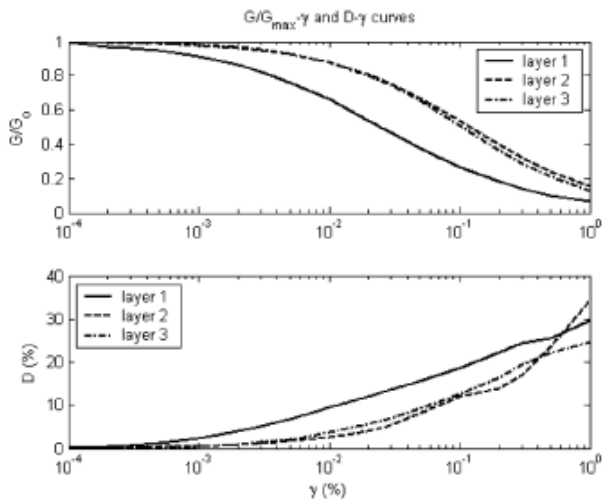


Figure 2. Shear modulus reduction and damping curves of the 140m deep soil profile.

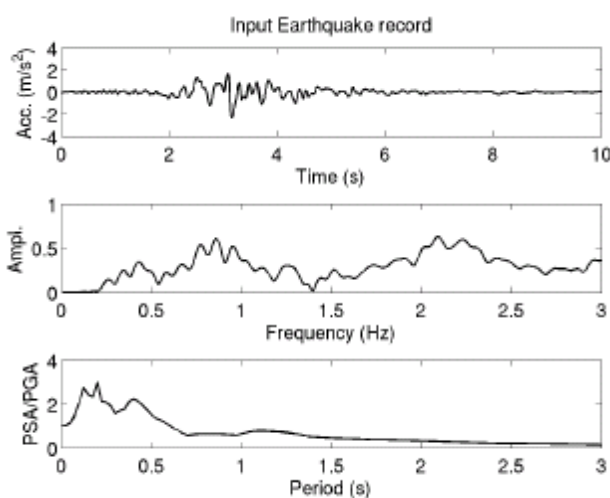


Figure 3. San Rocco, Friuli 1976 Italy earthquake ground motion.

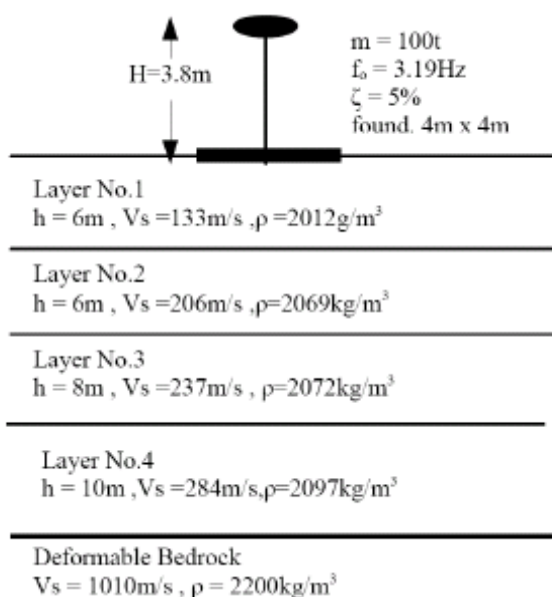


Figure 4. Simplified representation of the water tower on the shallow soil profile of 30m.

ral frequency of the soft shallow profile is found at 2.1Hz. The shear modulus reduction and damping curves assigned to this benchmark soil profile are shown in Figure 5. These curves were obtained by the simulation of cyclic shear tests for each soil layer. The system is subjected to the same earthquake ground motion as the first configuration, which is the San Rocco, 1976 Friuli, Italy.

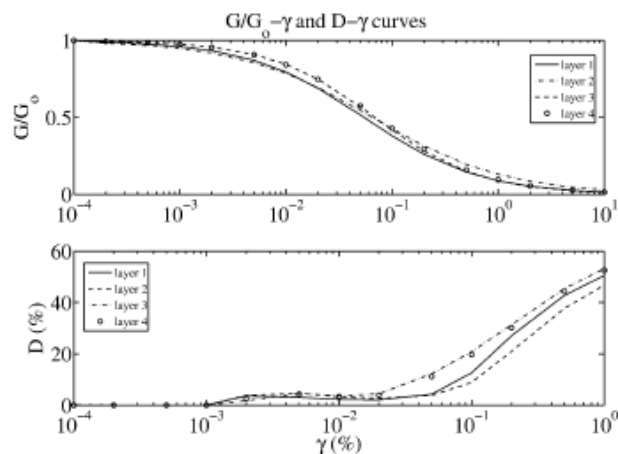


Figure 5. Shear modulus reduction and damping curves of the 30m soil profile.

The third soil-foundation-structure configuration consists of the same system of the water tower on the shallow soil profile of Figure 4 and Figure 5, but this time subjected to the stronger record of the Aegion, 1995 Aegion, Greece earthquake of Figure 6.

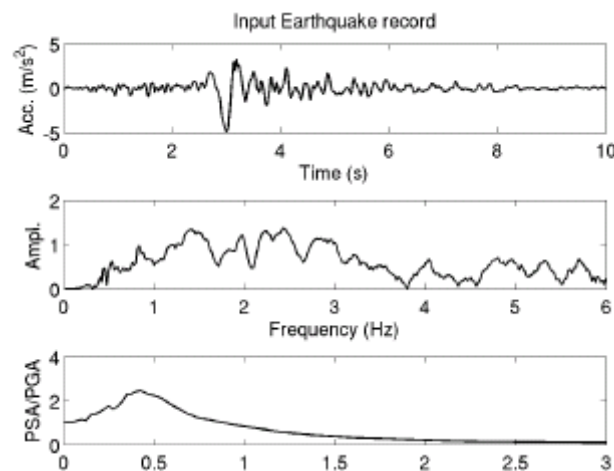


Figure 6. Aegion, 1995 Aegion, Greece earthquake record.

## COMPARATIVE RESULTS

The two different soil-foundation-structures are subjected to two different ground motions. The strong ground shaking assures the nonlinear soil behavior, which in turn modifies the system response.

### Residential building

The simplified residential building resting on the deep soil profile is subjected to the San Rocco earthquake ground motion. The nonlinear behavior of the soil is excited and the shear modulus of the upper soil layer reduces to 30% of the maximum value for linear elastic response. On the other hand, the material damping through hysteretic behavior increases from 2% (initial value) to 18%, suggesting increased energy dissipation during the strong ground shaking.

The shear strain at a depth of 2m under the foundation level is plotted in Figure 7. The presence of the structure and its vibration are taken into consideration when calculating the shear strain in the soil. The amplitude of the shear strain reduces by 50%, but most important the amplitude in the frequency domain reduces and shifts down to lower frequencies than the linear elastic fundamental frequency of the soil at 0.76Hz. Moreover, the response is almost negligible above the frequency of 2Hz. The abovementioned conditions may be important for the earthquake design of underground structures, as well as the dynamic behavior of the foundation soil.

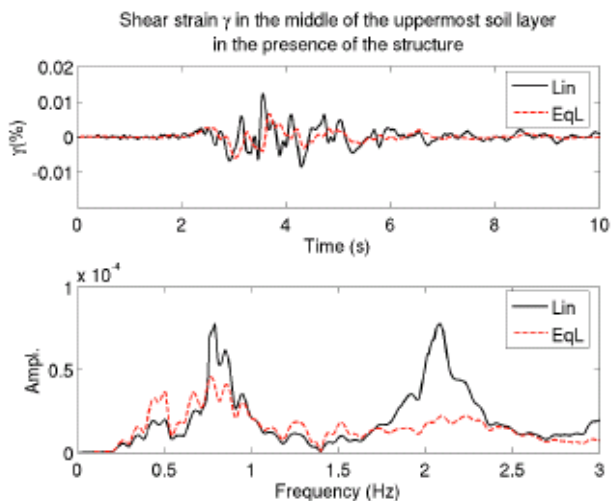


Figure 7. Shear strain at depth of 2m below the foundation level. The time history (top) and the Fourier spectrum (bottom) of the shear strain are calculated for linear (solid line) and equivalent linear (dashed line) soil behavior.

The demand spectrum at the foundation level is shown in Figure 8. It is clear that the nonlinear soil behavior reduces the spectral values of the acceleration at the foundation. The increased energy dissipation along with the interaction of the foundation with the soil decrease the amplitude of the acceleration entering the system, leading to different seismic design.

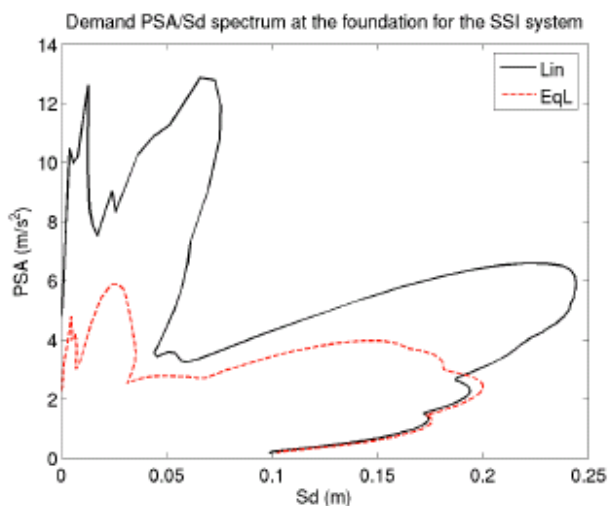


Figure 8. Demand spectrum at the foundation level for linear (solid line) and equivalent linear (dashed line) soil behavior.

#### Water tower subjected to the San Rocco earthquake record

The simplified water tower resting on the shallow soil profile is subjected to the San Rocco earthquake record. The large weight of the structure along with the rather small founda-

tion dimensions create an additional wave field emanating away towards the halfspace. This wave field is added to the incoming incident wave field from the earthquake ground shaking, contributing to the increase of the shear strain in the uppermost soil layers. Figure 9 shows the shear strain at a depth of 2m below the foundation for equivalent linear soil behavior. The presence of the structure increases the shear strain exhibited by the soil more than 50%.

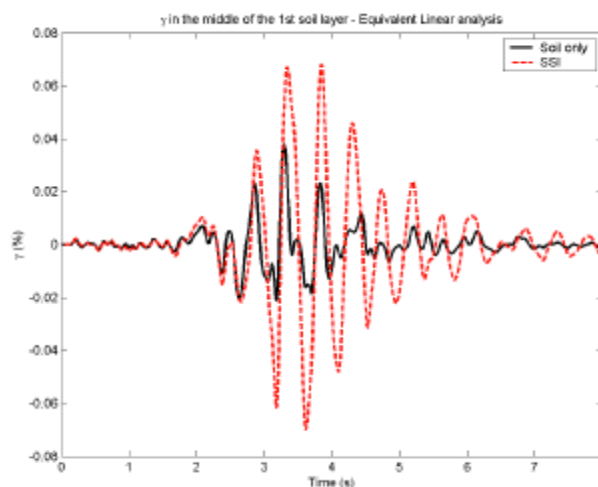


Figure 9. Shear strain time history at a depth of 2m below the foundation for equivalent linear soil behavior. The response of the free field soil response (solid line) is compared with the response of the SFSI response (dashed line).

Nevertheless, the soil-foundation-structure interaction does not seem to affect much the demand spectrum of the structure, as seen in Figure 10. The existence of the structure increases the acceleration and displacement spectral values for certain periods.

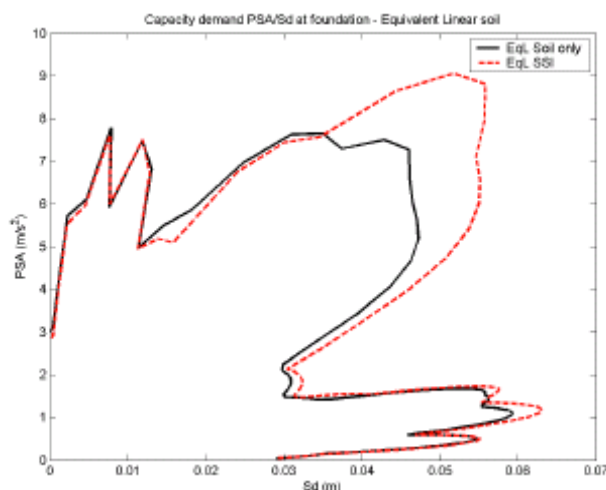


Figure 10. Demand spectrum at the foundation level for equivalent linear soil behavior, at the free field (solid line) and in the presence of the structure (dashed line).

#### Water tower subjected to the Aegion earthquake record

Next the simplified system of the water tower on the shallow soil profile is subjected to the stronger ground motion of the Aegion, 1995 Aegion, Greece earthquake. The soil behaves in a nonlinear way due to the intensity of the ground shaking, which can be witnessed by the minor increase of the shear strain time history at a depth of 2m under the foundation, shown in Figure 11. However, most important is the shifting of the soil response to lower fre-

quency values due to nonlinear behavior, attested in Figure 11 at the bottom, where the Fourier amplitude of the shear strain is plotted. The fundamental frequency of the soft soil shifts from 2.1Hz down to 1.4Hz, due to the soil softening.

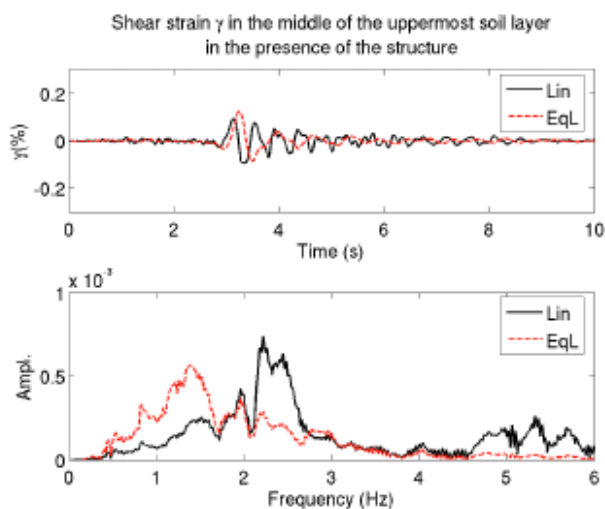


Figure 11. Shear strain time history (top) and Fourier amplitude (bottom) at a depth of 2m below the foundation level, for linear (solid line) and equivalent linear (dashed line) soil behavior.

The structural system is greatly affected by the nonlinear soil behavior, as well as by the interaction with the soil. The response at the top of the structure is shown in Figure 12. The softening of the soil due to nonlinear behavior causes the acceleration and velocity response to reduce by 70% and 50% respectively, while the displacement at the top is less affected due to its lower frequency content. The reduction in the acceleration suggests less conservative seismic design for the structure. On the other hand, the design has to accommodate for the important displacement and drift exhibited by the structure.

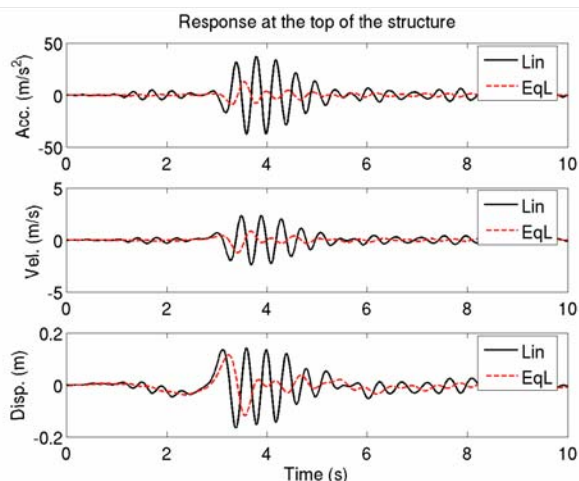


Figure 12. Response at the top of the structure for linear (solid line) and equivalent linear (dashed line) soil behavior.

The most impressive effect, however, of the nonlinear soil behavior is plotted in Figure 13. The demand spectrum of the structure for linear soil behavior decreases dramatically for equivalent linear soil behavior. The acceleration spectral values for nonlinear soil reduce more than 70% from the values for linear soil, while the displacement is less affected by the soil softening.

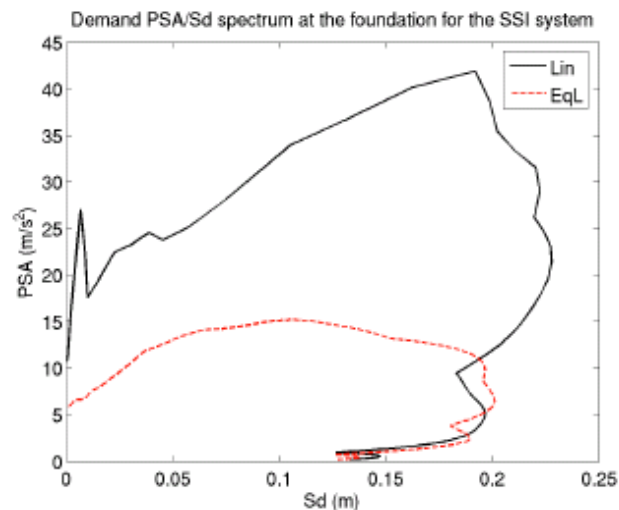


Figure 13. Demand spectrum at the foundation for linear (solid line) and equivalent linear (dashed line) soil behavior.

## CONCLUSIONS

The primer effects of the SFSI are the stiffness degradation of the soil–foundation system and the increase of the energy dissipation in the soil, by hysteretic action and radiation. Naturally, the fundamental frequency of the complete soil–foundation– structure system decreases from the fixed base case and the amplitude of the response diminishes as well. The nonlinear soil behavior has essentially a supplementary action, as it further decreases the soil– foundation system stiffness and increases the damping in the soil from the linear case. Consequently, the nonlinear soil behaviour causes the natural frequency of the system to shift to lower frequencies to a greater extent from the linear elastic or viscoelastic case. Finally, the amplified energy dissipation in the soil leads, in most cases, to a decrease in the response amplitude.

As the nonlinear soil behavior and the SFSI affect the response of the system, the spectral acceleration and displacement values are equally influenced. Consequently, the demand spectra are modified from the traditional linear elastic or viscoelastic approach. The crucial trend is two-fold:

- the incorporation of a SFSI approach mostly modifies the shape of the demand spectrum, by amplifying or diminishing the spectral values,
- the introduction of an equivalent linear soil approximation in the substructure SFSI approach decreases significantly the spectral values from the linear case.

Concerning the effect of the SFSI and the nonlinear soil behavior on the soil, their combined action increases the shear strain immediately underneath the foundation, which may lead to different seismic design concept of lifelines and underground structures.

## Acknowledgements

This study was performed in the framework of the European research project entitled New Methods for Mitigation of Seismic Risk of Existing Foundation (acronym NEMISREF, EC contract No G1RD-CT-2002-00702, EC project No GRD1-2001-40457) under the coordination of Professors Arezou Modaressi and Didier Clouteau of Ecole Centrale Paris. The author deeply acknowledge their contribution to this study.

## REFERENCES

Vucetic, M. (1994). Cyclic threshold shear strains in soils. *Journal of Geotechnical Engineering Division – ASCE* 120(12), 2208–2228.

Gazetas, G. (1983). Analysis of machine foundation vibrations: state of the art. *Soil Dynamics and Earthquake Engineering* 2(1), 2–42.

Pitilakis, D. (2006). Soil-Structure Interaction Modeling Using Equivalent Linear Soil Behavior in the Substructure Method. Ph.D. thesis, LMSS-Mat, Ecole Centrale Paris, France.

Schnabel, P., J. Lysmer, and H. Seed (1972). SHAKE: a computer program for earthquake response analysis of horizontally layered sites. Report EERC-72-12, Earthquake Engineering Research Center, University of California, Berkeley, CA, U.S.A.

Modaressi, H. and E. Foerster (2000). *CyberQuake*. France: BRGM.

Pitilakis, D., M. Dietz, D. M. Wood, D. Clouteau, and A. Modaressi (2008). Numerical simulation of dynamic soil-structure interaction in shaking table testing. *Soil Dynamics and Earthquake Engineering* 28(6), 453–467.



## A NUMERICAL APPROACH TO THE SEISMIC PROBLEM OF STEEL PILE-SOIL INTERACTION UNDER ENVIRONMENTAL AND SECOND-ORDER GEOMETRIC EFFECTS

Asterios LIOLIOS<sup>1</sup>, George MICHALTSOS<sup>2</sup>  
and Konstantinos LIOLIOS<sup>3</sup>

### ABSTRACT

*A numerical approach for the dynamic soil-pile interaction, considered as an inequality problem of structural engineering, is presented. So, the unilateral contact conditions due to tensionless and elastoplastic softening/fracturing behaviour of the soil as well as due to gapping caused by earthquake excitations are taken into account. Moreover, soil-capacity degradation due to environmental effects and second-order geometric effects for the pile behaviour due to preexisting compressive loads are taken into account. The numerical approach is based on a double discretization and on mathematical programming. First, in space the finite element method (FEM) is used for the simulation of the pile and the unilateral contact interface, in combination with the boundary element method (BEM) for the soil simulation. Next, with the aid of Laplace transform, the problem conditions are transformed to convolutional ones involving as unknowns the unilateral quantities only. So the number of unknowns is significantly reduced. Then a marching-time*

*approach is applied and finally a nonconvex linear complementarity problem is solved in each time-step.*

Keywords: Dynamic soil-pile interaction, unilateral contact numerical approach

## INTRODUCTION

Dynamic soil-pile interaction can be considered as one of the so-called inequality problems of structural engineering (Liolios, 1989a). As wellknown (Panagiotopoulos, 1993), the governing conditions of these problems are equalities as well as inequalities. Indeed, for the case of the general dynamic soil-structure interaction, see e.g. Wolf (1988) and Beskos (1993), the interaction stresses in the transmitting interface between the structure and the soil are of compressive type only. Moreover, due to in general nonlinear, elastoplastic, tensionless, fracturing etc. soil behaviour, gaps can be created between the soil and the structure. Thus, during e.g. strong earthquakes, separation and uplift phenomena are often appeared, as the praxis has shown, (Savidis et al, 1999).

The mathematical treatment of the so-formulated inequality problems can be obtained by the variational or hemivariational inequality approach (Panagiotopoulos, 1993, Antes & Panagiotopoulos, 1992). Numerical approaches for some dynamic inequality problems of structural engineering have been also presented, see e.g. Antes & Panagiotopoulos (1992) and Liolios (1989b).

The present paper deals with a numerical treatment for the inequality dynamic problem of soil-pile interaction where soil-capacity degradation due to environmental effects and second-order geometric effects for the pile behaviour due to preexisting compressive loads are taken also into account. In the problem formulation, the above considerations about gapping as well as soil elastoplastic/softening behaviour are taken into account. The proposed numerical method is based on a double discretization and on methods of non-linear programming. So, in space the finite element method (FEM) coupled with the boundary element method (BEM), and in time a step-by-step method for the treatment of convolutional conditions are used. In each time-step a non-convex linear complementarity problem is solved with reduced number of unknowns. Finally, the presented procedure is applied to an example problem of dynamic pile-soil interaction, and some concluding remarks useful for the Civil Engineering praxis are discussed.

## METHOD OF ANALYSIS

### Spatial discretization. Coupling of FEM and BEM

A spatial discretization is applied for the soil-pile system by coupling the FEM and BEM in the wellknown way, see e.g. Brebbia et al.(1984). For simplicity, the pile is first considered as linearly elastic, and discretized into usual beam/frame finite elements. Each pile node is considered as connected to the soil on both sides through two unilateral constraints (interface soil-elements). Every such interface element consists of an elastoplastic-softening spring and a dashpot, connected in parallel (Figure 1), and appears a compressive force  $r(t)$  at the time-moments  $t$  only when the pile node comes in contact with the soil.

Further, let  $v(t)$  denote the relative retirement displacement between the soil-element end and the pile-node, and  $g(t)$  the existing gap. Then the unilateral contact behaviour of the soil-pile interaction is expressed in the compact form of the following linear complementarity conditions:

$$v \geq 0, \quad r \geq 0, \quad r.v = 0. \quad (1)$$

The soil-element compressive force is in convolutional form (Wolf, 1988)

<sup>1</sup> Professor, Democritus University of Thrace, Dept. Civil Engineering, Inst. Structural Mechanics and Earthquake Engineering, GR-671 00 Xanthi, Greece. (e-mail: [liolios@civil.duth.gr](mailto:liolios@civil.duth.gr))

<sup>2</sup> Professor, National Technical University of Athens, Dept. Civil Engineering, Structural Engineering Division, Athens, Greece. (e-mail: [michalts@central.ntua.gr](mailto:michalts@central.ntua.gr))

<sup>3</sup> PhD Candidate, Democritus University of Thrace, Dept. Environmental Engineering, Inst. Ecological Engineering and Technology, GR-671 00 Xanthi, Greece. (e-mail: [kliolios@env.duth.gr](mailto:kliolios@env.duth.gr))

$$r = S(t)*y(t), \quad y = w - (g + v), \quad (2a,b)$$

or in form used in Foundation Analysis (Scott, 1981)

$$r = c_s(\partial y/\partial t) + p(y). \quad (2c)$$

Here  $c_s$  is the soil damping coefficient,  $w=w(t)$  the pile node lateral displacement,  $y=y(t)$  the shortening deformation of the soil-element, and  $p(y)$  the spring force. By  $*$  is denoted the convolution operation.  $S(t)$  is the dynamic stiffness coefficient for the soil and can be computed by the BEM (Wolf, 1988). Function  $p(y)$  is mathematically defined by the following, in general nonconvex and nonmonotone constitutive relation

$$p(y) \in \Theta P(y), \quad (2d)$$

where  $\Theta$  is Clarke's generalized gradient and  $P(\cdot)$  the symbol of superpotential nonconvex functions (Panagiotopoulos, 1993). So, (2d) expresses in general the elastoplastic-softening soil behaviour, where unloading-reloading, gapping, degrading, fracturing etc. effects are included.

For the herein numerical treatment,  $p(y)$  is piece-wise linearized in terms of non-negative multipliers as in plasticity (Maier, 1971, Liolios, 1989). So the problem conditions for the assembled soil-pipeline system are written in matrix form according to the finite element method:

$$\underline{M} \ddot{\underline{u}}(t) + \underline{C} \dot{\underline{u}}(t) + (\underline{K} + \underline{G}) \underline{u}(t) = \underline{f}(t) + \underline{A}^T \underline{r}(t) \quad (3)$$

$$\underline{y} = \underline{A}^T \underline{u} - \underline{u}_g - \underline{g} - \underline{B} \underline{z}, \quad \underline{r} = \underline{S} * \underline{y}, \quad (\text{or } \underline{r} = \underline{E} \underline{y}), \quad (4),(5)$$

$$\underline{\omega} = \underline{B}^T \underline{r} - \underline{H} \underline{z} - \underline{k}, \quad \underline{\omega} \leq 0, \quad \underline{z} \geq 0, \quad \underline{z}^T \underline{\omega} = 0, \quad (6)$$

$$\underline{u}(t=0) = \underline{u}_o, \quad \dot{\underline{u}}(t=0) = \dot{\underline{u}}_o, \quad \underline{g}(t=0) = \underline{g}_o \quad (7)$$

Here (3) is the dynamic equilibrium condition, (4)-(6) include the unilateral and the piece-wise linearized constitutive relations and (7) are the initial conditions. As usually,  $\underline{M}$ ,  $\underline{C}$  and  $\underline{K}$  are the mass, damping and stiffness matrix, respectively;  $\underline{G}$  is the geometric stiffness matrix depending linearly on pre-existing stress state (Chen and Lui, 1981, Maier, 1971);  $\underline{u}$ ,  $\underline{f}$  are the displacement and the force vectors, respectively;  $\underline{u}_g(t)$  is the vector of (possible) seismic ground displacement;  $\underline{A}$ ,  $\underline{B}$  are kinematic transformation matrices;  $\underline{z}$ ,  $\underline{k}$  are the nonnegative multiplier and the unilateral capacity vectors; and  $\underline{E}$ ,  $\underline{H}$  are the elasticity and unilateral interaction square matrices, symmetric and positive definite the former, positive semidefinite the latter for the elastoplastic soil case. In the case of soil softening, some diagonal entries of  $\underline{H}$  are nonpositive (Maier, 1971, 1973). For the case of nonlinear pile behaviour, either the

linear terms  $\underline{C} \dot{\underline{u}}$  and  $\underline{K} \underline{u}$  can be replaced by the nonlinear

matrix functions  $\underline{C}(\underline{u})$  and  $\underline{K}(\underline{u})$ , or the local nonlinearities (e.g. elastoplasticity) are included in appropriate internal unilateral constraints (Maier, 1971, Liolios, 1993).

Thus the so-formulated problem is to find  $(\underline{u}, \underline{r}, \underline{g}, \underline{z})$  satisfying (1)-(7) when  $(\underline{f}, \underline{u}_g, \underline{u}_o, \dot{\underline{u}}_o, \underline{g}_o)$  are given.

#### Time discretization. The Convolutional LCP.

Assuming that the unilateral quantities  $\underline{z}$  and  $\underline{r}$  include all local nonlinearities and unilateral behaviour, the procedure of Liolios (1993) can be used. So, applying the Laplace transform to (3)-(7), except (6)<sub>4</sub>, and after suitable elimination of unknowns and back transforming to time domain, we arrive eventually at

$$\underline{\omega}(t) = \underline{D}(t) * \underline{z}(t) + \underline{d}(t). \quad (8)$$

Thus, at every time-moment the problem of rels. (6)<sub>2,3,4</sub> and (8) is to be solved. This problem is called here Convolutional Linear Complementarity Problem (CLCP), has a reduced number of unknowns and is solved by time discretization. So, for the time moment  $t_n = n \Delta t$ , where  $\Delta t$  is the time step, we arrive eventually at a non-convex linear complementarity problem [6]:

$$\underline{\omega}_n = \underline{D} \underline{z}_n + \underline{d}_n, \quad \underline{z}_n \geq 0, \quad \underline{\omega}_n \leq 0, \quad \underline{z}_n^T \underline{\omega}_n = 0. \quad (9)$$

Alternatively, the above inequality problem of rels. (1)-(7) can be solved in time by direct time integration methods as in Liolios (1989a). So, some algebraic manipulations and a suitable elimination of unknowns lead to the same discretized LCP (9).

Solving problem (9) by available computer codes of non-linear mathematical programming (Maier, 1973), we compute which of the unilateral constraints are active and which not in each time-step  $\Delta t$ . Due to soil softening, matrix  $\underline{D}$  is not strictly positive definite in general. But as numerical experiments have shown, in most civil engineering applications of soil-pile interaction this matrix is P-copositive. Thus the existence of a solution is assured (Maier, 1971, 1973).

#### NUMERICAL EXAMPLE

The example problem of Liolios (1989a) is reconsidered here for comparison reasons. The steel IPB300 H-pile depicted in Figure 1(a) has a length  $L = 12$  m and is fully embedded into a clay deposit. The pile has a stiffness  $EI = 52857$  KN.m<sup>2</sup>, is fixed at the bottom and free at the top. The effects of the over structural framing are approximated by a lumped mass  $2$  KN.m<sup>-1</sup>.sec<sup>2</sup> and a rotational inertia  $2$  KN.m.sec<sup>2</sup>. The pile is subjected to a vertical constant top force of  $120$  KN and to a dynamic horizontal top force with the time history shown in Figure 2(a). The elastoplastic-softening soil behaviour due to environmental effects is, according to eqn. (2b), shown in Figure 2(b)-(diagramme  $p$ - $y$ ) - where branch OA has the exponential form  $p(x,y) = p_u \cdot [1 - \exp(-100y)]$ , with  $p_u = 375[1 - 0.5 \exp(-0.55x)]$ , and for the branch AB holds  $p(x,y) = 0.75 p_p \cdot (-3\xi^2 + 2\xi^3) + p_p$ , with  $\xi = (y - 0.02)/0.06$ . For unloading-reloading paths the inclination is  $100p_u$ .

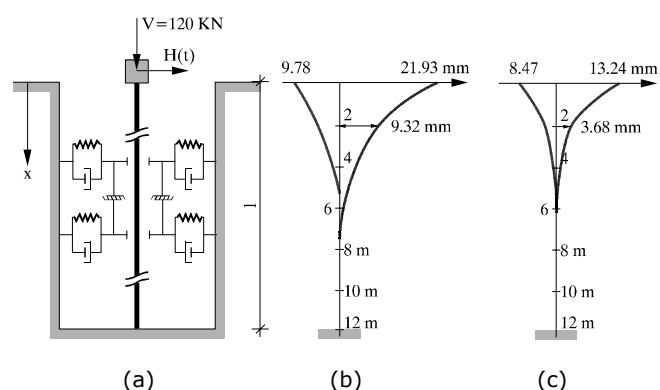


Figure 1: The numerical example: (a) The soil-pile system model, (b) Maximum horizontal pile displacements, (c) Final soil-pile gaps.

Some response results from the ones obtained by applying the herein presented numerical procedure are indicatively reported. So the maximum values of the pile horizontal displacements and the final gaps along the pipeline due to permanent soil deformations are shown in Figures 1(b) and 1(c), respectively. These results are in good agreement with those of Liolios (1989a).

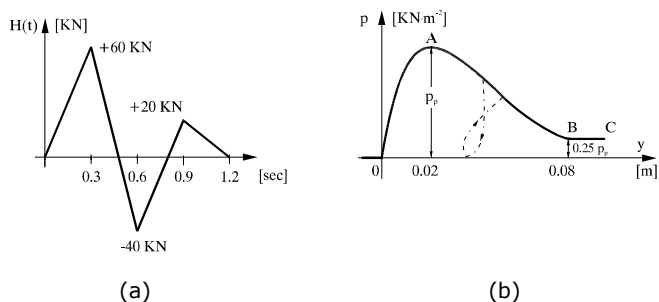


Figure 2: The numerical example: (a) Dynamic loading diagramme, (b) Diagramme p-y of the soil behaviour.

## CONCLUSIONS

As the above indicative results of the numerical example show, unilateral contact effects due to tensionless soil capacity and to gapping, soil-capacity degradation due to environmental effects and second-order geometric effects for the pile behaviour due to preexisting compressive loads may be significant and have to be taken into account for the dynamic soil-pile interaction. These effects can be numerically estimated by the herein presented procedure, which is realizable on computers by using existent codes of coupling the FEM and BEM as well as of optimization algorithms. Thus, the presented approach can be useful in the praxis for the earthquake resistant construction, design and control of piles.

## REFERENCES

- Antes, H. & Panagiotopoulos, P.D., *The Boundary Integral Approach to Static and Dynamic Contact Problems. Equality and Inequality Methods*, Birkh@user Verlag, Basel, Boston, Berlin (1992).
- Beskos, D.E., Application of the Boundary Element Method in Dynamic Soil-Structure Interaction, in: Gulkan, P. and Clough, R.W. (Eds.), *Developments in Dynamic Soil-Structure Interaction*, Kluwer, London, (1993).
- Brebbia, C.A., Telles, J.C.F. & Wrobel, L.C., *Boundary Element Techniques*, Springer-Verlag, Berlin and New-York, (1984).
- Chen, W.F. and Lui, E.M., *Structural Stability*, Elsevier, New York, (1981).
- Liolios, A.A., (1989a), A numerical approach to the dynamic nonconvex unilateral problem of soil-pile interaction. In: C.M. Dafermos, G. Ladas & G. Papanicolaou (eds.), *Differential equations*, pp. 437-443. Marcel Dekker, Inc., Basel, (1989).
- Liolios, A.A., (1989b), A Linear Complementarity Approach to the Nonconvex Dynamic Problem of Unilateral Contact with Friction between Adjacent Structures, *Jnl Applied Mathematics and Mechanics (ZAMM)*, (1989), 69(5), 420-422.
- Liolios, A.A., A Boundary Element Convolutional Approach to Unilateral Structural Dynamics, in: Antes, H. (Ed.), *IABEM 93-Extended Abstracts*, Inst. Appl. Mech., Techn. Univ. Braunschweig, (1993).
- Maier, G., Mathematical Programming Methods in Structural Analysis, in: Brebbia, C. and Tottenham, H., (Eds.), *Variational Methods in Engineering*, Vol.II, pp. 8/1-8/32, Southampton Univ. Press, Southampton, (1973).
- Maier, G., *Incremental Elastoplastic Analysis in the Presence of Large Displacements and Physical Instabilizing Effects*, Int. Jnl Solids and Structures, Vol. 7, 345-372, (1971).
- Panagiotopoulos, P.D., *Hemivariational Inequalities and Applications*, Springer Verlag, Berlin (1993).

Savidis, S.A., Bode, C., Hirschauer, R. & Hornig, J. Dynamic Soil-Structure Interaction with Partial Uplift. In: L. Fryba & J. Naprstek, (eds.), *EURODYN '99, Proc. 4<sup>th</sup> European Conference on Structural Dynamics*, Prag 1999, pp. 957-962. Rotterdam: Balkema.

Scott, R., *Foundation Analysis*, Prentice-Hall, London, (1981).

Wolf, J.P., *Soil-Structure-Interaction Analysis in Time Domain*, Prentice-Hall, Englewood Cliffs, N.J. (1988).



## RETAINING WALL-SOIL-STRUCTURE INTERACTION EFFECTS DUE TO SEISMIC EXCITATION

George PAPAZAFEIROPOULOS<sup>4</sup>, Prodromos N. PSARROPOULOS<sup>5</sup>, and Yiannis TSOMPANAKIS<sup>3</sup>

### ABSTRACT

*Retaining walls are very frequently used in engineering practice to support, apart from soil layers, structures founded on the retained soil layers. During a seismic event it is evident that the dynamic response of each component of this complex system (i.e., wall, soil and structure) may affect substantially the response of the rest and vice versa. This phenomenon, which could be adequately described as "dynamic wall-soil-structure interaction" (DWSSI), is a rather complicated issue that combines: (a) the dynamic interaction between the wall and the retained soil layers, and (b) the "standard" dynamic interaction of a structure with its underlying soil layers. In the present study, using two-dimensional numerical simulations, the impact of the wall flexibility and structure stiffness on the dynamic response of the overall system is investigated. Emphasis is given on the relation between the dynamic behavior of the overall system and the dynamic properties of each component (one-dimensional soil layer-structure and wall-soil-structure). Primarily, the response of a simple structure lying on a single infinite soil layer is investigated. Subsequently, a retaining wall is included in the numerical models. A parametric study is performed in order to examine at what extend the presence of the wall may affect the amplification factors of the various components, and consequently the distress imposed on the structure (with respect to its position and its fundamental eigenperiod). In addition, the eigenperiod of the soil-structure system is calculated via analytical methods. Despite the fact that there exist many open issues to be resolved, the results of the current study provide a clear indication of the direct dynamic interaction between a retaining wall and an adjacent structure.*

Keywords: dynamic response, soil-structure interaction, amplification factor, soil spring.

### INTRODUCTION

It is generally accepted that during a seismic event structures founded on soft soil exhibit much different dynamic behaviour than those founded on rigid rock. Therefore,

<sup>4</sup> M.Sc. Student, Technical University of Crete, Greece, gpapazafeiropoulos@yahoo.gr

<sup>2</sup> Lecturer, Hellenic Air Force Academy, Athens, Greece, prod@central.ntua.gr

<sup>3</sup> Asst. Professor, Technical University of Crete, Greece, jt@science.tuc.gr

structures founded on soft soil cannot be modelled as if they were founded on rigid rock, by assuming that they are totally fixed at their base. Their dynamic characteristics change substantially due to soil compliance, which has to be taken into account during their seismic design. This problem is widely known as *dynamic soil-structure interaction problem* (DSSI). Soil compliance is usually taken into account by using a number of springs and dashpots, which are located at the level of the structure's foundation, and are supposed to substitute totally the underlying soil. The calculation of these springs and dashpots is a sophisticated procedure, which has been coped with (semi-) analytical solutions (Veletsos and Meek, 1974, Gazetas, 1983). Using spring constants, various seismic norms (e.g., NEHRP-97) provide simple formulas to calculate the modified (due to DSSI) structural eigenperiod. Nevertheless, dynamic interaction between the soil and the structure remains a complex and unresolved issue, given that the nonlinearities (material and/or geometrical) present in the overall system behavior are usually not taken into account. However, the issue of DSSI (taken into consideration in a simplistic way by most seismic norms) is considered a-priori to be beneficial for a structure, which seems not to be always the case (Mylonakis and Gazetas, 2000).

In contrast, retaining walls are extensively used worldwide for serving various purposes in structures and infrastructures. Deep excavations, bridge abutments, or harbor quay-walls are some of the cases where a rigid or a flexible retaining wall is constructed. Despite their structural simplicity, the seismic response of retaining walls (that retain even a single soil layer) is a rather complicated problem. The major complexity of the problem is the dynamic interaction between the wall and the retained soil, especially when material and/or geometry nonlinearities are present (Kramer, 1996, Wu and Finn, 1999). This interaction is known as *dynamic wall-soil interaction* (DWSI). Consequently, the performance of retaining walls during earthquakes is a subject being still examined by many researchers, experimentally, analytically, or numerically (Veletsos and Younan, 1997, Psarropoulos et al., 2005). However, regarding the seismic design of retaining systems, the DWSI is generally ignored by the seismic norms (EC8, 2004, EAK, 2000).

In both the aforementioned cases (DSSI and DWSI), the phenomenon of "simple" dynamic interaction with soil material occurs. Nevertheless, in many real cases retaining walls are used to support structures founded on the retained soil. It is evident that during a seismic event the dynamic response of each component of this complex system (wall, soil layer, and structure) may affect substantially the response of the others. The presence of the retaining wall will affect not only the ground surface shaking of the retained soil, but the dynamic response of any type of retained structure as well. In addition, the existence of a structure behind the wall is expected to alter the dynamic earth pressures developed on the wall. Therefore, the phenomenon of *dynamic wall-soil-structure interaction* (DWSSI) is a complicated problem that includes: (a) the dynamic interaction between a wall and the retained soil layers, and (b) the "standard" one-dimensional dynamic soil-structure interaction of a structure with its underlying soil.

The aforementioned issues are not considered with the proper realism in the current seismic norms used in modern engineering practice, such as the Eurocode 8 (EC8 2004) or the Greek Seismic Code (EAK 2000). However, when structures (even with a single degree of freedom) have foundation that do not lie on a homogeneous halfspace, but nearby a rigid or a flexible retaining wall, their seismic response becomes much more complicated, mainly due to the existence of the aforementioned double interaction, rather than the simple well-known interaction between the structure and the underlying soil. In essence, the existence of a

wall imposes a vertical boundary on the overall soil-structure system which makes the whole model stiffer, and consequently reduces its eigenperiod. Thus, an eigenperiod lower than the one described by the NEHRP-97 provisions is expected.

The objective of the present study is to examine more thoroughly the phenomenon of *dynamic wall-soil-structure interaction*. For this purpose, two-dimensional plane-strain numerical simulations are performed, utilizing the finite-element method, in order to investigate some of the most important aspects of this complex phenomenon. Firstly, the influence of the soil compliance on the structural response is investigated, with the absence of the retaining wall (as shown in Figure 1), while emphasis is given on the amplification of the base acceleration, a fact generally underestimated by the seismic norms. The structure is essentially a single-degree-of-freedom (SDOF) system, comprised of a concentrated mass, a column, and a rigid footing. The resonant frequencies of the structure can be estimated, and the interpretation and verification of the results, with the well-established NEHRP-97 provisions, can be easily performed. Subsequently, a retaining cantilever wall adjacent to the structure is included in the numerical models. A parametric study has been conducted in order to examine how the location of the structure may affect the amplification factors in characteristic locations of the model. In addition, the parametric study investigates at what extent the presence of the wall may affect the response of the structure with respect to its position. In all cases, the wall is characterized by its height  $H$  and its relative flexibility  $d_w$ , while the soil is considered as uniform viscoelastic material with constant shear-wave velocity  $V_s$ , density  $\rho$ , and critical damping ratio  $\xi$ . In general, dynamic response of any system depends on the seismic excitation characteristics (both in the time domain and in the frequency domain). Without any loss of generality, harmonic excitations have been considered in this study, since any arbitrary seismic excitation can be analysed into a series of harmonic functions with selected amplitudes and frequencies (Fourier series). Results provide a clear indication of the direct dynamic interaction between a retaining wall and its retained structures. That fact justifies the necessity for a more elaborate consideration of this interrelated phenomenon on the seismic design of the retaining walls and the nearby structures.

## EFFECTS OF DYNAMIC SOIL-STRUCTURE INTERACTION (DSSI)

Initially, the retaining wall was not considered during the analysis of the dynamic system. Thus, the soil layer behaves as if it was extended to infinity for both horizontal directions. Such cases, in which structures have to be founded on compliant soil, are not rare in civil engineering practice. In order to examine the effects of DSSI on structures, one-dimensional (1-D) numerical simulations of the system depicted in Figure 1 were conducted. The simulations were performed utilizing the finite-element code ABAQUS (2003), which is capable of performing dynamic linear analyses using Rayleigh type of material damping (resulting to a critical damping ratio of  $\xi$  for the frequencies of interest). The soil was discretized using four-node quadrilateral plain-strain elements. Kinematic constraints were used at the two vertical boundaries of the soil layer in order to simulate the 1-D soil layer response. For more accurate simulation, the vertical kinematic constraints were placed far away from the structure. Regarding the ground motion, harmonic excitation has been selected as the dynamic loading. Although soil nonlinearity is expected to have a significant impact, it was not examined in this preliminary investigation of this complex interaction phenomenon. To avoid inertial effects on the response of the structure (which would make the interpretation of the results of the investigated dynamic interaction issues much more complicated) the structure was modelled as a lumped mass  $m$

on top of a weightless column of flexural stiffness  $K_{STR}$ , discretized with beam elements. The weightless column was considered to be fixed at a rigid, weightless foundation, which is located on the surface of the soil layer (i.e., without any embedment). The interface between the foundation and the underlying soil is considered to be fully bonded, thus no sliding of the footing is allowed and its dynamic response is identical to the response of the surrounding soil. This assumption is generally valid for cohesive soils and small displacements.

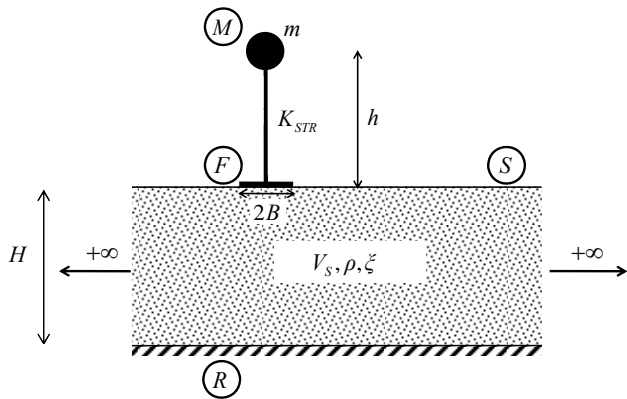


Figure 1. The examined 1-D model: a SDOF system founded on the surface of an infinite soil layer

The response of the structure and its foundation were studied via properly defined transformation functions that define the amplification in various locations shown in Figure 1: the bedrock (R), the free-field of the soil (S), the foundation (F) of the SDOF and the top (M) of the SDOF where its mass is located. Consequently, the Amplification Factor between two arbitrary points X and Y of the model, denoted as  $AF(XY)$ , is defined by:

$$AF(XY) = \frac{FFT[Y(t)]}{FFT[X(t)]} \quad (1)$$

where  $FFT[Y(t)]$  and  $FFT[X(t)]$  are the Fast Fourier Transforms of the corresponding time histories of points X and Y, respectively. Displacement-, velocity-, or acceleration- time histories can be used in the above equation, provided that both Y(t) and X(t) are expressed in terms of the same quantity. Two characteristic amplification factors AF are considered here: (a) the  $AF(RM)$  which is the total amplification between the rigid rock layer and the lumped mass of the SDOF, and (b) the  $AF(RF)$  which is the amplification between the rigid rock and the foundation of the SDOF.

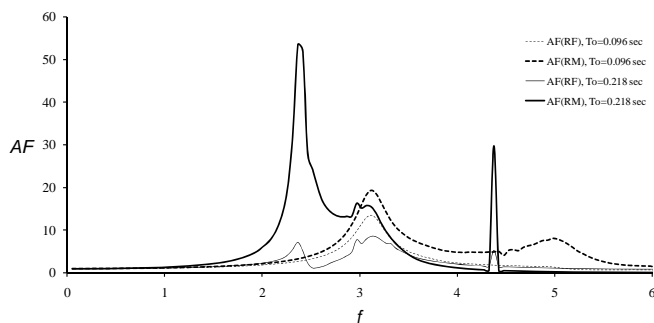


Figure 2. The variation of the steady state AFs, versus the frequency of the imposed harmonic excitation

For any structure founded on rigid rock its eigenperiod  $T_0$  is given by:

$$T_0 = 2\pi \sqrt{\frac{m}{K_{STR}}} \quad (2)$$

If two structures with arbitrary characteristics and eigenperiods equal to  $T_{01}=0.218$  sec and  $T_{02}=0.096$  sec are assumed on the top of the model presented in Figure 1, then the amplification factors depicted in Figure 2 will result. The bold lines correspond to the amplification of the structures' lumped mass, and the thinner ones refer to the amplification of the structures' foundation level. By inspecting Figure 2 the following trends can be noticed:

(a) All curves have a local peak around the frequency equal to  $f=3.15$  Hz. These peaks are due to the resonance of the underlying soil. The resonant frequency of the soil layer is given by:

$$f_0 = \frac{V_s}{4H} \quad (3)$$

and for  $V_s=100$ m/s and  $H=8$ m considered in this simulation, Eq. (3) results to  $f_0=3.125$  Hz, which is very close to the aforementioned value.

(b) The curves showing the total amplification factor of the SDOF,  $AF(RM)$ , have another peak at different frequencies, while at the same frequencies the value of the amplification factor of the foundation,  $AF(RF)$ , is small. These frequencies are the resonant frequencies of the structures and they appear to be independent of the behavior of the underlying soil. These two frequencies are equal to  $\bar{f}_{01} = 2.4$  Hz (corresponding to period  $\bar{T}_{01} = 0.417$  sec) for the structure with  $T_{01}=0.218$  sec, and  $\bar{f}_{02} = 5$  Hz (corresponding to period  $\bar{T}_{02} = 0.2$  sec) for the structure with  $T_{02}=0.096$  sec. Note that  $\bar{T}_{01} > T_{01}$  and  $\bar{T}_{02} > T_{02}$ , more specifically  $\bar{T}_{01}/T_{01} = 1.91$  and  $\bar{T}_{02}/T_{02} = 2.08$ , due to the impact of DSSI.

Figure 3 presents two possible modelling types for the foundation of SDOF systems. At the left, the original fixed-base soil-structure system is depicted, while at the right the equivalent SDOF system of the sift soil layer, substituted by two representative springs, is shown. According to the NEHRP-97 provisions (Gazetas, 1991), the eigenperiod of a structure founded on compliant soil is calculated by:

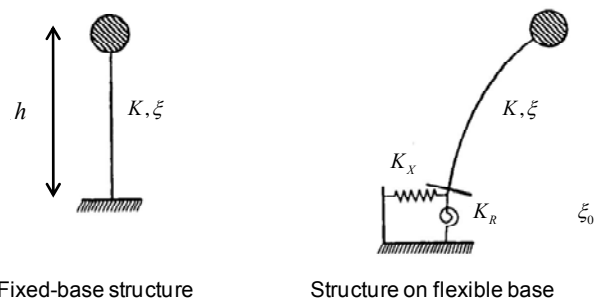


Figure 3. A SDOF system lying on rigid rock (left), and a SDOF system lying on deformable soil (right)

$$\bar{T} = T \sqrt{1 + \frac{K_{STR}}{K_X} \left( 1 + \frac{K_X h^2}{K_R} \right)} \quad (4)$$

where  $\bar{T}$  is the eigenperiod of the structure lying on deformable soil and  $T$  is the eigenperiod of the same structure being totally fixed at its base, while  $K_{STR}$  is the flexural stiffness of the column:

$$K_{STR} = \frac{3EI}{h^3} \quad (5)$$

$E$ ,  $I$ ,  $h$  denote the Young modulus, the moment of inertia, and the height of the column of the SDOF. Parameters  $K_X$  and  $K_R$  are the horizontal and rotational equivalent stiffness of the springs simulating the underlying soil respectively, which for the strip foundation lying on the surface of a homogeneous soil (see Figure 4) are given by:

$$K_X \approx \frac{2.1G}{2-\nu} \left( 1 + \frac{2B}{H} \right) \quad (6)$$

$$K_R \approx \frac{\pi GB^2}{2(1-\nu)} \left( 1 + \frac{B}{5H} \right) \quad (7)$$

The parameters in Equations (6) and (7) are shown in Figure 4. For the examined structure they are equal to:  $h=6$  m,  $E=30$  GPa, and  $I=0.018$  m<sup>4</sup> (for dimensions 1.0m x 0.6m) and its foundation has width  $2B=3.2$  m. In addition, the underlying soil layer has  $G=18$  MPa and  $\nu=0.3$ . According to Eqs. (5), (6) and (7) the stiffnesses parameters can be easily calculated:  $K_{STR}=7.5$  MN/m,  $K_X=31.129$  MN/m, and  $K_R=107.539$  MNm. Therefore, Equation (4) results to  $\bar{T}/T \approx 1.94 \approx \bar{T}_{O1}/T_{O1} \approx \bar{T}_{O2}/T_{O2}$ , thus, the NEHRP-97 provisions are verified.

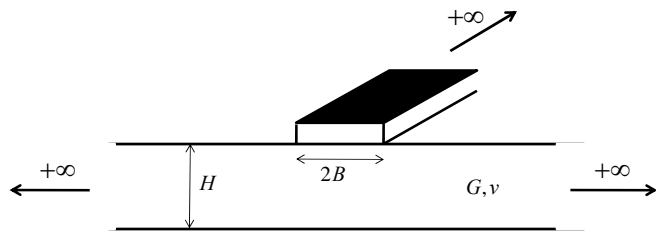


Figure 4. A rigid strip footing lying on an infinite soil layer for plane strain conditions

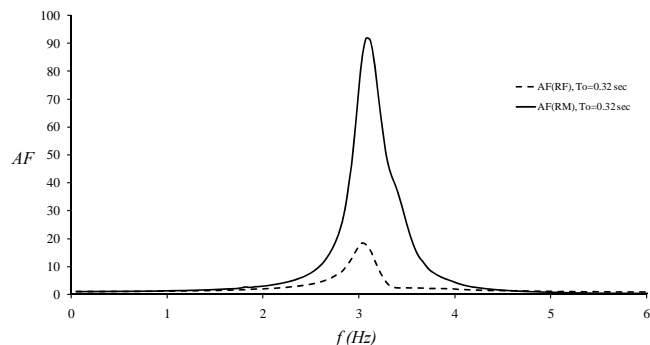


Figure 5. The variation of the steady state AFs versus the frequency of the imposed harmonic excitation for the case of double soil-structure resonance

Considering the case when the structure's eigenperiod is equal to the eigenperiod of the underlying soil layer. Then, if the amplification factors are plotted against the frequency  $f$  of the harmonic excitation then the curves shown in Figure 5 are produced. In these curves, both amplification factors ( $AF(RM)$  and  $AF(RF)$ ) present a peak at the resonant frequency of the soil layer. No other peaks exist, and it can be observed that the amplification factors are both much

higher than the ones observed in Figure 2, e.g.,  $AF(RM)$  is almost equal to 100. This phenomenon, in which the amplification factor of the SDOF is very high, compared to the amplification factor of its foundation, is called "double resonance". If this occurs, then the structure alone, and the soil layer also, are in conditions of resonance and the overall vibrating system is also in resonance. Consequently, the dynamic response of the structure increases dramatically (as one can see by comparing Figures 2 and 5), and failure will ensue. Such a case has occurred in the Mexico city, during the 1985 earthquake, the destructive impact of which is widely known. This system, which is characterized by double soil-structure resonance, is selected in order to study the influence of a retaining wall (rigid or flexible) adjacent to the structure.

### EFFECTS OF DYNAMIC WALL-SOIL-STRUCTURE INTERACTION (DWSSI)

As it was previously mentioned, prescriptive seismic norms are not capable of taking realistically into consideration the main components of the dynamic wall-soil-structure interaction: (a) the dynamic interaction between a retaining wall and the retained soil layer, and (b) the "standard" 1-D dynamic soil-structure interaction, i.e., the foundation of a structure on a soil layer and the related kinematic or inertial interaction with it. Therefore, in a case of a complex wall-soil-structure system, elaborate numerical modelling of the whole problem is unavoidable, as it is not realistic to study the wall-soil system and the soil-structure system independently. In order to examine more efficiently the DWSSI phenomenon, numerical analyses were conducted and the results are obtained in terms of amplification factors. The analytical methodology of Veletsos and Younan (1997) has permitted the assessment of the effects and the relative importance of the factors involved. The 1-D soil layer is now considered to be retained by a vertical, rigid or flexible wall; it is free at its upper surface and fixed on a rigid base (thus no radiation damping is expected to occur). The properties of the wall are described by its thickness  $t_w$ , mass per unit of surface area  $\mu_w$ , modulus of elasticity  $E_w$ , Poisson's ratio  $\nu_w$ , and critical damping ratio  $\xi_w$ . The base of both the wall and the soil stratum were considered to be excited by a space-invariant horizontal harmonic motion, assuming an equivalent force-excited system.

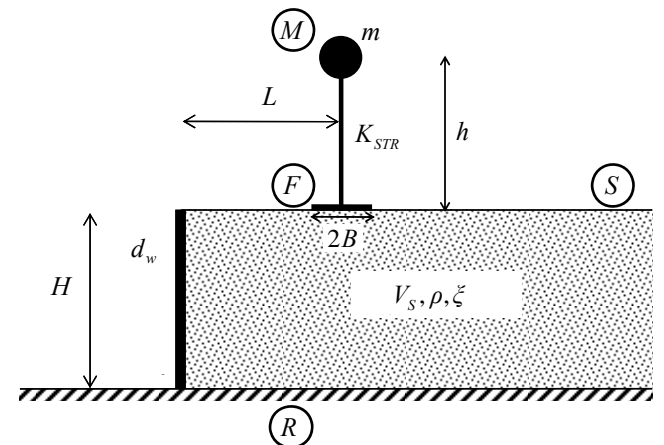


Figure 6. The retaining wall-soil-structure system examined in this study: a wall retaining a soil layer of height  $H$  on which a SDOF system is founded at distance  $L$

In the present study, in order to examine the effects of DWSSI on the retained structures, two-dimensional (2-D) numerical simulations of the retaining system depicted in Figure 6 were conducted. The simulations were performed utilizing also the finite-element code ABAQUS (2003), which is capable of performing dynamic linear analyses using Rayleigh type of material damping (resulting to a critical damping ratio of  $\xi$  for the frequencies of interest). The wall

was discretized using beam elements of unit longitudinal dimension and thickness equal to  $t_w = 0.20\text{m}$ .

The main parameters that affect the response of the system are the relative flexibility of the fixed-base wall derived by:

$$d_w = \frac{GH^3}{D_w} \quad (8)$$

and the dimensionless distance of the structure from the wall, defined by the ratio  $L/H$ . Parameter  $D_w$  in Eq. (8) denotes the flexural rigidity per unit of length of the wall, and is given by:

$$D_w = \frac{E_w t_w^3}{12(1-\nu_w^2)} \quad (9)$$

Two rather extreme cases were examined in this study: (a) a rigid fixed-base wall ( $d_w = 0$ ), and (b) a very flexible fixed-base wall ( $d_w = 40$ ). Given the value of  $d_w$ , the modulus of elasticity of the wall  $E_w$  is evaluated using equations (8) and (9), while the Poisson's ratio  $\nu_w$  is taken as 0.2. The wall is presumed to be massless, in order to avoid inertial effects on the structural response, which would further increase the complexity of the problem. The simplifying assumptions that no de-bonding or relative slip is allowed to occur at the wall-soil and the structure-soil interfaces were used.

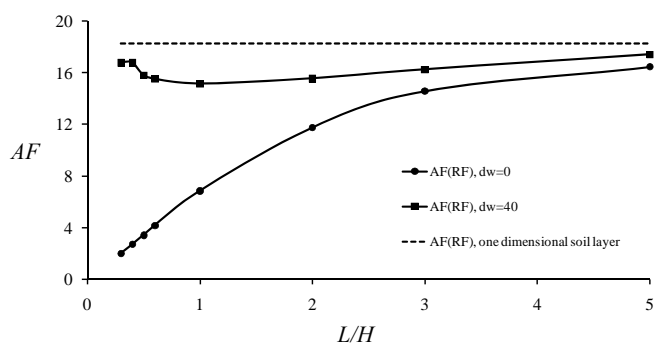


Figure 7. Variation of AF between the rigid rock (R) and the foundation of the SDOF (F) with the dimensionless distance from the wall  $L/H$ ; AF for the case of 1-D soil layer is also shown

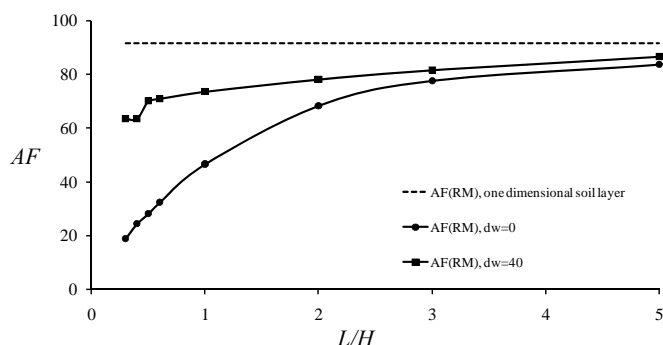


Figure 8: Variation of the Amplification Factor between the rigid rock (R) and the top of the SDOF (M) with the dimensionless distance from the wall  $L/H$ ; AF for the case of 1-D soil layer is also shown

It has to be stressed that the eigenperiod of the structure is affected by two primary factors: (a) the underlying soil compliance has an increasing effect on the structure eigenperiod, and (b) the presence of the retaining wall imposes a vertical (rigid or flexible) boundary to the soil layer, thus it makes the soil-structure system stiffer and it has a decreasing effect on the structure eigenperiod. Therefore, the

value of the structure's eigenperiod will be lower than the one given by Equation (4).

In Figure 7, the maximum amplification factor  $AF(RF)$  is plotted versus the dimensionless distance of the structure from the wall,  $L/H$ , for the two extreme cases of wall flexibility:  $d_w=0$  and  $d_w=40$ . It is obvious that the presence of a rigid wall has a decreasing effect on the maximum amplification for values of  $L/H$  lower than 5. It can be observed that as the distance ratio  $L/H$  decreases the system becomes stiffer, so the observation of lower amplification values is rational. For the case of flexible retaining wall, this reduction is not so intense. As the structure moves away from the wall, the wall has gradually lower influence on the structural response and the structural response approaches its behavior when founded on the 1-D soil layer. The same trends are detected in Figure 8 which presents the variation of the maximum amplification factor  $AF(RM)$ , with increasing dimensionless distance of the structure from the wall, for the two extreme values of wall flexibility.

Note that for all values of  $L/H$ , in both figures (7 and 8) the system is in resonance, thus, the maximum possible amplification factor can be obtained. It is also noteworthy that for  $L/H=1$ , the amplification factor  $AF(RF)$  reaches a local minimum of 15. Actually, AF does not get lower than this value, for any value of  $L/H > 0.3$ . The corresponding curve for the  $AF(RM)$  in Figure 8 does not follow this tendency, as the amplification of the structure's foundation increases and the amplification of the lumped mass decreases. This is attributed to the fact that the inertial effects of the lumped mass of the structure are gradually increasing, provided that the structure is relatively close to the wall. The flexibility of the retaining wall plays also an important role on the dynamic response of the structure. It can be seen in both figures that for all cases of  $L/H$ , flexible wall produces higher amplifications, both for the structure's foundation and the structure's lumped mass. The lowest amplification corresponds for the perfectly rigid retaining wall ( $d_w=0$ ).

In Figure 9 the amplification factor  $AF(FM)$  is shown as a function of the dimensionless distance of the structure from the wall  $L/H$ . In this diagram, a remarkable effect of the presence of the retaining wall is shown: while the other amplification factors generally reduce as the structure approaches the wall, this amplification factor becomes higher. Therefore, it is obvious that if the  $AF(RF)$  or  $AF(RM)$  are low, this does not mean that the amplification of the structure alone is also low. Structural engineers must be aware of the DWSSI phenomenon, as most seismic norms regard only the  $AF(RF)$  (which is not always realistic) only for the DSSI phenomenon, and may lead to unsafe design. Thus, the necessity of a unified retaining wall-soil-structure system and the understanding of the response of its components is imperative, in order to deal realistically with DWSSI phenomena.

## CONCLUSIONS

The scope of the present study was to investigate preliminarily the dynamic interaction between retaining walls, retained soil, and retained structures. It has been presented that the existence of a retaining wall may alter considerably the dynamic response of a structure founded on the retained soil. In the examined cases it was proven that the characteristics of the wall affect substantially the dynamic behaviour of the whole system. The presence of a rigid wall imposes a boundary that clearly alters the 1-D conditions of the backfill, while a flexible wall has less impact on the structural response. Furthermore, it has been shown that the amplification of the structure alone can be higher than that of 1-D conditions, as it comes closer to the retaining wall. In general, the results of this investigation provide a clear indication of the direct dynamic interaction between the wall, the retained soil, and the retained struc-

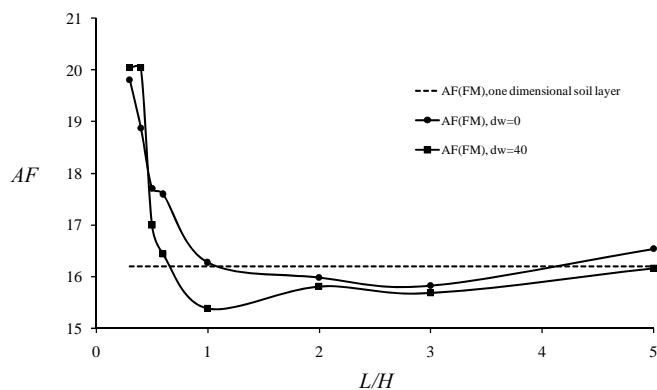


Figure 9: Variation of the Amplification Factor between the foundation (F) and the top of the SDOF (M) with the dimensionless distance from the wall  $L/H$ ;  $AF$  for the case of 1-D soil layer is also shown

tures. That fact justifies the necessity for a more elaborate consideration of this interrelated phenomenon during the seismic design (both in seismic norms and in engineering practice), taking into account not only the DSSI conditions, but the DWSSI imposed by a nearby retaining wall as well.

## REFERENCES

ABAQUS (2003) Analysis User's Manual Version 6.4, ABAQUS Inc., USA

EAK (2000) Greek Seismic Code, Ministry of Public Works, Athens, Greece

EC8 (2004) Eurocode 8: Design of structures for earthquake resistance, European standard CEN-ENV-1998-1, European Committee for Standardization, Brussels

Gazetas G (1983) "Analysis of machine foundation vibrations: state of the art", *Soil Dynamics and Earthquake Engineering* 2(1):2-42

Gazetas G (1991) "Formulas and charts for impedances of surface and embedded foundations", *Journal of Geotechnical Engineering Division - ASCE* 117(9):1363-1381

Kramer S (1996) Geotechnical Earthquake Engineering, Prentice Hall

Mylonakis G, and Gazetas G (2000) "Seismic soil-structure interaction: beneficial or detrimental?" *Journal of Earthquake Engineering* 4(3): 277-301

NEHRP-97 (1997) Recommended provisions for seismic regulations for new buildings and other structures, Building Seismic Safety Council, Washington, DC

Psarropoulos PN, Klonaris G, and Gazetas G (2005) "Seismic earth pressures on rigid and flexible retaining walls", *Soil Dynamics and Earthquake Engineering* 25(7-10): 795-809

Veletsos AS, and Meek JW (1974) "Dynamic behavior of building-foundation systems", *Earthquake Engineering and Structural Dynamics*, 3: 121-138

Veletsos AS, and Younan AH (1997) "Dynamic Response of Cantilever Retaining Walls", *ASCE Journal of Geotechnical and Geoenvironmental Engineering* 123(2):161-172

Wu G, and Finn WDL (1999) "Seismic lateral pressures for design of rigid walls", *Canadian Geotechnical Journal* 36(3): 509-522



## USING ACTIVE FAULT DATA FOR ASSESSING SEISMIC HAZARD: A CASE STUDY FROM NE AEGEAN SEA, GREECE

Spyros PAVLIDES<sup>6</sup>, Theodoros TSAPANOS<sup>7</sup>, Nikos ZOUROS<sup>8</sup>, Sotiris SBORAS<sup>9</sup>, George KORAVOS<sup>10</sup> and Alexandros CHATZIPETROS<sup>11</sup>

## ABSTRACT

*Seismic hazard is commonly assessed by using seismicity records and local geotechnical conditions. It is however of imperative importance to accurately define the probable seismic sources of the broader study area and assess their seismic potential, as earthquake intensities are expected to increase in the close vicinities of active faulting. In this paper, the procedure for identifying seismically active faults in NE Aegean and surroundings is described, while their earthquake potential and expected ground acceleration are also estimated. Based on the existing data, the maximum expected earthquake magnitude is 6.7 for onshore faults and 7.2 for offshore ones, while the corresponding ground displacements are 0.75 and 5.27 m respectively. Despite onshore faults are considered more hazardous, due to their immediate proximity to inhabited areas, the offshore fault hazard is considerable too, due to their proximity to the islands. Based on the instrumental seismicity, as well as the mapped active faults, conclusions are drawn for the expected ground acceleration for the main urban centres of the area in case of a strong earthquake. The results of this paper may be used for targeted measures during construction projects, complementing the existing earthquake building code.*

Keywords: Seismic Hazard Assessment, Aegean, Active faults, Greece

## INTRODUCTION

The North Aegean region is a geotectonically complex area, because its geodynamic status is directly affected by the North Anatolian Fault Zone (NAFZ), its westward continuation in the Aegean Sea, known as the North Aegean Trough (NAT) and the West Anatolia Graben System (WAGS) in Asia Minor with significant historical seismicity (Papazachos and Papazachou, 1989; Kiratzi and Louvari, 2003; Papazachos and Kiratzi, 1996). As a result of the interaction between those tectonic systems, there is a strong diversity in fault trending and character (Pavlidis et al., 1990; Koukouvelas and Aydin, 2002; Kreemer et al., 2004; Papanikolaou et al., 2006). These faults are located on both local islands as well as offshore, where they define the seafloor morphology. Furthermore, the faults on the Turkish coast should not be ignored in a seismic hazard analysis of the area, as they are situated in short distance from residential areas and are possible seismic sources.

According to the Greek National Statistic Agency (2001

<sup>6</sup> Professor, Dept. of Geology, Aristotle University of Thessaloniki, Greece, pavlides@geo.auth.gr

<sup>7</sup> Professor, Dept. of Geophysics, Aristotle University of Thessaloniki, Greece, tsapanos@geo.auth.gr

<sup>8</sup> Assoc. Professor, Dept. of Geography, University of the Aegean, Mytilene, Greece, nzour@aegean.gr

<sup>9</sup> Geologist MSc, Dept. of Geology, Aristotle University of Thessaloniki, Greece, ssmpporas@geo.auth.gr

<sup>10</sup> Dr. Geologist, Dept. of Geophysics, Aristotle University of Thessaloniki, Greece, gkoravos@geo.auth.gr

<sup>11</sup> Dr. Geologist, Dept. of Geology, Aristotle University of Thessaloniki, Greece, ac@geo.auth.gr

consensus), the population of North Aegean Prefecture is 204,108 residents while the population of Turkish coast cities and towns is several million. The definition of active faults and their seismic potential is therefore of paramount importance for seismic hazard assessment and civil protection.

The first step towards quantitative seismic hazard analysis for the area is the recognition and identification of active faults in the study area. This is not easy in this case, as the majority of the faults are either offshore, or do not deform recent geological formations. The following chapter describes the methodology used and is proposed as a general best practice guide for related studies.

## ACTIVE FAULTS

### Methodology

As mentioned above, the study area faults are variable in strike and character. A large percentage of them are affected by the local shear stress field, showing predominantly horizontal displacement, as derived from the focal mechanism of shallow earthquakes in the area. However, there are also many normal faults, while the majority of all faults are either normal with left-lateral component or right-lateral component.

In this complex tectonic environment, the determination of the fault activity and the fault classification in active or possibly active faults is based on the following criteria (see summary flow chart in Figure 1):

- *Fault geometry*: the relation between the fault strike and the local stress field is very important for possible future reactivations. If the angle between the fault strike and the main strain axis approaches the optimum value ( $90^\circ$  in relation to  $\sigma_3$  axis in normal faults and  $45^\circ$  in relation to  $\sigma_1$  and  $\sigma_3$  axes in strike-slip faults), it is likely that this fault will be activated either primarily, generating a seismic event, or secondarily due to distant triggering.
- *Geologic age*: the age of the last reactivation of the fault is the one of the most recent deformed material. Faults that deform Upper Pleistocene – Holocene sediments are *a priori* active. Older faults can also be considered as active as long as they match the rest of the present criteria.
- *The morphologic impact on relief (morphotectonic signature)*: the identification of past earthquake ground ruptures, easily affected by exogenic procedures, is an important and valuable indicator of recent fault activity; its weathering degree is directly dependant to the elapsed time since the last reactivation. Morphotectonic signatures may also be various other structures, such as sharp fault scarps, the differential and intense deep erosion at the upper part of a fault scarp, an observed linear arrangement of recent geomorphic features, etc. Analysis and evaluation of the morphologic impact requires careful study of geomorphic features and their association (or not) to faults.
- *The seismotectonic characteristics*: some faults are associated to historic or instrumental seismicity; in this case they are classified as active. In cases they produced surface ruptures during an event, it is easy to correlate them with specific tectonic structures. The determination of seismic faults that have not produced surface effects is based on the association of focal mechanisms with already mapped faults.
- *The morphotectonic indices*: together with the morphotectonic structures, the morphotectonic indices are strong proof for the activity level of a fault zone. This kind of indices can be fault scarp sinuosity, drainage basin asymmetry, valley width/height ratio, etc. There are many indices that can be used for drawing conclusions in tectoni-

cally active regions, but in all cases they must be used in combination with geologic and tectonic data (Pavlidis, 2003).

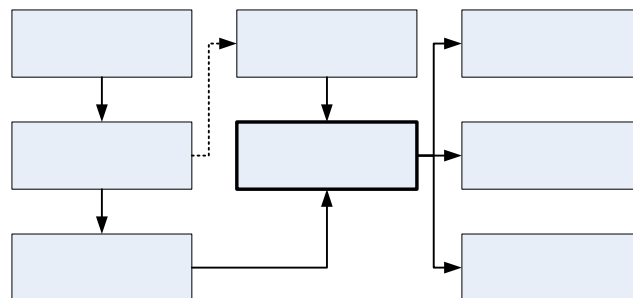


Figure 1. Procedure flow diagram for the characterization of active faults in the study area.

After applying the above mentioned criteria to individual faults, together with field confirmation, they can be characterized as active, possibly active or inactive. This classification refers to fault zones and not individual fault planes. An additional reason is that in many occasions active faults are hard to trace by surface prospecting, due to of recent sedimentation or human influence on morphology. Therefore, fault zone definition is important and adds, if taken into account, additional safety to construction planning.

The methodology applied for characterization of faults in the study area is summarized in Figure 1. Even if it wasn't possible to apply all the criteria to every studied fault, the combination of at least two of them is in many cases enough in order to characterize a fault as active.

### Active fault maps

All active faults in the study area are presented in the summary map (Figure 2), as well as in more detailed maps for each island. In each local map, expected magnitude and displacement are also presented. They were estimated using Pavlidis and Caputo (2004) relationships.

It is important to note that the faults depicted in the maps should rather be considered as fault zones, instead of individual faults. Their exact trace has been identified by comparing various published data with field results. Faults located at Turkey were mainly extracted from Şaroğlu et al. (1992), but also from several related papers (Genç et al., 2001; Gürer et al., 2001; Konak 2002; Flerit et al., 2003; Ocakoğlu et al., 2004, 2005; Altinok et al., 2005; Süzen et al., 2006)

### Lemnos Island

Lemnos is located very close to the North Aegean Trough, a large tectonic structure that represents the continuation of the major North Anatolian Fault Zone in the North Aegean territory. It is considered to be a highly active and seismically dangerous territory (Pavlidis et al., 1990; Tranos, 1998). The main active faults of Lemnos island are shown in Figure 2 and are the following (numbers in parentheses indicate their respective maximum expected earthquake magnitude).

- The *Mourtzouflos fault*, whose biggest part is offshore, intersects with the island on the Mourtzouflos cape at the NW part of the island (6.4).
- The *Kaspakas fault*. It prescribes the NW part of a longitudinal hill-chain and directly affects Myrina, the capital city of the island and Kaspakas (6.4).
- The *Kondia – Kotsina fault*. It concerns a complex structure striking NE-SW which crosses the island and affects the coastline (6.7).

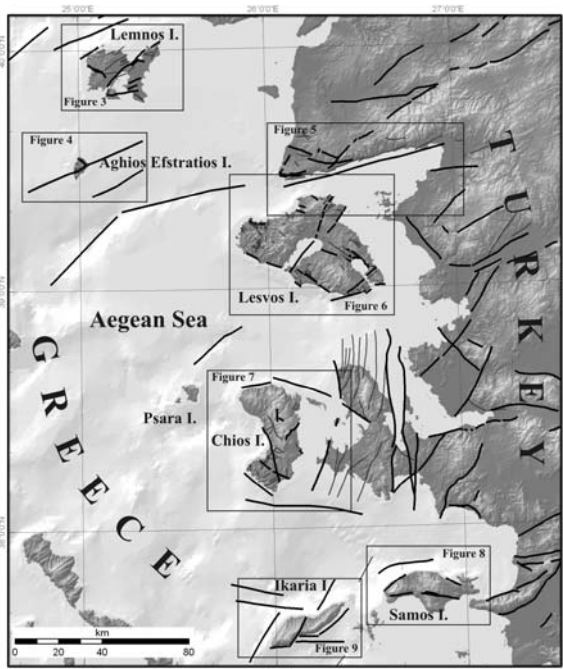


Figure 2. Overview map of the study area and its main faults. Thick lines indicate active or possibly active faults, while thin lines indicate the remaining mapped faults of the area. Numbered boxes correspond to more detailed maps that follow.

- The Fanos – Aghia Sophia fault, striking WSW-ENE and dips to the S. Despite its potential of 6.5 magnitude, it is considered less hazardous due to its position and dip direction.

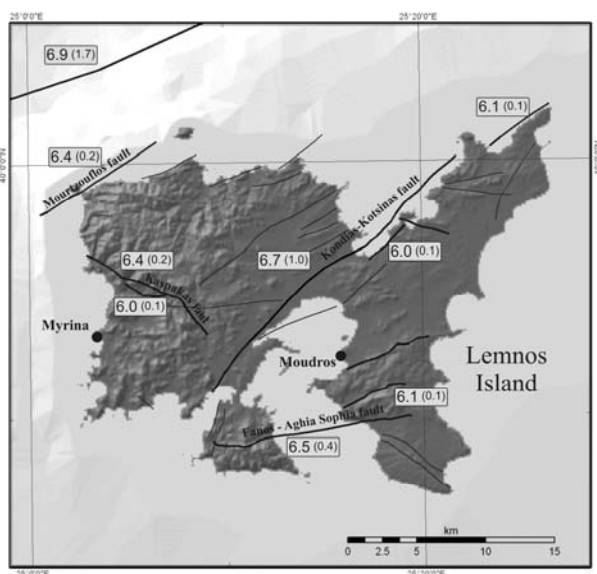


Figure 3. Lemnos map including the mapped faults. Numbers in boxes represent the expected earthquake magnitude and the expected displacement (m, in parenthesis) for potential fault activation.

#### Aghios Efstratios Island

Aghios Efstratios suffered serious damage during the great earthquake in 1968 ( $M_s$  7.1). The seismic fault bisects the island, strikes NE-SW and extends from both ends to the sea (Figure 4). A related antithetic fault striking NW-SE defines the northern coast of the island, having a seismic potential of 6.1 (Pavlidis and Tranos, 1991).

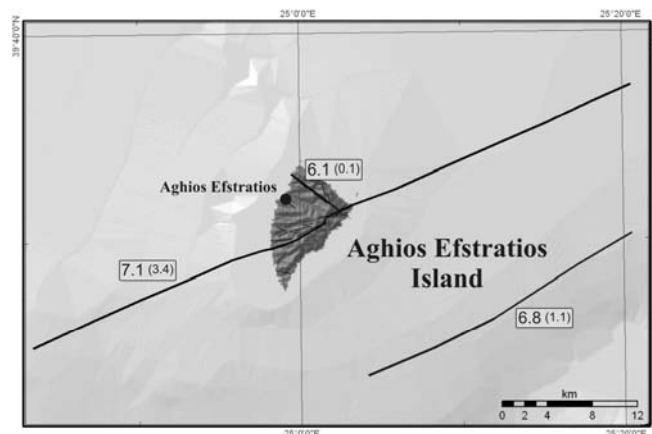


Figure 4. Aghios Efstratios fault map. Numbers indicate the expected earthquake magnitude and displacement (m, in parenthesis) in case of potential activation of specific faults. The main right-lateral fault that bisects the island was activated during the 1968 event.

#### Edremit area

The Edremit fault shows high seismic potential and it's one of the most hazardous seismic sources for the broader area (Figure 5). It defines the south coastline of Biga Peninsula (Turkey), right opposite of the northern shore of Lesvos, while its synthetic and antithetic faults are possible seismic sources of lower potential (Yilmaz and Karacik, 2001).

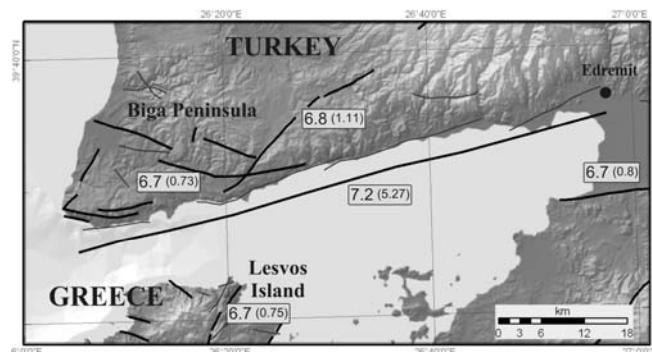


Figure 5. Edremit area fault map. Numbers indicate the expected earthquake magnitude and displacement (m, in parenthesis) in case of potential activation of specific faults.

#### Lesvos Island

Lesvos is the most populated island and the capital of the prefecture, so its seismic potential has special social-economic meaning not only regionally but also broadly. The most significant faults – potential seismic sources (Figure 6) are the following (Soulakellis et al., 2006):

- The right-lateral Aghia Paraskevi fault (Fytikas et al., 1999) was the one activated when the 1867 earthquake (6.8) occurred. It cuts off the central part of the island from N to S, while its visible length onshore has earthquake potential 6.7. This means that it continues to the sea, to the Kalloni gulf possibly, as it arises from the microseismic epicenters distribution.
- The NW-SE trending faults on the southern shore of the island play an important role in shaping the coastal morphology. According to the length, the maximum earthquake potential is 6.6-6.8. Their SW dip direction, however, reduces the seismic risk for the island's settlements.
- The faults in the Gulf of Gera comprise a zone that has particular importance because of the short distance from the town of Mytilene. The earthquake potential reaches

the value of 6.5.

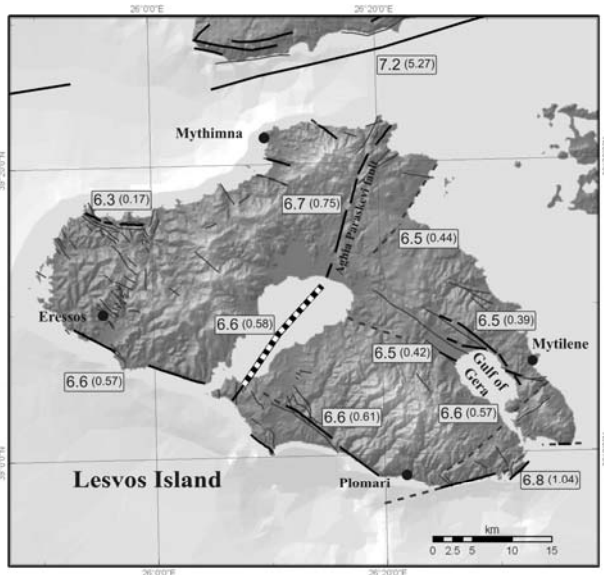


Figure 6. Lesvos Island fault map. Numbers indicate the expected earthquake magnitude and displacement (m, in parenthesis) in case of potential activation of specific faults.

#### Chios Island

Chios was the place where the deadliest seismic event in Greek history occurred (1881) with (Ms 6.5). Many faults cut through the island (Besenecker et al., 1971a, b), but for most of them there is no indication of recent activity. Several faults in the nearby Turkish coast are also susceptible for active deformation (Altinok et al., 2005, Ocakoğlu et al., 2005). The major active faults of the region are (Figure 7):

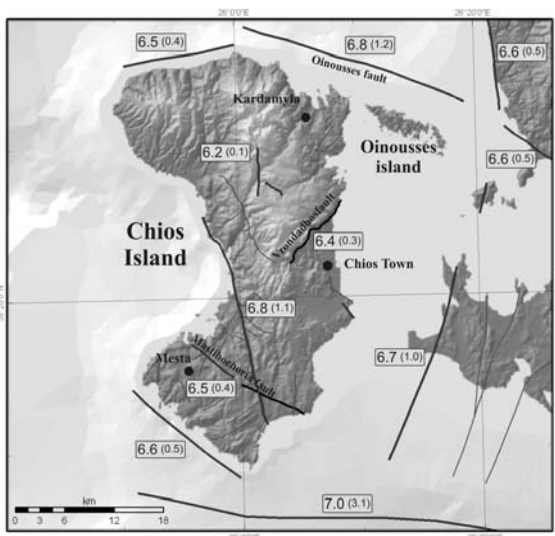


Figure 7. Chios Island fault map. Numbers indicate the expected earthquake magnitude and displacement (m, in parenthesis) in case of potential activation of specific faults.

- The Mastihochoria fault. It runs through the island from coast to coast striking NW-SE and is considered as the fault that generated the great 1881 earthquake whose highest intensity value was recorded in the territory of southern Chios. The earthquake potential is 6.5, although there is a chance of continuation towards the sea rising up the earthquake potential.
- The Vrontadhos fault is very near to the warren of Chios – Vrontadhos and constitutes an important seismic source. It consists of a series of smaller faults with a mean strike from NE to SW that affect the morphology.

Even though it is not that long (maximum potential 6.4), there are sufficient proofs of recent activity.

- The offshore fault of Oinousses and the offshore faults of northern and southern Chios coast (having potential 6.8, 6.5 and 6.6 respectively) are very possible seismic sources. The Oinousses fault however, is considered the causative fault of the great 1949 earthquake (Ms 6.7).

#### Samos Island

In Samos island major faults have shaped the plains at the southern part and the shoreline at the northern part (Figure 8). They are faults with clear neotectonic character and significant length (Mountrakis et al., 2003).

- The Pythagorion fault, striking WNW-ESE, is the prominent fault of the island having earthquake potential on the order of 6.6. Pythagorio village is mainly situated on the hanging-wall and partly on the fault trace, so this fault is essential for possible activation.
- The Vathy and Karlovasi faults (earthquake potential 6.3 and 6.5 respectively) define the linear shorelines. However, the dip direction (to the NE and NW respectively) decrease seismic hazard for occupied areas.
- There is a major offshore fault north of Samos with earthquake potential of 6.8 and great possibility of future seismic source.

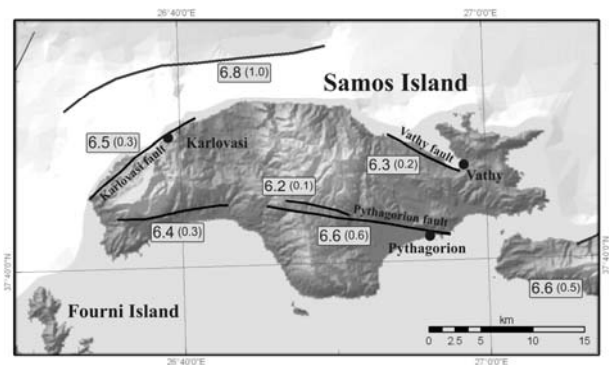


Figure 8. Samos Island fault map. Numbers indicate the expected earthquake magnitude and displacement (m, in parenthesis) in case of potential activation of specific faults.

#### Ikaria

There are not many onshore faults on Ikaria. There are many offshore faults in the broader area though (Figure 9):

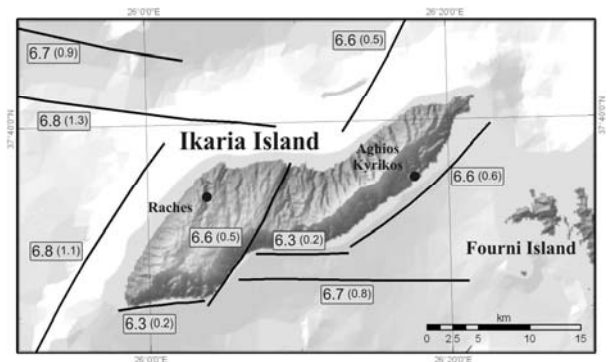


Figure 9. Ikaria Island fault map. Numbers indicate the expected earthquake magnitude and displacement (m, in parenthesis) in case of potential activation of specific faults.

- The major fault of Ikaria intersects the island almost at the middle, striking NE-SW, and having earthquake potential on the order of 6.6.

- The steep slopes at the southern coast of Ikaria are shaped and controlled by three faults, striking WSW-ENE and NE-SW and dipping to the south, and the seismic potential varies from 6.3 to 6.6.
- A number of probable seismic sources in the broader marine area of Ikaria – Fourni islands have seismic potential between 6.6 and 6.8, due to their location in respect to inhabited areas however, their hazard is lower.

## SEISMIC HAZARD ASSESSMENT

### Ground acceleration

Seismic hazard at a site is the expected value of intensity  $Y$  in this location, in a determined time space, with defined possibility of exceeding this value. The term seismic intensity can be related with macroseismic intensity  $I$ , or in value with one of the ground motion parameters (eg logarithm of ground acceleration  $A$ , velocity  $V$  or displacement  $D$ ). Various models have been used for seismic hazard evaluation. The extreme values method of Gumbel, for example, can be considered as a useful tool for calculating seismic hazard parameters. On the other hand, Knopoff and Kagan (1977) suggested that this method is probable to show problems in calculating the parameters of seismic hazard. This happens because methodology works well when we have seismic data for short time spaces (eg per 1 year), but this is feasible only for recent catalogues that were contacted by instrumental recordings. From the data we used it seems that this methodology cannot be applied to the present study. To overcome this incompatibility, we used the maximum likelihood method (Kijko and Sellevoll, 1989, 1992). Using this method we succeed to overcome the previous difficulty.

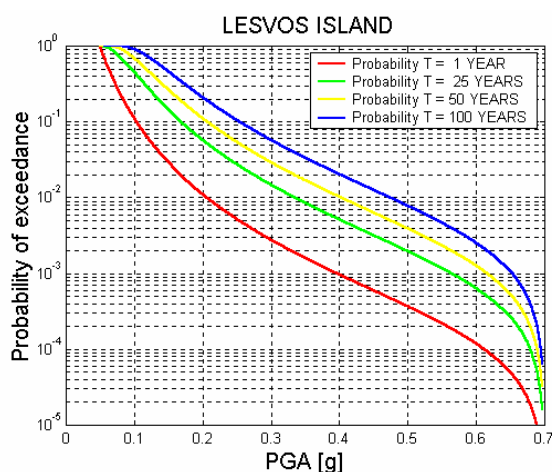


Figure 10. Probability that the given peak ground acceleration (PGA) values will not exceeded in 1, 25, 50 and 100 years at Lesvos island.

The Poisson model was used to determine earthquake hazard by Cornell (1968) and McGuire (1976). The algorithm of this model is described by the definition of the seismic zones, the seismic parameters (focal depth, seismic rate, maximum magnitude, b-parameters values, etc), and the relationship of strong ground motion absorbency. In this paper, instead of this model, the model of Kijko and Graham (1998) was used, which among other benefits it is also independent from seismic zone definition which in case of misjudging them, seismic hazard gets under- or overestimated.

Seismic hazard is defined by Lomnitz (1974) as the possibility of a "critical earthquake" occurrence during a specific period of time. This critical earthquake is called "design earthquake". The concept of the "design earthquake" was used for determining the "design acceleration" according to methodology that was developed by Kijko and Graham

(1998, 1999). This methodology concerns a scenario planning for earthquake occurrence in short distances from the study site and the seismic hazard that will follow.

Thus, according to the new relationship of absorbance for the region of Greece, as it was conducted from Skarlatoudis et al. (2003) concerning seismic ground acceleration, ground velocity and ground displacement, while seismic hazard was evaluated, for the island of Lesvos, using ground acceleration. It must be mentioned that all evaluations were conducted for intermediate soil types since the broader area of Lesvos Island was examined. We also declare that the attenuation law used takes into account the type of the faults. For the island of Lesvos the tectonic features illustrated in Figure 6 (of the present paper) considered. The diagram in Figure 10 shows the possibility of ground acceleration exceeding for the next  $t$  years (that is 1, 25, 50 and 100 years). Seismic ground acceleration unit is in  $g$  (where  $g$  is gravity acceleration).

The map in Figure 11 shows earthquake hazard (in  $g$ ) for the broader study area.

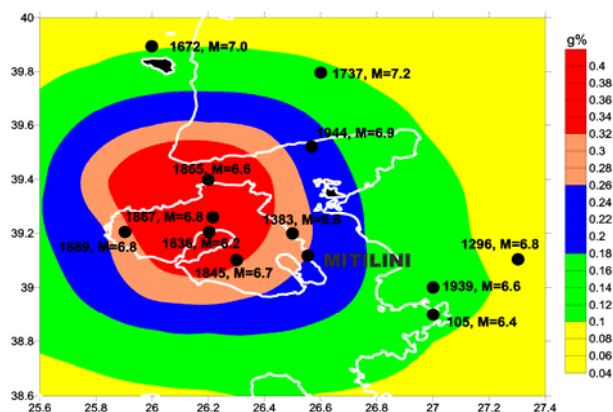


Figure 1. A seismic hazard map for the broader area of Lesvos island. The hazard is expressed in terms of PGA values for intermediate soil conditions with 10% probability of exceedance at least once in 50 years.

It is a smoothed map of seismic hazard of the region, expressed as ground acceleration. It is shown that the possibility of exceeding the value of ground acceleration at least once the next 50 years is 10%. The map also depicts the large earthquake epicenters that occurred in the broader area from 105 until 1944. According to all above, ground acceleration in the town of Mytilene is 0.23g, a value that is in accordance with G.A.R. (2000, zone II), while for the territory of the gulf of Kalloni and surrounding areas (Molyvos, etc.) ground acceleration is between 0.34 and 0.36g, so they should belong to the just next zone III of G.A.R.. This suggestion does not abrogate Antiseismic Regulation (G.A.R. 2000), however maps, diagrams and values produced in this paper can be used as a local map of seismic hazard. Earthquakes that occur in Greece cause damages when intensity exceeds VI or when ground acceleration is over 0.11g or when ground velocity exceeds 8cm/sec (Papazachos and Papazachou, 1997).

### Operating basis earthquake

The *operating basis earthquake (OBE)* is the earthquake for which a structure is designed to remain operational (Krinitsky, 2002). In simpler words, it is the earthquake that can occur during the lifetime of a construction. This time space is determined to 100 years (Kijko et al., 2002). According to this definition, an installation remains functional and damages be readily repairable from an earthquake not exceeding the OBE. The judgment needed to determine functioning and repair requirements makes the OBE an engineering decision. So it is very important for an engineer to have knowledge for this earthquake magnitude in order to

design a structure.

If it is assumed that the constructions in the region are crucial, then their lifetime period is 100 years. Figure 12 shows earthquake magnitudes versus time period, during a time space of 1-1000 years, for different values of the possibility of exceeding a specific magnitude value (1, 10, 37, 50, 63, and 90%). Repeating period for various magnitudes is defined by the 63% possibility of exceeding curve, when we assume the Poisson curve for the number of seismic events.

So, let's assume that the structures in the study area have lifetime 100 years. OBS takes into account the strongest expected earthquake for this period of time. According to Figure 12, the 63% possibility of exceeding curve suggests that an earthquake with 100 years repeating time period has magnitude  $M=6.3$ . Thus, this would be the operating basis earthquake and subsequently a construction should be designed in such way that it should be operational after an  $M=6.3$  earthquake occurs. It is interesting the fact that, according to Gutenberg-Richter method, the mean time period of recurrence of a  $M \geq 6.3$  earthquake for the same area is 103 years, which is close enough to the OBS's time period. Figure 13 shows the possibility that ground acceleration won't exceed during a given time a specific value in the study area.

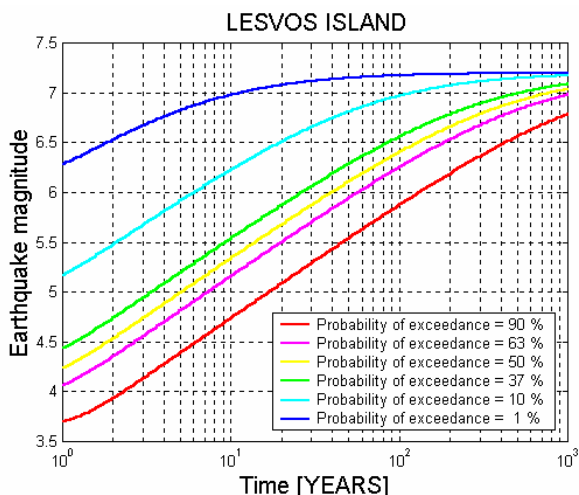


Figure 12. Magnitude expected to be exceeded as a function of time for different probability levels of exceedance

Combining the two figures (Figure 12 and Figure 13) it is possible to estimate the seismic acceleration value that will be produced by an earthquake with 100 years recurrence period and 6.3 magnitude, on the 63% possibility of exceeding curve, which is no other than OBE. If a construction is designed in the area, with 100 years recurrence period and possibility of exceeding 63%, then can easily be estimated that the value is 0.23 g. We get into the conclusion that construction planning in the region of the island of Lesbos should be according to the G.A.R. (2000) regulations.

#### Acknowledgements

This paper is the result of a project co-financed by Region of North Aegean and the General Secretariat for Research and Technology. Interactive fault maps of the area are available at <http://naseismic.geo.aegean.gr>.

#### REFERENCES

Altinok, Y., Alpar, B., Ozer, N. and Gazioglu, C. (2005), "1881 and 1949 earthquakes at the Chios-Cesme Strait (Aegean Sea) and their relation to tsunamis", *Natural Hazards and Earth System Sciences*, 5(5), pp. 717-725.

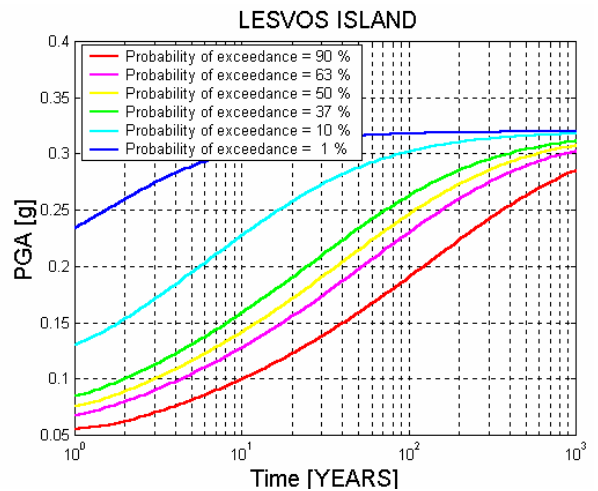


Figure 10. PGA (in g) expected to be exceeded as a function of time for different probability levels of exceedance

Besenecker, H., Durr, S., Herget, G., Kauffmann, G., Lutdke, G., Roth, W., and Tietze, K.W. (1971a). Geological map of Greece, Chios sheet (north part), 1:50,000 scale, Institute of Geological and Mineral Exploration, Athens.

Besenecker, H., Durr, S., Herget, G., Kauffmann, G., Lutdke, G., Roth, W., and Tietze, K.W. (1971b). Geological map of Greece, Chios sheet (south part), 1:50,000 scale, Institute of Geological and Mineral Exploration, Athens.

Cornell, C.A. (1968), "Engineering seismic risk analysis", *Bulletin of the Seismological Society of America*, 58, pp. 1583-1606.

Flerit, F., Armijo, R., King, G.C.P., Meyer, B. and Barka, A. (2003). Slip partitioning in the Sea of Marmara pull-apart determined from GPS velocity vectors. *Geophysical Journal International*, 154(1), pp. 1-7.

Fytikas M., Lombardi S., Papachristou M., Pavlides S., Zouros N. Soulakellis N. (1999), "Investigation of the 1867 lesbos (NE Aegean) earthquake fault pattern based on geochemical data", *Tectonophysics*, 308, pp. 249-261

Genč, C.S., Altunkaynak, S., Karacik, Z., Yazman, M. and Yilmaz, Y. (2001). The Çubukludağ graben, south of Izmir: Its tectonic significance in the Neogene geological evolution of the western Anatolia. *Geodinamica Acta*, 14(1-3), pp. 45-55.

Gürer, O.F., Bozcu, M., Yilmaz, K. And Yilmaz, Y. (2001). Neogene basin development around Söke- Kuşadası (western Anatolia) and its bearing on tectonic development of the Aegean region. *Geodinamica Acta*, 14(1-3), pp. 57-69.

Kijko, A. and Sellevoll, M.A. (1989), "Estimation of earthquake hazard parameters from incomplete data files. Part I. Utilization of extreme catalogs with different threshold magnitudes" *Bulletin of the Seismological Society of America*, 79, pp. 645-654.

Kijko, A. and Sellevoll, M.A. (1992), "Estimation of earthquake hazard parameters from incomplete data files. Part II. Incorporation of magnitude heterogeneity", *Bulletin of the Seismological Society of America*, 82, pp. 120-134.

Kijko, A. and Graham, G. (1998), "'Parametric-historic' procedure for probabilistic seismic hazard analysis. Part I. Estimation of maximum regional magnitude  $m_{max}$ ", *Pageoph*, 152, pp. 413-442.

Kijko, A. and Graham, G. (1999), "'Parametric-historic' procedure for probabilistic seismic hazard analysis. Part II.

Assessment of seismic hazard at specified site", *Pageoph*, 154, pp. 1-22.

Kijko, A., Retief, J.P. and Graham, G. (2002), "Seismic hazard assessment for Tulbagh, South Africa: Part I – Assessment of seismic hazard", *Natural Hazards*, 26, pp. 175-201.

Kiratzis, A. and Louvari, E. (2003), "Focal mechanisms of shallow earthquakes in the Aegean Sea and the surrounding lands determined by waveform modelling: A new database", *Journal of Geodynamics*, 36(1-2), pp. 251-274.

Konak, N. (2002). Geological Map of Turkey: Izmir, scale 1:500000 General Directorate of Mineral Research and Exploration

Knopoff, L. and Kagan, Y. (1977), "Analysis of the theory of extremes as applied to earthquake problem", *Journal of Geophysical Research*, 82, pp. 5647-5657.

Koukouvelas, I.K. and Aydin, A. (2002), "Fault structure and related basins of the North Aegean Sea and its surroundings", *Tectonics*, 21(5).

Kreemer, C., Chamot-Rooke, N. and Le Pichon, X. (2004), "Constraints on the evolution and vertical coherency of deformation in the Northern Aegean from a comparison of geodetic, geologic and seismologic data", *Earth and Planetary Science Letters*, 225(3-4), pp. 329-346.

Krinitzsky, E.L. (2002), "How to obtain earthquake ground motions for engineering design", *Engineering. Geology*, 65, pp. 1-16.

Lomnitz, C. (1974), *Global tectonics and earthquake risk*, Elsevier Scientific Publishing Company, 320 pp.

McGuire, R.K. (1976), "EQRISK: FORTRAN computer program for seismic risk analysis", *U.S.G.S. Open-File Report*, 76-79, 90 pp.

Mountrakis, D., Kiliyas, A., Vavliakis, E., Psilovikos, A. and Thomaidou, E. (2003). Neotectonic map of Samos Island (Aegean Sea, Greece): implication of Geographical Information Systems in the geological mapping, *4<sup>th</sup> European Congress on Regional Geoscientific Cartography and Information Systems, Bologna, Italy, Proceedings*, 1, pp. 11-13.

Ocakoğlu, N., Demirbağ, E. and Kuşçu, I. (2004). Neotectonic structures in the area offshore of Alaçati, Doğanbey and Kuşadası (western Turkey): Evidence of strike-slip faulting in the Aegean extensional province. *Tectonophysics*, 391(1-4 SPEC.ISS.), pp. 67-83.

Ocakoğlu, N., Demirbağ, E. and Kuşçu, I. (2005). Neotectonic structures in Izmir Gulf and surrounding regions (western Turkey): Evidences of strike-slip faulting with compression in the Aegean extensional regime. *Marine Geology*, 219(2-3), pp. 155-171.

Papanikolaou, D., Alexandri, M. and Nomikou, P. (2006), "Active faulting in the north Aegean basin", *Geological Society of America*, Special Paper 409, pp. 189-209.

Papazachos, C.B. and Kiratzis, A.A. (1996), "A detailed study of the active crustal deformation in the Aegean and surrounding area", *Tectonophysics*, 253(1-2), pp. 129-153.

Papazachos, B. and Papazachou, K. (1989). *Earthquakes of Greece*, Ziti Editions, Thessaloniki, Greece.

Papazachos, B. and Papazachou, K. (1997). *Earthquakes of Greece*, Ziti Editions (new edition), Thessaloniki, Greece.

Pavlidis, S. (2003). *Geology of Earthquakes*, University Studio Press, Thessaloniki, Greece.

Pavlidis, S. and Caputo, R. (2004). Magnitude versus faults' surface parameters: quantitative relationships from the Aegean Region, *Tectonophysics*, 380, pp. 159-188.

Pavlidis, S. and Tranos, M. (1991), "Structural characteristics of two strong earthquakes in the North Aegean: Ierissos (1932) and Agios Efstratios (1968)", *Journal of Structural Geology*, 13, pp. 205-214.

Pavlidis, S., Mountrakis, D., Kiliyas, A. and Tranos, M. (1990), "The role of strike-slip movements in the extensional area of Northern Aegean (Greece). A case of transtensional tectonics", *Annales Tectonicae*, IV n.2 (Special Issue), pp. 196-211.

Şaroğlu, F., Emre, Ömer, E. and Kuşçu I. (1992). Active fault map of Turkey (1:2,000,000 scale), *MTA Publishing Office, Ankara, Turkey*.

Skarlatoudis, A., Papazachos, C.B., Margaritis, B.N., Theodulidis, N., Papaioannou, Ch., Kalogeras, I., Scordilis, E.M. and Karakostas, V. (2003). Empirical peak ground motion predictive relations for shallow earthquakes in Greece, *Bull. Seismol. Soc. Am.*

Soulakellis, N., Novak, I., Zouros, N, Lowman, P. and Yates, J. (2006). "Fusing Landsat-5/TM imagery and shaded relief maps in tectonic and geomorphic mapping: Lesbos Island, Greece", *Photogrammetric Engineering and Remote Sensing*, 6, pp. 693-700.

Süzen, M.L., Toprak, V. and Rojay, B. (2006). High-altitude Plio-Quaternary fluvial deposits and their implication on the tilt of a horst, western Anatolia, Turkey. *Geomorphology*, 74(1-4), pp. 80-99.

Yilmaz, Y. and Karacik, Z. (2001). Geology of the northern side of the gulf of Edremit and its tectonic significance for the development of the Aegean grabens. *Geodinamica Acta*, 14(1-3), pp. 31-43.



## DEGRADATION OF PILE FOUNDATIONS' RESPONSE DUE TO CRACKING: ADVANCED AND SIMPLIFIED NUMERICAL APPROACH

Emilios COMODROMOS<sup>12</sup>, Mello PAPAPOPOULOU<sup>13</sup> and Ioannis RENTZEPERIS<sup>14</sup>

### ABSTRACT

*Capacity-based design of pile foundations tends to be obsolete among scientific community, whereas a new displacement-based design concept is considered more adequate, rendering the deflection of the piles, rather than their capacity, a crucial parameter for the design of a pile founded structure under lateral loading. With the aim of investigating the degradation of piles' response under lateral loads due to soil yielding as well as pile cracking, an advanced methodology allowing for cracking effects of concrete is presented, making use of 3-D nonlinear analysis including a subroutine simulating the cracking mechanism.*

<sup>12</sup>Associate Professor, University of Thessaly, Volos GR, ecomo@civ.uth.gr

<sup>13</sup> Ph.D. Student, University of Thessaly, Volos GR, ml@geostatiki.gr

<sup>14</sup> Ing. Dr., C.E.O. of Egnatia Odos S.A., Thessaloniki GR, irentze@egnatia.gr

In attempting to reduce the extreme calculation demands and to render the method value-engineering, even in the more complicated case of a pile group, a simplified approach is implemented, combining the structural beam theory, with the 3-D nonlinear analysis. Moreover, interesting conclusions have also been drawn regarding the dependence of both pile capacity and response on axial force magnitude. Finally the degradation of pile group response has also been estimated allowing for cracking and pile group interaction.

Keywords: pile cracking, pile group response

## INTRODUCTION

Capacity-based design of pile foundations tends to be obsolete among scientific community, whereas a new displacement-based design concept is considered more adequate, rendering the deflection of the piles, rather than their capacity, a crucial parameter for the design of a pile founded structure under lateral loading. For simplicity reasons, in most cases the performance-based design analysis is limited to superstructures, while the response of pile foundations on which a superstructure is based is not taken into account. This capacity-based design, still used in many cases, limits the soil-structure interaction mechanism to the determination of the bearing capacity of a pile group. One of the challenges that could render the performance-based design more reliable is to include the pile foundation response in the analysis. Therefore a new deformation-based design concept is considered more adequate for pile foundations.

Many procedures exist for estimating the response of single piles and pile groups under lateral loading, ranging from application of empirical relationships and simple closed-form solutions to sophisticated nonlinear numerical procedures. Until currently, simplified numerical approaches allowed for nonlinearities arising only from soil-pile interaction. The most representative and effective among such methods, used for determining the response of single piles under lateral loading, is the well-known 'p-y' method (Reese, 1977). On the basis of the experience gained from the research studies performed over the past decades, empirical relationships were proposed to estimate the reduction factors with respect to the stiffness of a group due to the interaction between the piles. Most of these methods disregard the effect of cracking on the response of reinforced concrete piles.

Advanced computational methods, powerful constitutive models and sophisticated numerical techniques have been developing rapidly the last three decades. Despite the development and continuous advances in numerical methods and powerful computer manufacturing, a 3-D nonlinear analysis remains computationally demanding in both geotechnical modeling and CPU-time. For this reason, a straightforward analysis of a superstructure, based on a pile foundation, cannot practically be applied, when soil nonlinearity and effects from pile group response cannot be ignored. However, hybrid methods or even the fine notion of the substructuring technique can facilitate this goal providing the ability of adopting a performance-based design approach for superstructures allowing for pile foundation response.

With the aim of investigating the degradation of piles' response under lateral loads due to soil yielding as well as pile cracking, an advanced methodology allowing for cracking effects of concrete is presented, making use of 3-D nonlinear analysis including a subroutine simulating the cracking mechanism. Appropriate design values for soil and pile were determined by back-figuring from experimental data. Furthermore, values for concrete strength and deformation modulus as well as information regarding cracking regions were revealed. It was found that initial bending

stiffness of pile can be used to estimate bending moment, provided that the calculated value is less than the cracking moment. Further loading increment initiates cracking in concrete and bending stiffness of the pile must be reduced, otherwise bending moments will be overestimated.

Finally, in attempting to reduce the extreme calculation demands and to render the method value-engineering, even in the more complicated case of a pile group, a simplified approach is implemented, combining the structural beam theory, with the 3-D nonlinear analysis. Structural software codes incorporating nonlinear moment-curvature response of concrete sections are able to accurately predict the response of either a single concrete pile or a pile group undergoing cracking, provided that nonlinearity of soil response and interaction between piles are taken into account.

## EXPERIMENTAL DATA

In order to investigate the response of a bridge pile foundation under horizontal loading, a static load test has been carried out. The subsoil at the specific location is given in Fig. 1. The horizontal load was applied using hydraulic jacks having a capacity of 2500 kN. Reaction was transferred to the pile located behind the tested pile at a distance of 3.0 m from the test pile, equivalent to a spacing of 3.75D. The test pile was instrumented with an inclinometer as well as 13 fiber-optic sensors (FOS) of very high resolution. On the upper part of the pile, the FOS (SA-1 to SA-5 and SB-1 to SB-5) were placed in pairs so that curvature could be deduced from the data of the lateral load test. Figure 2 illustrates the pile load test layout.

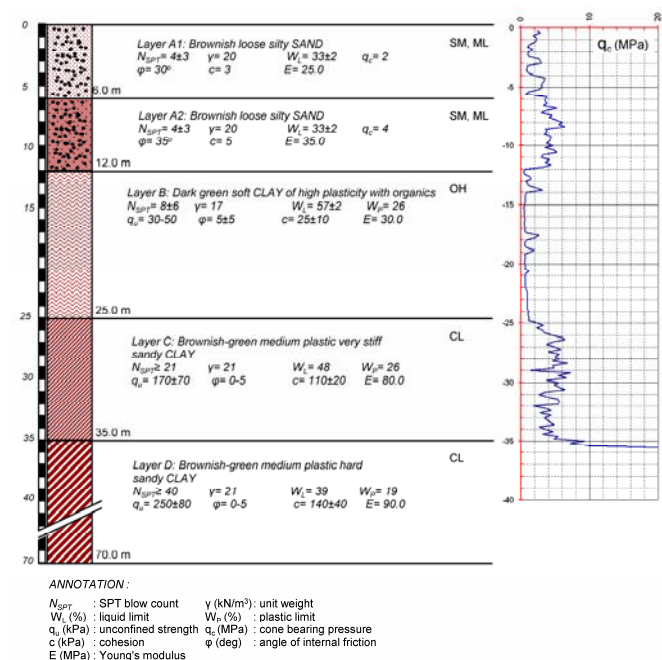


Figure 1. Geotechnical soil profile in the project area (after Comodromos et al., 2009a)

The loading sequence adopted in the pile test included an initial loading up to 0.40 MN in steps of 0.00, 0.10, 0.25, 0.30, 0.40, 0.20, 0.10 MN (cycle H1). Subsequently, the load was increased until the ultimate pile capacity was reached. More specifically, the second loading/unloading cycle (cycle H2) was applied with the following steps: 0.10, 0.20, 0.40, 0.47, 0.55, 0.40, 0.32, 0.20, 0.00 MN. Figure 3 shows the results of the loading test together with the load-displacement curve derived from the application of the 'p-y' method. It can be seen that the 'p-y' prediction, even less stiff, provides an acceptable prediction for loading less than 300 kN. From that level, the effect of cracking provokes significant reduction in the bending stiffness of the pile,

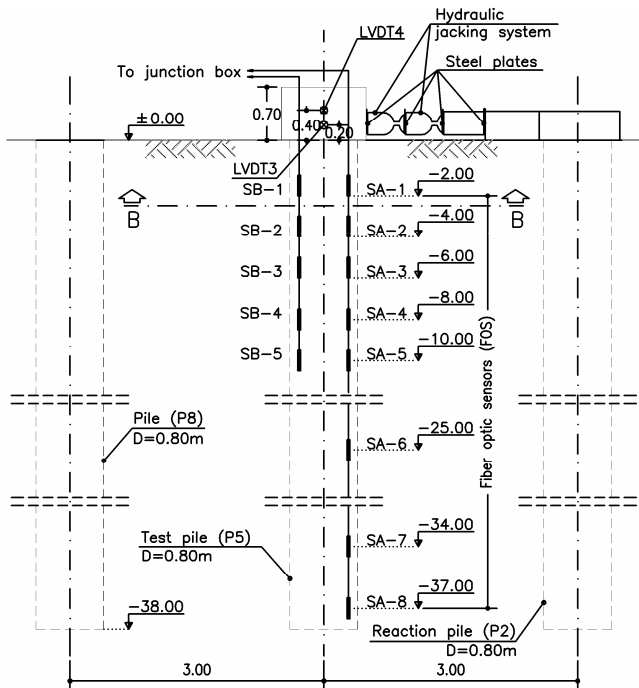


Figure 2. Pile test layout

rendering it less resistant. The applied 'p-y' method was not able to allow for concrete cracking and therefore a significant discrepancy is observed for higher values of loading. Further information on the experimental setup can be retrieved from Comodromos et al. (2009).

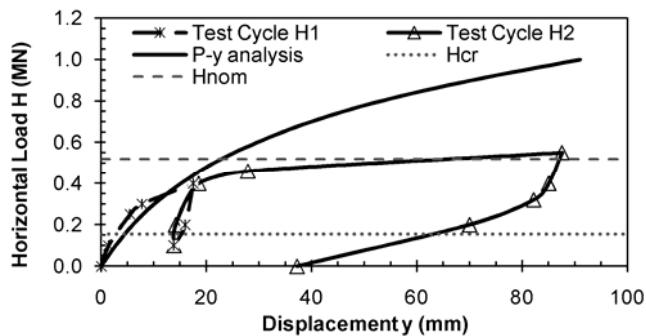


Figure 3. Pile test load-displacement curve together with that provided from the application of the 'p-y' method (after Comodromos et al., 2009b)

Figure 4 provides helpful information in explaining the reason of this divergence, by illustrating the strain development with loading, as recorded by FOS SA-2 (tension side) and SB-2 (compression side). Obviously, when no cracking occurs, the pile behaves as linear elastic body and therefore the strain at the FOS are of the same magnitude. On the contrary, when cracking occurs, the strain on the side under tension is higher than that on the side under compression, as illustrated in Fig. 4.

Consecutive increase of loading provokes enlargement of cracking area, demonstrated by larger difference between tensile and compressive strains. Evidently, at those levels of loading, the bending stiffness of the pile decreases, rendering the pile less resistant and the load-displacement response nonlinear. It is obvious from Figure 4 that at loading step H1-1 (0.10 MN), no cracking occurs since the tensile and compressive strains are the same. Loading step H1-2 (0.25 MN) provokes a partial but limited cracking as indicated by the curves of tensile and compressive strains of this step. At the end of loading step H1-3 (0.30 MN), the tensile strain is 2.5 times higher than the compressive one.

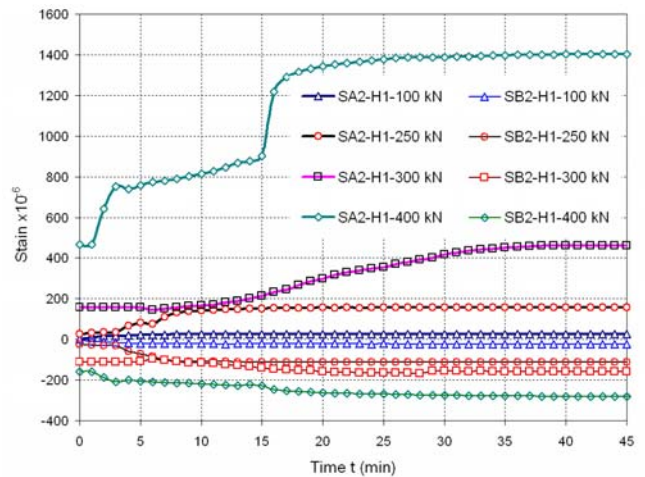


Figure 4. Evolution of tensile and compressive strains for loading steps of cycle H1

Further increase of loading to 0.40 MN (step H1-4) leads to a tensile strain that is 5.0 times higher than the compressive one, revealing the significant extent of cracking.

In attempting to investigate and reveal the effects of cracking on the response of the pile, a 3-D nonlinear analysis, simulating the pile test at the maximum possible accuracy was carried out.

### THREE-DIMENSIONAL NONLINEAR ANALYSIS

#### Numerical Simulation

The numerical simulation of the pile load test was performed using the finite difference code FLAC<sup>3D</sup> (Itasca, 2007). The existence of the pile in front of the tested pile at a distance of 3.0 m affects its response by leading to an overestimation of the pile head stiffness and the ultimate resistance as well, since it is located within the region of passive resistance of the soil. For this reason, the pile test back-analysis included all the three piles presented in Figure 2. A very fine mesh that enabled the reinforcement steel bars, simulated by cable elements, to be placed at their exact location was proposed. Figure 5 illustrates the finite difference mesh consisting of 87332 elements, 87424 nodes, 342 cable elements and 351 structural nodes. The elastic perfectly plastic Tresca constitutive model was used to simulate the behavior of clayey layers, whereas the elastic perfectly-plastic Mohr-Coulomb constitutive model was used to simulate the behavior of the silty and sandy layers. The values of soil properties as defined through the back-analysis iterative process are given in Table 1. The Young's modulus of concrete and steel was taken equal to  $E_c = 29$  GPa and  $E_s = 200$  GPa according to Eurocode EN1992 1-1 2001. The behavior of concrete was considered as linear elastic for compressive stresses or for tensile stresses less than the tensile strength. In case the latter was exceeded, which means a crack formation, the tensile strength was set equal to zero and the tensile stress was released and redistributed to the neighboring elements. In addition, the modulus of elasticity in the direction perpendicular to the crack formation was reduced to zero (Cedolin et al. 1982). Linear elasticity was considered for the reinforcement steel bars simulated by one-dimensional elements. The bond between the steel bars and the concrete was taken equal to the concrete tensile strength according to Eurocode 2.

Due to the fact that soil has a limited capacity in sustaining tension, interface elements were introduced to allow pile separation from the surrounding soil. With the value of 10 GPa/m that has been taken for both normal and shear interface stiffness ( $k_n$  and  $k_s$ , respectively) as explained by Comodromos and Pitilakis (2005), no additional displace-

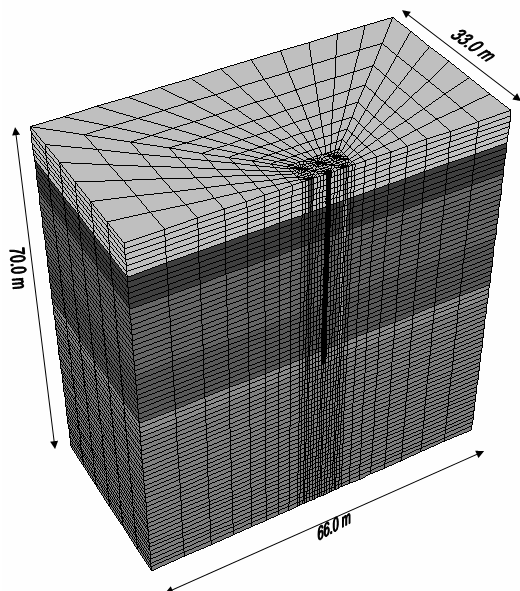


Figure 5. Finite difference mesh for simulating the pile test

ments were attributed to the pile due to the deformation of the springs representing the interface. Further details on the numerical model can be derived from Comodromos et al. (2009).

It should be finally clarified that the applied numerical approach corresponds to 'smeared' cracking models. It is reliable for partially cracked sections, while the use of very small elements may improve the results at the expense of further computational demands, (Cedolin et al., 1982). Discrete cracking models (Ngo and Scordelis, 1967), on the other hand, are more adequate for including discrete propagation of cracks, but are not convenient for predefining crack patterns requirement; therefore, the method is unpopular and its applicability very rare.

Table 1. Geotechnical data used in the 3-D analysis

STRATA	A1	A2	B	C	D
Bottom Elevation (m)	-6.0	-12.0	-25.0	-35.0	-70.0
Bulk Modulus $K$ (MPa)	20.8	38.9	33.3	266.7	300.0
Shear Modulus $G$ (MPa)	9.6	12.9	11.1	27.6	31.0
Angle of Friction $\phi$ (deg)	30.0	33.0	5.0	---	---
Dilation Angle $\psi$ (deg)	0.0	0.0	0.0	---	---
Cohesion $c$ (kPa)	3.0	5.0	25.0	---	---
Undrained Shear Strength $S_u$ (kPa)	---	---	---	110.0	140.0
Unit weight $\gamma$ (kN/m <sup>3</sup> )	20.0	20.0	17.0	21.0	21.0
Friction angle at the interface $\phi_i$ (deg)	30.0	33.0	3.0	---	---
Adhesion along the interface $c_a$ (kPa)	3.0	5.0	15.0	45.0	65.0

When applied loads are high enough to produce concrete cracking, the foundation response is significantly affected by undergoing substantial decrease in pile stiffness ( $E_p I_p$ ). Concrete tensile strength is the determinant factor for the development of cracking. However, its value is indirectly estimated based on compression strength and empirical relationships (Eurocode 2 2001; ACI 1995). More specifically, Eurocode 2 proposes the relationship given in Equation 1 for estimating the mean tensile strength of concrete  $f_{ctm}$ , while the tensile strength  $f_{ct}$  is assumed to vary between the limits of 0.70 and 1.30 of  $f_{ctm}$ , depending on the specific conditions of the problem:

$$f_{ctm} = 0.30 f_{ck}^{2/3} \quad (1)$$

where  $f_{ck}$  stands for the compressive strength of the concrete (20 MPa for grade C20/25).

On the other hand, ACI (1995) proposes Equation 2 for estimating the tensile strength of concrete:

$$f_{ct} = 2 \sqrt{f_{ck}} \quad (2)$$

where  $f_{ck}$  and  $f_{ct}$  are expressed in kg/cm<sup>2</sup>.

The application of the above relationships provide a range of 1.54 to 2.86 MPa (Eurocode ENV1997 1-1 2001) and 2.82 MPa (ACI). Given the uncertainties in estimating the appropriate tensile strength, a conservative tensile strength value is usually applied. Such an approach might significantly affect the prediction for pile response, particularly in the case of pile foundations in soils of limited shear strength. In such cases, pile load tests can play an important role in value engineering and design optimization. A full-scale test may contribute to the elimination of practically all the uncertainties arising from soil and reinforced concrete nonlinear behaviors, which govern the mechanism of pile-soil interaction.

## Numerical Results

The most appropriate value for the tensile strength of concrete was defined after a parametric numerical analysis and was found equal to 2.0 MPa. This value is slightly less than the values proposed by Eurocode and ACI 318-05 (2005), but this can be explained by the fact that when the test was carried out, the concrete was aged 21 days. The predicted load-displacement curve is presented in Fig. 6 together with the test results, demonstrating remarkable agreement. It should be underlined at this point that both relationships include the effect from the pile P8 (the pile in front of the tested pile) and that of the reaction pile P2. To establish the response of the single pile and to quantify the effect arising from the existence of piles in front and behind the tested pile, a numerical analysis was performed using the same numerical model, with the exception of the aforementioned piles. The numerically established response of the single pile is also illustrated in Fig. 6. It can be seen that up to an applied load of 0.30 MN, the curves corresponding to the response of the tested and the single pile coincide. This should be attributed to the fact that for applied loads less than 0.30 MN, the pile P8 remains out of the soil-resisting zones developed in front of the tested pile. For higher loads, the displacement field in front of the pile extends to the pile P8, which now resists together with the surrounding soil. The effect on both pile head stiffness and ultimate resistance remains constant as loading increases.

As the majority of pile foundations are rather fixed-head and their mode of deformation is clearly different from that of the free-head pile condition corresponding to the tested pile, an additional analysis of a single fixed-head pile was carried out. As anticipated, the response of the fixed-head pile (Fig. 6) is considerably more resistant and stiff, which should be attributed to two factors. The first and well known is the pile deformation mode, which in the case of the free-head pile exhibits higher displacements for the same load due to higher slope level. The second and more influential factor, in the particular case, is the effect of cracking. For the same load, the deformation mode of the free-head pile exhibits higher curvature, resulting to an earlier development of cracking and therefore a greater reduction in bending stiffness than in the case of fixed-head pile. As a result, the response of the free-head pile is much more affected than that of the fixed-head pile. Both effects are illustrated in Fig. 7, where exaggerated deformed modes of the free- and fixed-head piles are given. It also indicates that the effect of cracking is limited to the upper part of the pile for the fixed-head pile, whereas in the case

of the free-head pile the effect is more aggravated and extended to a deeper level.

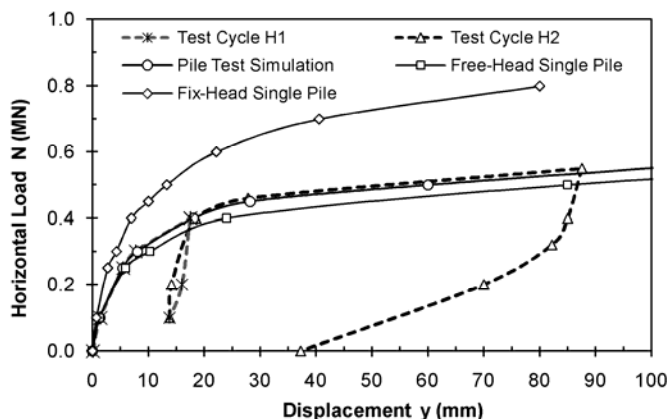


Figure 6. Measured and numerically predicted load-displacement curves for the pile test; predicted response for free and fixed-head single pile (after Comodromos et al., 2009b)

Curvature estimated from double differentiation of horizontal displacement retrieved from an inclinometer is averaged between the sequential points of records. Therefore, measurements should be taken at very close intervals in the area of cracking where the values of curvatures are increasing rapidly. Furthermore, the displacement field produced from inclinometer data should be fitted using polynomial splines (Georgiades et al. 1992; Smethurst and Powrie 2007). Figure 8 illustrates the horizontal displacement field, retrieved from the inclinometer and fitted using a series of five-order polynomial splines, together with the displacements predicted from the 3-D analysis. The curves are in acceptable agreement. The relationships corresponding to inclinometer exhibit lower curvature values than those corresponding to the 3-D analysis. This should be attributed, among others, to the fact that the thickness of the elements in the 3-D analysis was 0.25 m, while measurements from the inclinometer were taken at an interval of 1.0 m. Obviously, averaging has larger effect when the interval is prolonged, smoothing the values of curvature. The first conclusion to be drawn, regarding the element size in a numerical analysis, is that small elements are required when flexurally dominant problems are to be examined. This is also valid for the measurement intervals of the inclinometers.

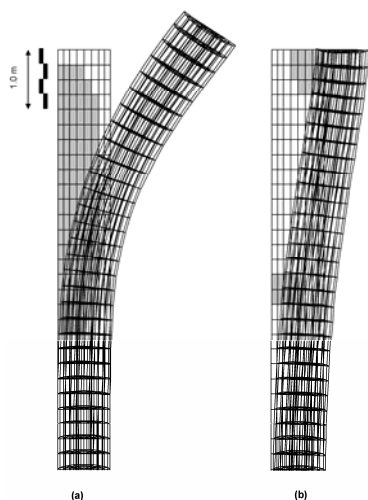


Figure 7. Comparison of cracked region and deformed mode of free-head (a) and fixed head (b) pile as predicted by FLAC<sup>3D</sup> for lateral loading of 0.4 MN (displacement exaggerated by a factor of 100) (after Comodromos et al., 2009b)

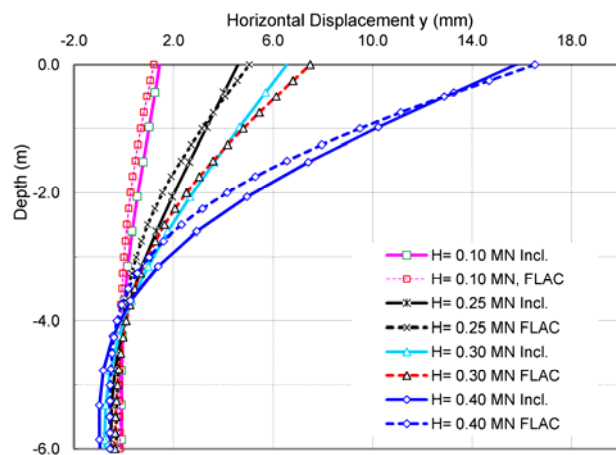


Figure 8. Comparison of horizontal displacements retrieved from inclinometer to those predicted by FLAC<sup>3D</sup>

## EVALUATION OF CRACKING EFFECTS USING THE STRUCTURAL BEAM THEORY

### Formulation

According to the Euler's beam theory, once the pile deflection function is determined, the bending moment  $M$  can easily be obtained using the following equation:

$$M(z) = E_p I_p \varphi = E_p I_p \frac{d^2 y(z)}{dz^2} \quad (3)$$

where  $M$  = bending moment;  $E_p$  = effective pile elastic modulus;  $I_p$  = effective pile moment of inertia; and  $y$  = horizontal pile displacement.

Despite the fact that the above formulae are valid in the case of uncracked behavior, for simplification, it is widely used in field measurements and back-analysis process even when partial cracking occurs (Smethurst & Powrie 2007). The effect of cracking is then introduced by empirically reducing the bending stiffness. A more accurate procedure in estimating the bending moment is given by Equation 4:

$$M = E_p I_p \varphi = (E_c I_c + E_s I_s) \varphi \quad (4)$$

Figure 10 illustrates the variation of bending stiffness ( $E_p I_p$ ) with cracking level for the specific section and reinforcement of the tested pile. A very interesting approach for estimating the bending stiffness of the pile and the bending moment of cracked sections as a function of the curvature is provided by the moment-curvature relationship derived from the beam theory (Park & Paulay 1975). This model has been incorporated in many structural software codes that can provide the moment-curvature response for a given reinforced concrete section, consisting of known grades of concrete and steel. The structural code Sofistik (2003) which allows for cracking effects has been used. Piles have been simulated using one-dimensional beam elements. The stress-strain relationships for grade C20/25 concrete and grade S500 steel are given in Figure 11 according to Eurocode 2.

To determine the pile response, a serviceability analysis was considered and therefore no partial factors of safety have been applied. The tensile strength of concrete ( $f_{ct} = 2.0$  MPa) has been also taken into account.

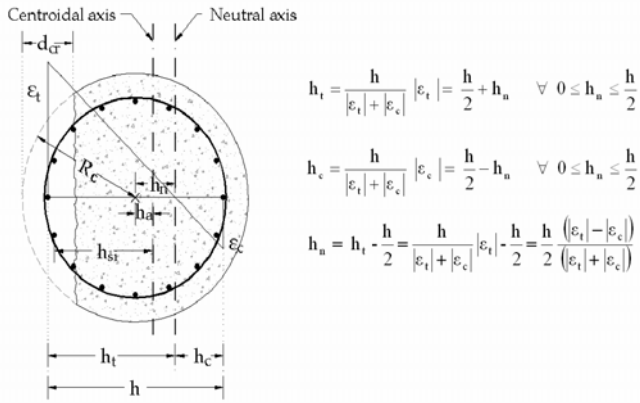


Figure 9. Formulation and definition for a circular reinforced concrete section under flexural deformation (after Comodromos et al., 2009b)

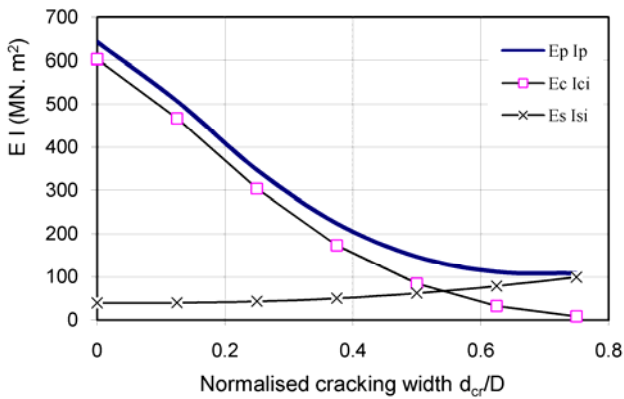


Figure 10. Variation of pile bending stiffness with normalized cracking width

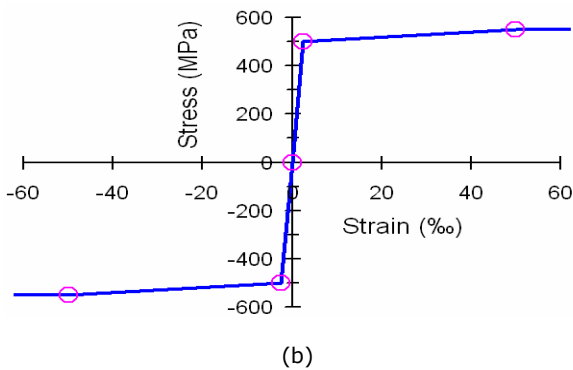
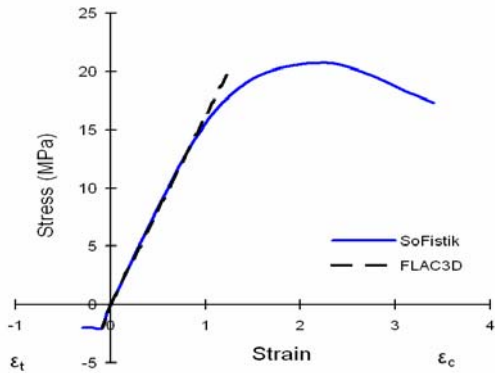


Figure 11. Concrete (a) and steel (b) stress-strain relationship according to Eurocode2

## Results from One-Dimensional Nonlinear Numerical Analysis

Figure 12 shows the variation of bending stiffness of the pile with bending moment for the tested pile (axial load  $N = 0.0$  MN) using the SOFISTIK (2003) computer code. Bearing in mind that the piles of a bridge foundation carry axial load at the same time and that the existence of a compressive force leads to higher values of ultimate bending moment, the same figure illustrates the bending stiffness degradation in the cases where piles carry compressive loads of 0.5 and 2.0 MN. The shape of the curves is similar to that derived by Reese and Van Impe (2001). The rightmost portion of the curves shows a small part where the bending stiffness remains constant. This part corresponds to linear elasticity where no cracking occurs, while the point at the edge of this part indicates the cracking moment  $M_{cr}$  corresponding to the maximum tensile stress that the concrete

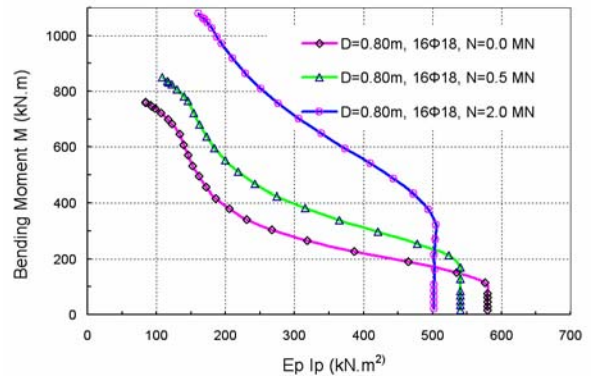


Figure 12. Variation of bending stiffness with bending moment for the tested pile and for axial loads of 0.0, 0.5 and 2.0 MN

accommodated. Figure 13 illustrates bending moment distribution along the pile using FLAC<sup>3D</sup> and Sofistik in the case of horizontal loading of  $H = 0.1$  MN and  $H = 0.4$  MN. Both methods allow for cracking and the results are in close agreement. When neglecting the cracking effects, taking into account the initial value of bending stiffness of the pile, bending moment is significantly over predicted (solid line with diamonds). In this case, the maximum predicted values are of the order of 1.5 MN.m, which is almost twice the ultimate bending moment capacity of the pile.

Figure 14 summarizes the experimental and numerical results. It can be seen that the 3-D nonlinear analysis allowing for cracking, represented by the dashed line with no mark symbols, is the most effective, providing almost identical

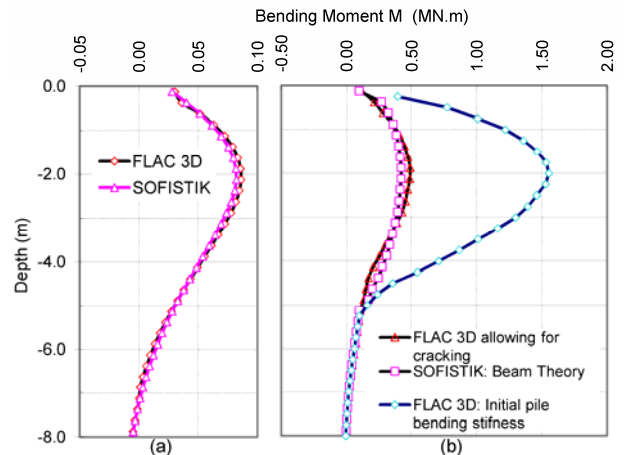


Figure 13. Comparison of bending moment predicted by FLAC<sup>3D</sup> and Sofistik,  $H=0.1$  MN (a) and FLAC<sup>3D</sup> and Sofistik and initial pile bending stiffness,  $H = 0.4$  MN (b).

tical response to that of the test. The high accuracy of this method renders its implementation very attractive, but when taking into account the extreme demands in computation time and capacity it can be seen that its applicability is mainly limited to research purposes. On the contrary, the 'p-y' method in which cracking effects are neglected is the most simplified providing the results instantly. It is not able, however, to follow the response of the pile when cracking occurs and therefore a significant discrepancy is observed from the point of cracking initiation. When combining the 'p-y' method for simulating the soil reaction with one-dimensional nonlinear analysis allowing for cracking, an acceptable response (dashed line with circle symbols) can be attained. The advantages of the first two methods (satisfactory either in accuracy or time demands) are combined in that last approach rendering the method quite attractive.

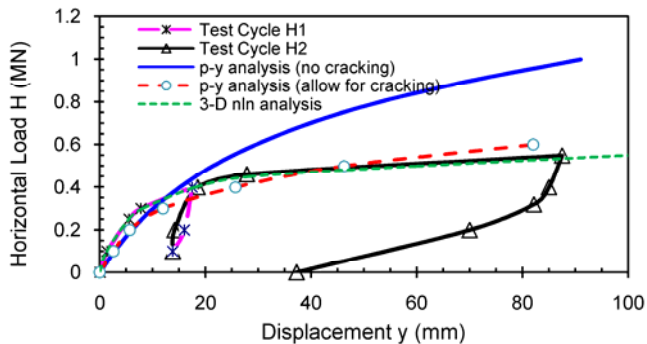


Figure 14. Summary of experimental and numerically established pile response

Even if a 3-D nonlinear analysis to estimate the post-cracking response of a pile may be applied in the case of a single pile, it is evident that it is not feasible in the case of a pile group. On the contrary, the approximation by a nonlinear analysis, in which one-dimensional beam elements allowing for cracking are used to simulate piles and 'p-y' curves are applied for simulating the soil reaction, can easily be implemented. The effect of the interaction between the piles can be introduced by using appropriate guidelines or research results. Figure 15 presents the response prediction of a fixed head single pile (continuous regular line). To estimate the response of a 3 x 3 group in a spacing of 3.0D, a soil reaction reduction factor  $R = 0.25$  can be applied according to CFEM (1992) and NAVFAC DM-7.2 (1982). The response of the group can then be estimated and is given by the continuous bold line. In case of further accuracy, in which the response of the characteristic piles of the group is required, the results of specific research can be used. Based on the results of Comodromos and Pitilakis (2005) in the case of a fixed head 3 x 3 pile group, the corner pile carries the 115% of the mean load while the central pile carries the 70% of the mean load. With these assumptions the response of these characteristic piles can be evaluated and are also displayed in Figure 15.

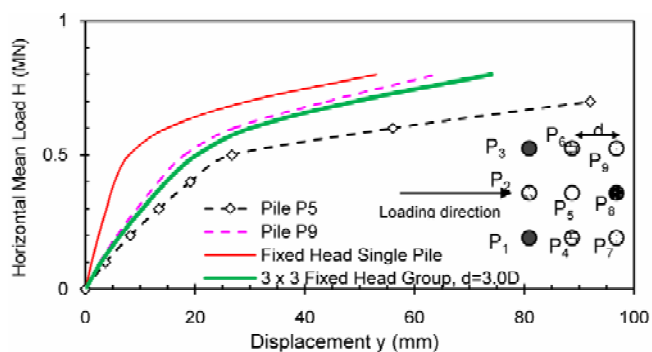


Figure 15. Response prediction for pile group and characteristic piles

## CONCLUSIONS

Capacity-based design of pile foundations tends to be obsolete among scientific community, whereas a new displacement-based design concept is considered more adequate, rendering the deflection of the piles, rather than their capacity, a crucial parameter for the design of a pile founded structure under lateral loading. A methodology allowing for cracking effects of concrete on the response of laterally loaded piles has been presented. The proposed method makes use of 3-D nonlinear analysis including a subroutine analysis, simulating the cracking mechanism and development. Experimental data are used to adjust concrete and soil values for deformation and shear strength parameters. It was found that initial bending stiffness of pile can be used to estimate bending moment provided that the calculated value is less than the cracking moment,  $M_{cr}$ . Further loading increment initiates cracking in concrete and bending stiffness of the pile must be reduced, otherwise pile deformations will be underestimated and bending moments overestimated.

In attempting to reduce the extreme calculation demands and to render the method value-engineering, the structural beam theory was combined with the 3-D nonlinear analysis. It has been demonstrated that this combination provides prediction accuracy within acceptable limits and at the same time contributes to the reduction of computational demands. Moreover, the combination of the 'p-y' method for simulating the soil reaction with one-dimensional nonlinear analysis allowing for cracking provides also satisfactory results. Bearing in mind that the application of a 3-D nonlinear analysis allowing for cracking effects is not feasible, the approach of the nonlinear one-dimensional analysis combined with the widely used 'p-y' method is capable of providing satisfactory results. In that case the interaction between the piles can be introduced using appropriate guidelines or research results.

## REFERENCES

- American Concrete Institute (2005) ACI building code requirements for structural concrete and commentary, ACI: 318-05. Detroit.
- Canadian Geotechnical Society (1992). Canadian foundation engineering manual, Vancouver, B.C., Canada.
- Cedolin L, Darwin D, Ingrassia AR, Pecknold EA and Schnobrich W C (1982) "Concrete cracking." *Chap 4 in State of the art report on Finite element analysis of reinforced concrete*, ASCE, N.Y.
- Comodromos EM and Pitilakis KD (2005) "Response evaluation of horizontally loaded fixed-head pile groups using 3-D nonlinear analysis", *Int. J. Numer. Analyt. Meth. Geomech.* 29(6): 597-625
- Comodromos EM, Papadopoulou MC, Rentzeperis IK (2009a) 'Pile Foundation Analysis and Design using Experimental Data and 3-D Numerical Analysis', *Computers and Geotechnics*, 36(5): 819-836
- Comodromos EM, Papadopoulou MC & Rentzeperis IK (2009b) "The effect of cracking on the response of pile test under horizontal loading" *Journal of Geotechnical and Geoenvironmental Engineering*, DOI: 10.1061/(ASCE)GT.1943-5606.0000069
- Eurocode 2 (2001) Design of concrete structures - Part 1: General rules and rules for buildings together with the United Kingdom National Application Document. ENV 1992-1-1, London
- Eurocode 7 (2003) Geotechnical design - Part 1: General rules together with the United Kingdom National Application Document. DD ENV 1997-1. London.

Foundations and earth structures (1982) Design manual 7.2 NAVFAC DM-7.2. Department of the Navy, Naval Facilities Engineering Command.

Georgiadis M, Anagnostopoulos C and Saflekou S (1992) "Centrifugal testing of laterally loaded piles in sand" *Can. Geotech. J.*, 29(2): 208-216.

Itasca Consulting Group (2007) FLAC<sup>3D</sup>, Fast Lagrangian analysis of continua user's and theory manuals, Version 3.1. Minneapolis

Ngo D and Scordelis AC (1967) "Finite element analysis of reinforced concrete beams", *J. Amer. Concr.Inst.*, 64(3): 152-163.

Park R and Paulay T (1975) Reinforced concrete structures, John Wiley & Sons Ltd, New York.

Reese LC (1977) "Laterally loaded piles: Program documentation", *J. Geotechn. Engng Div.*, 103: 287-305

Reese LC and Van Impe WF (2001) Single piles and pile groups under lateral loading, Balkema, Rotterdam

Sofistik AG (2003) Sofistik: Finite element code and user's manuals, Munich

Smethurst JA and Powrie W (2007) "Monitoring and analysis of the bending behaviour of discrete piles used to stabilize a railway embankment", *Géotechnique* 57(8): 663-677



## DYNAMIC SHEAR MODULUS AND DAMPING RATIO CURVES OF SAND/RUBBER MIXTURES

Anastasios ANASTASIADIS<sup>1</sup>, Kiriazis PITILAKIS<sup>2</sup> and Kostas SENETAKIS<sup>3</sup>

### ABSTRACT

*Experimental and theoretical studies during the last two decades have striven to evaluate the use of granulated rubber as a lightweight material in civil engineering applications. Several geotechnical structures using soil/rubber mixtures or clean granulated rubber especially in USA and Western Europe proved the efficiency of this solution. Most studies have focused on the monotonic behavior as well as the compressibility and permeability characteristics of granulated tire rubber and soil/rubber mixtures. Only few studies have examined the cyclic behavior and dynamic characteristics of granulated tire rubber and soil/rubber mixtures in order to examine the performance of these applications in earthquake loading. The present work is an effort to study the dynamic characteristics of soil/rubber mixtures using a fixed-free torsional resonant column device. Specimens were prepared using different percentages of granulated tire rubber and a medium poor graded sand. The experimental results at low dynamic shearing strains indicate a significant reduction of shear stiffness and increase of damping ratio as the percentage of rubber in-*

*creases. High amplitude resonant column tests indicate that the normalized shear modulus and damping ratio curves increase the "flexibility" and damping as the percentage of rubber increases. The effect of mean confining pressure and moisture content on the dynamic properties of sand/rubber mixtures has a similar trend like on clean sands.*

Keywords: granulated tire rubber, resonant column, shear modulus, damping ratio

### INTRODUCTION

The growing disposition of end-of-life tyres on stockpiles has added on the environmental diminution especially in developing countries. Lee et al. (1999) report that 250 million scrap tires are discarded every year in landfills and illegal tire dumps in U.S.A., while Foose et al. (1996), based on statistical data, report that the estimated amount of disposed scrap tyres in U.S.A. is about 5 billion. Edesca (2006) reports that 2 million scrap tires are discarded every year in Europe.

In recent years, many developing and developed countries including Greece, have legislated laws concerning the limitation of the disposed tyres and the encouragement of recycling and re-use of tyres in variant applications. The main utilization of disposed tyres until recently was focused on industrial applications. However, the interesting physical and mechanical properties of granulated tire shreds (low density, high elasticity, high drainage capacity, high damping capacity, relatively high deformability of rubber solids), has encouraged the use of this material in civil engineering applications, especially in geo-structures as construction material and landfills as drainage layer (Edil, 2004, Edesca, 2006).

Experimental investigation on the compaction characteristics (Humphrey and Manion, 1992, Bosscher et al., 1993, Edil and Bosscher, 1992 and 1994, Edesca, 2006), compressibility characteristics (Beatty, 1981, Edil and Bosscher, 1992 and 1994, Edesca, 2006) and mechanical properties (Masad et al., 1996, Foose et al., 1996, Lee et al., 1999, Zornberg et al., 2004, Edesca, 2006) of clear granulated rubber and soil/rubber mixtures indicate satisfactory behaviour and potentially efficient use of recycled tire shreds in construction projects as a lightweight material.

Granulated tire rubber exhibits temperature-dependent physical and mechanical properties and high compressibility. However volumetric compressibility of clear rubber and soil/rubber mixtures is relatively low due to the small compressibility of rubber solids (Beatty, 1981). Edil and Bosscher (1994) report a significant reduction of soil/rubber specimens compression for percentages of sand above 40% by mixture volume, while Zornberg et al. (2004) report a critical percentage of rubber which separate the mixture behavior from sand-like (where dilatant behavior is observed) to rubber like (where contractive behavior is observed).

Although the static behavior of rubber and sand/rubber mixtures has been extensively examined during the last two decades, only few studies have focused on the cyclic behavior and dynamic characteristics of granulated rubber and soil/rubber mixtures. Feng and Sutter (2000) performing low to high amplitude resonant column tests on a uniform sand with different percentages of granulated tire rubber, report a significant reduction of shear stiffness and increment of damping ratio as the percentage of rubber increases. Pamukcu and Akbulut (2006) performing low amplitude resonant column tests on sand/rubber mixtures, indicate that up to an optimum percentage of granulated rubber by sand/rubber weight both low strain shear modulus and damping ratio increases.

In the present study, low to high amplitude torsional resonant column tests were performed on dry and saturated

<sup>1</sup> Lecturer, Civil Engineering Department, Aristotle University of Thessaloniki, [anas@civil.auth.gr](mailto:anas@civil.auth.gr)

<sup>2</sup> Professor, Civil Engineering Department, Aristotle University of Thessaloniki, [kpitilak@civil.auth.gr](mailto:kpitilak@civil.auth.gr)

<sup>3</sup> Civil Engineer MSc., Aristotle University of Thessaloniki, [ksenetak@civil.auth.gr](mailto:ksenetak@civil.auth.gr)

mixtures of a medium, poor graded sand and a uniform granulated tire rubber, using different percentages of tire rubber. This study is part of an extensive program including experimental tests and theoretical analyses which is in progress at the Laboratory of Soil

Mechanics, Foundations and Geotechnical Earthquake Engineering of Aristotle University of Thessaloniki which intends to examine and quantify the efficiency and capability to improve the ground and soil - structure response under seismic loads using physical and synthetic materials.

## MATERIALS, SAMPLE PREPARATION AND TESTING PROGRAM

### Materials

Torsional resonant column tests were performed on four dry sand/rubber specimens with percentages of rubber equal to 0, 15, 35, and 100% by weight of dry mixture and two saturated sand/rubber specimens with percentages of rubber equal to 0 and 15% by weight of dry mixture.

The sand used in this study is a washed medium fluvial sand with mean grain size  $D_{50} = 0.60\text{mm}$ , and coefficient of uniformity  $C_u = 2,70$ . The specific gravity of sand solids is assumed equal to  $G_{s,sand} = 2,67$ . The tire rubber used is a granulated material composed of recycled waste tires, with mean grain size  $D_{50} = 2,75\text{mm}$  and coefficient of uniformity  $C_u = 2,37$ . According to ASTM D6270-98 specification, the specific gravity of tire rubber solids is assumed as  $G_{s,rubber} = 1.10$ . Figure 1 shows the grain size distribution of the materials used in this study.

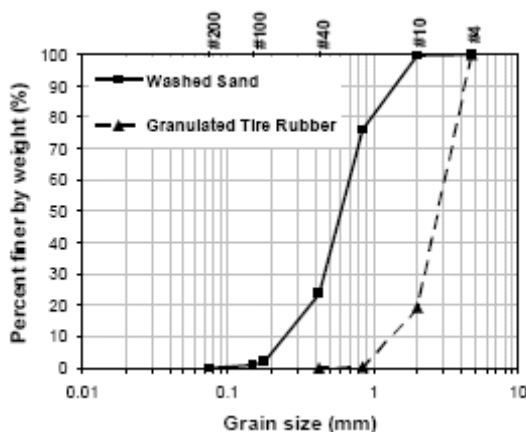


Figure 1. Grain size distribution of washed sand and granulated tire rubber used in this study

### Sample preparation

Resonant column tests were performed on 71,1mm diameter and 142,2mm high solid cylindrical specimens. Sand and tire rubber minerals were firstly dry mixed in the appropriate percentages in order to fabricate uniform sand/rubber samples. Specimens were then prepared in dry conditions into a mold inside the resonant column apparatus following the under-compaction method (Ladd, 1978). In order to prepare dense to very dense specimens, the samples were compacted into the mold in 14 layers of equal sand/rubber mass, using a metal rod tip tamper. To perform specimens of uniform density, the tips were increased at the top layers. Prior to resonant column testing full saturation and consolidation of the specimens were performed according to usual procedures.

### Testing program

All dynamic experiments were carried out using a Drnevich longitudinal-torsional resonant column device, in which the

base of the sample is rigidly fixed and the electromagnetic force is applied at the top-active end of the specimen. The torsional resonant column tests and analyses of the results were performed according to ASTM D4015-92 specification.

Table 1. Sand/rubber specimens tested

Sample code	Percentage of rubber by weight of sand/rubber mixture (%)	Test conditions	$e^{**}$	$\gamma_d^{**}$ (kN/m <sup>2</sup> )
100/0	0	Dry	0,588	16,49
85/15	15	Dry	0,471	14,85
65/35	35	Dry	0,450	12,53
0/100	100	Dry	0,472	7,34
100/0	0	Saturated	0,623	16,14
85/15	15	Saturated	0,493	14,72

\*\* initial values at  $\sigma_m = 0$

In order to study the shear modulus and damping ratio of the sand/rubber specimens at low dynamic shearing strains ( $G_{max}$  and  $D_{s,min}$ , respectively) and at low to medium dynamic shearing strains ( $G - \gamma - D_s$  curves), low amplitude and high amplitude torsional resonant column tests were performed in a series of subsequent increasing confining pressures. At each pressure, the specimen was allowed 80 minutes to equilibrate before the application of torsional force. Low amplitude resonant column test was performed firstly, followed by high amplitude test. After the high amplitude test, the specimen was allowed 60 minutes to recover its initial shear stiffness before the confining pressure increment. Table 2 summarizes the torsional resonant column testing program of the present study.

Table 2. Torsional resonant column testing program

Sample Code	Test conditions	$\sigma_m$ (kPa) regarding low amplitude R.C. tests	$\sigma_m$ (kPa) regarding high amplitude R.C. tests	$\gamma$ reference *** (%)
100/0	Dry	25, 50, 100, 200	50, 100, 200	$4,0 \times 10^{-4} - 6,8 \times 10^{-4}$
85/15	Dry	25, 50, 100, 200, 400	50, 100, 200, 400	$2,7 \times 10^{-4} - 3,9 \times 10^{-4}$
65/35	Dry	25, 50, 100, 200	50, 100, 200	$8,9 \times 10^{-4} - 1,1 \times 10^{-3}$
0/100	Dry	25, 50, 100	50, 100	$1,0 \times 10^{-4} - 2,3 \times 10^{-4}$
100/0	Saturated	50, 100, 200	50, 100, 200	$2,7 \times 10^{-4} - 8,9 \times 10^{-4}$
85/15	Saturated	25, 50, 100, 200	50, 100, 200	$4,3 \times 10^{-4} - 5,5 \times 10^{-4}$

\*\*\* dynamic shearing strain at which  $G_{max}$  and  $D_{s,min}$  of this study are defined

## EXPERIMENTAL RESULTS AND DISCUSSION

### Low amplitude dynamic parameters of dry specimens

Low amplitude resonant column tests are defined as those tests at which the dynamic shearing strain amplitude,  $\gamma$ , does not exceed the elastic threshold,  $\gamma_t^e$ . The elastic threshold is defined as the dynamic shearing strain which corresponds to a normalized shear modulus,  $G/G_{max}$  equal to 0,98 (Menq, 2003). In each confining pressure a specimen is tested, low amplitude resonant column measurements are performed before high amplitude measurements, in order to examine the dynamic parameters of maximum shear modulus,  $G_{max}$ , and minimum damping ratio,  $D_{min}$ . Due to the significantly low stiffness of granulated tire rubber, relatively high percentages of rubber in sand/rubber mixtures lead to more flexible specimens. Thus, the initial dynamic shearing strain, in which resonant column measurements are obtained, is expected to increase along with the increase in the percentage of rubber. Table 2 summarizes the reference dynamic shearing strain at which the low amplitude dynamic parameters are defined in this study. As shown in Table 2, shearing strain at which low amplitude measurements of this study are obtained is approximately  $5 \times 10^{-4}$  %,  $10^{-3}$  % and  $10^{-2}$  % for 0-15 %, 35 % and 100% percentage of rubber by mixture weight, respectively.

Figure 2 shows the effect of mean confining pressure on  $G_{max}$  and  $D_{min}$  of the dry sand specimen. It is noticed that  $G_{max}$  increases and  $D_{min}$  decreases approximately linearly with the logarithm of mean confining pressure. Empirical relations proposed in the literature concerning the estimation of maximum shear modulus and minimum damping ratio of granular soils are plotted in the same figures. The

experimental results are in good agreement with the empirical relations.

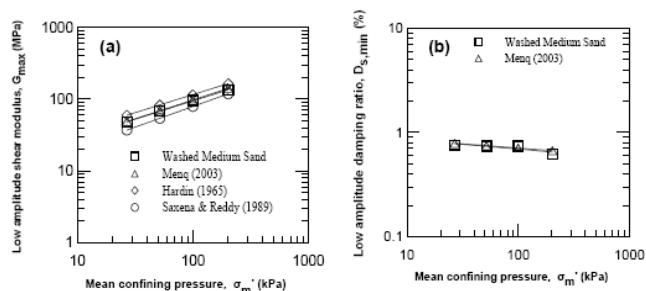


Figure 2. Low amplitude torsional resonant column tests on dry specimens: Low amplitude (a) shear modulus and (b) damping ratio of the washed medium sand versus mean confining pressure and corresponding theoretical values from empirical relations

Figure 3a shows the effect of mean confining pressure on  $G_{max}$  of all dry specimens tested. It is noticed that shear stiffness reduces significantly with an increase in the percentage of tire rubber due to the small contribution of rubber solids in the shear stiffness of the sand/rubber matrix.

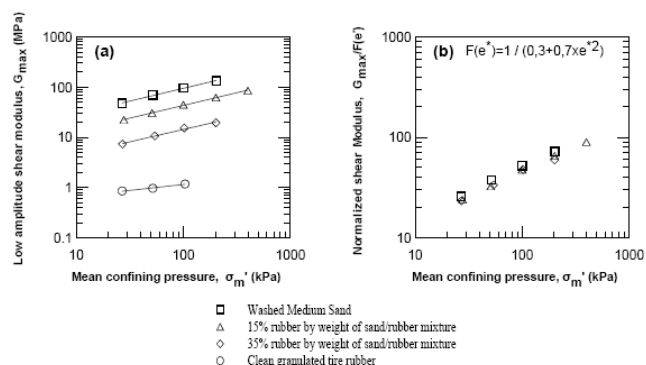


Figure 3. Low amplitude torsional resonant column tests on dry specimens: Low amplitude (a) shear modulus versus mean confining pressure and (b) normalized shear modulus with respect to void ratio function versus mean confining pressure of sand/rubber specimens for different percentages of granulated tire rubber by weight of mixture taking into account the rubber solids volume as part of the voids volume

However, the effect of mean confining pressure on  $G_{max}$  of sand/rubber mixtures follows the same trend like on sandy soils. It is remarkable that the clean tire rubber specimen exhibits approximately 100 times lower stiffness in comparison to the clean sand specimen. In Figure 3b the maximum shear moduli of the clean dry sand and the dry sand/rubber specimens, normalized with respect to the void ratio function, are plotted against mean confining pressure. The void ratio function used for the shear stiffness normalization is the traditional function proposed by Hardin (1978):

$$F(e^*) = \frac{1}{0.3 + 0.7 \times e^{*2}}$$

In equation (1)  $e^*$  is not the familiar void ratio but an equivalent void ratio in which the volume of rubber solids is assumed to be part of the whole volume of voids and the volume of solids consisting of the soil solids only. By taking this assumption into account, Figure 3b shows that the normalized maximum shear moduli of all mixtures are close to each other. Thus, empirical relations proposed in the literature for the estimation of maximum shear modulus of granular soils predict in a satisfactory manner the shear modulus of sand/rubber mixtures, assuming the volume of

rubber solids as part of the whole voids volume of the specimen.

Figure 4 shows the effect of mean confining pressure on  $D_{min}$  of all dry specimens tested. It is noticed that  $D_{min}$  decreases approximately linearly with the logarithm of mean confining pressure for all mixtures and that a significant increment on small strain damping ratio is observed as the percentage of rubber increases. Two possible mechanisms that contribute in the significant increment of damping ratio are the high damping capacity of rubber solids due to their high deformability and the thermoelastic damping occurring at sand-rubber interfaces due to the remarkably different properties of these two materials (Pamukcu and Akbulut, 2006).

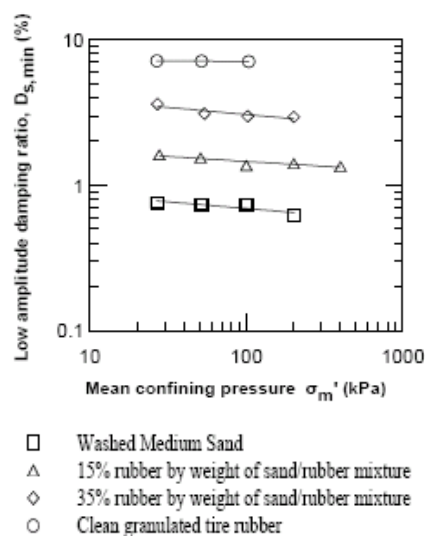


Figure 4. Low amplitude torsional resonant column tests on dry specimens: Low amplitude damping ratio of sand/rubber specimens versus mean confining pressure for different percentages of granulated tire rubber by weight of mixture

### High amplitude dynamic parameters of dry specimens

In order to examine the normalized shear modulus reduction and damping ratio ( $G/G_{max} - \gamma - D$  curves) at low to medium dynamic shearing strains, high amplitude resonant column tests were performed at different mean confining pressures.

Figures 5a and 5b show the  $G/G_{max} - \gamma - D$  curves of the clean dry sand specimen and corresponding curves proposed in the literature concerning granular soils (Menq, 2003). The experimental results show a reduction of normalized shear modulus and an increment of damping ratio when dynamic shearing strains exceed the elastic threshold.  $G/G_{max} - \gamma - D$  curves become less steep with the increase of the mean confining pressure. The experimental results are in good agreement with the proposed curves by Menq (2003). Figures 5c and 5d show the  $G/G_{max} - \gamma - D$  curves of the clean granulated rubber specimen. It is noticed that tire rubber exhibits a remarkably linear behavior for a wide range of dynamic shearing strains and that the effect of mean confining pressure on  $G/G_{max} - \gamma - D$  curves is negligible. The observed nonlinear behavior of the tire rubber specimen is possibly due to the granular fabric of the clean tire rubber specimen. Figures 5e and 5f show the  $G/G_{max} - \gamma - D$  curves of the dry sand/rubber specimen with 35% rubber by weight of mixture. The effect of mean confining pressure on the  $G/G_{max} - \gamma - D$  curves of the sand/rubber specimen has a similar trend like on the one of clean sand, but the dynamic curves of the mixture are less steep in comparison to the sandy specimen.

Figures 6b and 6d indicate that at relative low dynamic shearing strains the damping ratio is getting higher as the

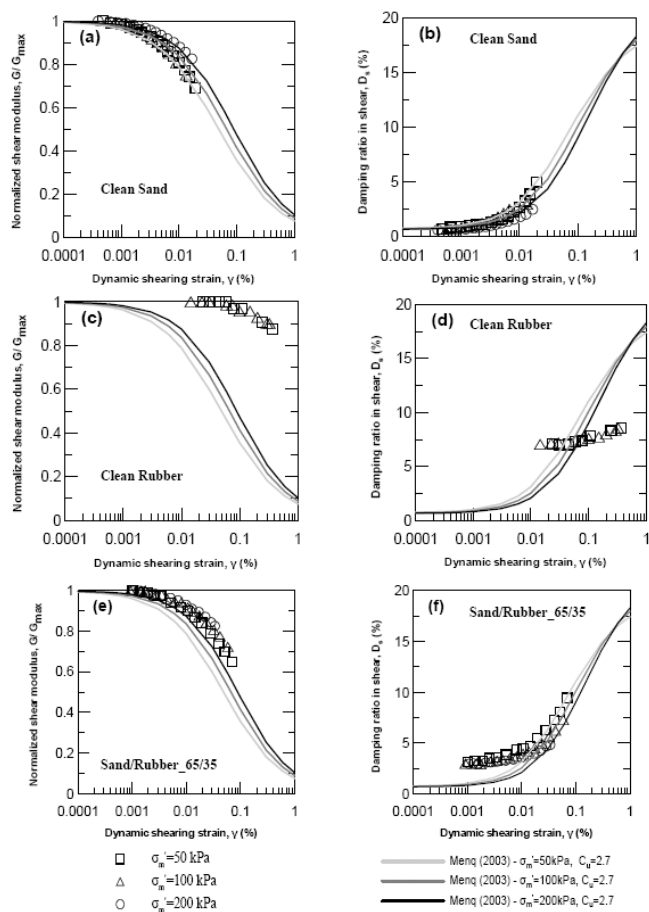


Figure 5. High amplitude torsional resonant column tests on dry specimens : Normalized shear modulus and damping ratio curves versus dynamic shearing strain of (a and b) clean dry sand specimen (c and d) clean dry granulated rubber specimen and (e and f) dry sand/rubber specimen with 35% granulated rubber by weight of mixture and corresponding empirical curves proposed in the literature

Figures 6 shows the effect of rubber percentage on  $G/G_{max} - \gamma - D$  curves of the dry sand/rubber specimens at two different mean confining pressures. Figures 6a and 6c indicate that normalized shear modulus curves become less steep with an increase in rubber percentage due to the more linear behavior of granulated tire rubber.

percentage of rubber increases, mainly due to the significant effect of rubber percentage in low amplitude damping ratio. However, at relative high dynamic shearing strains the damping ratio curves of different mixtures tend to converge. This trend is explained by the fact that an increase in rubber percentage, results in more linear behavior and lower reduction in specimens shear stiffness. Darendeli (2001) indicate that the mechanism of damping in soils at relatively high dynamic shearing strains is related to the non-linear stress-strain relationship. Thus, less steep  $G/G_{max} - \log \gamma$  reduction curves caused by an increase in the percentage of rubber, lead to less steep  $D_s - \log \gamma$  curves. This possible assumption is further confirmed by plotting  $D_s - D_{s,min}$  versus normalized shear modulus,  $G/G_{max}$ , of the sand/rubber specimens in the same figure (Figure 7). It is clearly shown that an elimination of the effect of low amplitude damping ratio on damping ratio curves, reduces significantly the effect of presence and percentage of rubber in the damping ratio at low to moderate dynamic shearing strains. In addition, the experimental results of this study concerning the relation between  $D_s - D_{s,min}$  and  $G/G_{max}$  of sand/rubber mixtures are in good agreement with available literature curves (Darendeli, 2001, Zhang et al., 2005) proposed for clean soils.

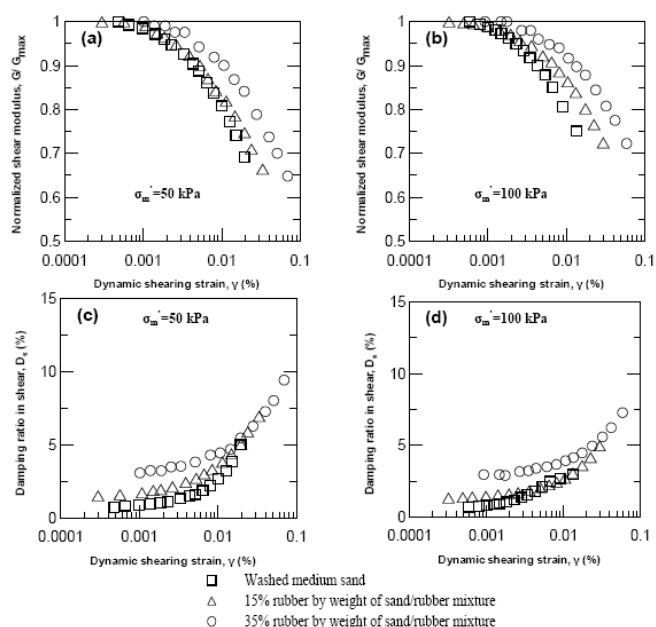


Figure 6. High amplitude torsional resonant column tests on dry specimens : Effect of percentage of granulated tire rubber on the normalized shear modulus and damping ratio curves of dry sand/rubber specimens at a mean confining pressure of (a and c) 50 kPa and (b and d) 100 kPa

Figure 7. High amplitude torsional resonant column tests on dry specimens : Normalized damping ratio curves with respect to low amplitude damping ratio ( $D_s - D_{s,min}$ ) versus normalized shear modulus ( $G/G_{max}$ ) of dry sand/rubber specimens at a range of granulated tire rubber 0% - 35% and mean confining pressure 50 400 kPa and corresponding literature curves

### Low and high amplitude dynamic parameters of saturated specimens

The effect of moisture on the dynamic properties of the clean sand and the sand/rubber specimens was investigated by performing additional torsional resonant column tests on the clean sand and on the sand/rubber specimen with 15% rubber by mixture weight, in saturated conditions.

The low amplitude dynamic parameters versus mean confining pressure of the saturated and dry specimens are plotted in the same figures (Figures 8a and 8b). In Figure 8a it is noticed that moisture has little effect on the low amplitude shear modulus. The observed differences on  $G_{max}$  between dry and saturated specimens are possibly a result of the different void ratios in which the specimens were prepared. In Figure 8b it is noticed that saturated specimens exhibit slightly higher low amplitude damping ratio in comparison to dry specimens. Taking into consideration that void ratio has negligible effect on damping ratio (Menq, 2003), a possible explanation on the damping ratio differences between dry and saturated specimens is the additional mechanism of viscous damping that saturated specimens exhibit. The main notice of the low amplitude torsional resonant column results is that moisture has a qualitatively similar effect on  $G_{max}$  and  $D_{min}$  of the clean sand and sand/rubber mixtures.

Figure 9 shows the effect of moisture on the corresponding low to medium amplitude dynamic parameters with respect to a mean confining pressure of 200 kPa. Figures 9a, b, c and d indicate that moisture content has negligible effect on the normalized shear modulus and damping ratio curves for both the clean sand and the sand/rubber specimens. Fig-

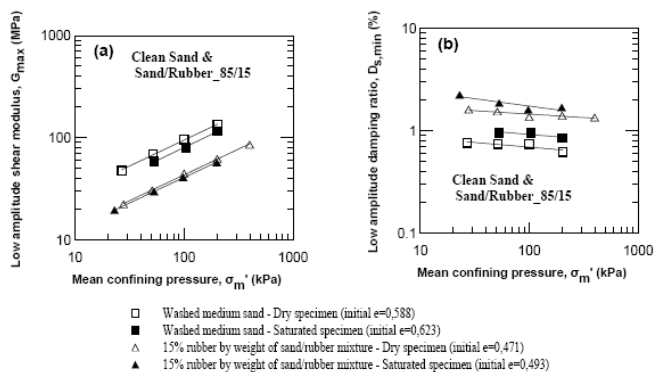


Figure 8. Low amplitude torsional resonant column tests on dry and saturated specimens : Effect of moisture on low amplitude dynamic parameters of clean sand and sand/rubber specimens (a) low amplitude shear modulus versus mean confining pressure and (b) low amplitude damping ratio versus mean confining pressure

ures 9e and 9f indicate that  $G/G_{max} - \gamma - D$  curves of saturated clean sand and sand/rubber specimens exhibit the same trend like the corresponding curves of dry specimens. The main conclusion of the high amplitude torsional resonant column results on dry and saturated specimens is that moisture has a qualitatively similar effect on  $G/G_{max} - \gamma - D$  curves for both clean sand and sand/rubber mixtures.

## CONCLUSIONS

Torsional resonant column tests were performed on mixtures of washed, medium, poor graded sand and a granulated tire rubber material with different percentages of rubber by weight of mixture.

Low amplitude and high amplitude resonant column tests were performed on dry and saturated sand/rubber mixtures in order to study the dynamic parameters of shear stiffness and damping ratio in a range of low to medium dynamic shearing strains.

Low amplitude resonant column results indicate a significant reduction in shear stiffness of sand/rubber specimens due to the negligible contribution of rubber solids on the shear stiffness of the sand/rubber matrix. The clean granulated rubber specimen exhibits approximately 100 times lower stiffness in comparison to the clean sandy specimen. Empirical relations concerning the estimation of shear modulus  $G_{max}$  of granular soils, as a function of void ratio and mean confining pressure, predict in a satisfactory manner the shear modulus  $G_{max}$  of sand/rubber mixtures, considering the rubber solids volume as part of the voids' volume.

Low amplitude damping ratio,  $D_{min}$ , of sand/rubber mixtures increases significantly with an increase in the percentage of rubber. Two possible mechanisms that contribute in the significant increase in damping ratio have been identified: the high damping capacity of rubber solids due to their high deformability and the thermoelastic damping occurring at the sand-rubber interfaces due to the remarkably different properties of these two materials. Low amplitude shear modulus and damping ratio values of sand/rubber specimens of this study are in good agreement with Feng and Sutter (2000).

$G/G_{max} - \gamma - D$  curves of sand/rubber mixtures become less steep with the increase in rubber percentage due to the approximately linear behavior of the granulated tire rubber. The effect of mean confining pressure on  $G/G_{max} - \gamma - D$  curves of sand/rubber mixtures present similar trend to the clean sands. However, both low amplitude and low to medium amplitude dynamic parameters of clean granulated tire rubber are unaffected by the mean confining pressure.

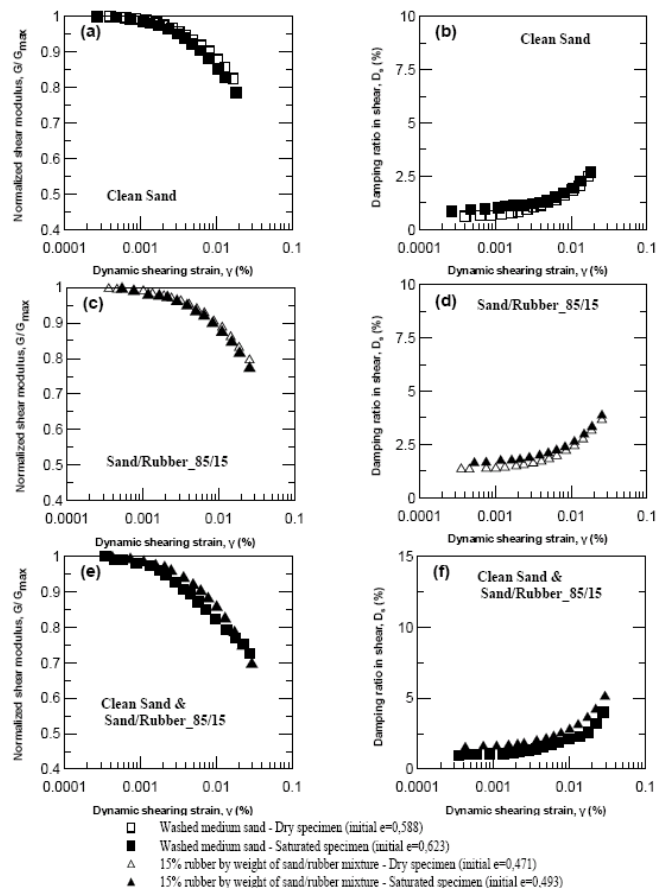


Figure 9. High amplitude torsional resonant column tests on dry and saturated specimens at a mean confining pressure of 200 kPa : Effect of moisture on low to medium amplitude dynamic parameters of clean sand and sand/rubber specimens (a, c and e) normalized shear modulus versus dynamic shearing strain and (b, d and f) damping ratio versus dynamic shearing strain

$D_s - \log \gamma$  curves of sand/rubber mixtures at relative low amplitude dynamic shearing strains are located higher, mainly due to the effect of presence and percentage of rubber on  $D_{s,min}$ .

However, at higher dynamic shearing strains (above 10-2%),  $D_s - \log \gamma$  curves of clean sand and sand/rubber mixtures tend to converge, due to the more linear behavior of mixtures with an increased percentage of rubber at relatively high dynamic shearing strains.

The effect of moisture on low and low to medium shear stiffness and damping ratio of sand/rubber mixtures has a similar trend to the clean sands. Saturated specimens exhibit higher damping ratio at low amplitude shearing strains due to the additional mechanism of viscous damping observing on saturated specimens. Low amplitude shear modulus and  $G/G_{max} - \gamma - D$  curves of sand/rubber mixtures are slightly affected by moisture content.

In order to quantify the effect of the presence and percentage of granulated tire rubber on the dynamic parameters of soil/rubber mixtures, additional experiments on granular soils of different grain size distributions and on soils that exhibit plasticity are needed. Moreover, the effectiveness of the use of granulated tire rubber on civil engineering projects should be investigated by additional theoretical one and two dimensional dynamic response analysis, in order to study the ground response, soil-structure interaction and behavior of geo-structures under dynamic loads. In this direction, an extensive experimental and theoretical program is under progress at the Laboratory of Soil Mechanics, Foundations and Geotechnical Earthquake Engineering of

AUTH. in order to study the efficiency of using granulated tire rubber in geotechnical and structural projects.

### Acknowledgement

The authors gratefully acknowledge the Ecoelastica S.A. company which provided the granulated rubber material used in this paper.

### REFERENCES

American Society of Testing and Materials, Annual Book of Standards, Volume 04.08, Soil and Rock :

ASTM Designation D6270-98 (1998) Standard test methods for use of scrap tires in civil engineering applications

ASTM Designation D4015-92 (1992) Standard test methods for modulus and damping of soils by the resonant column method

Beatty JR (1981) "Physical properties of rubber compounds", Chapter 10 of Mechanics of Pneumatic Tires, Clark SK Ed., U.S. Department of Transportation, National Highway Traffic Safety Admin., Washington, DC 20590, 871-885

Bosscher PJ, Edil TB, and Eldin N, (1993) "Construction and performance of shredded tire test embankment", Transportation Research Board, Washington, 44-52

Darendeli MB (2001) "Development of a new family of normalized modulus reduction and material damping curves", Ph.D. Thesis, University of Texas at Austin

Edeskar T (2006) "Use of tyre shreds in civil engineering applications – Technical and environmental properties", PhD Thesis, Lulea University of Technology, Department of Civil and Environmental Engineering, Division of Mining and Geotechnical Engineering

Edil TB (2004) "A review of mechanical and chemical properties of shredded tires and soil mixtures", *Recycled Materials in Geotechnics*, Geotechnical Special Publication, No.127, ASCE, Edited by AH Aydilek AH & Wartman J, 1-21

Edil TB and Bosscher PJ (1994) "Engineering properties of tire chips and soil mixtures", *Geotechnical Testing Journal*, 17 (4):453-464

Edil TB and Bosscher PJ (1992) "Development of engineering criteria for shredded waste tires in highway applications", Final Report to Wisconsin Departments of Transportation and Natural Resources, Research Report GT-92-9, Madison, WI.

Feng ZY and Sutter KG (2000) "Dynamic properties of granulated rubber/sand mixtures", *Geotechnical Testing Journal*, GTJODJ, 23(3):338-344

Foose GJ Benson CH and Bosscher PJ (1996) "Sand reinforced with shredded waste tires", *Journal of Geotechnical Engineering*, 122(9):760-767

Hardin BO (1978) "The nature of stress strain behavior of soils", *Proceedings of the Geotechnical Division Speciality Conference on Earthquake Engineering and Soil Dynamics*, ASCE, Pasadena, 1:3-90

Hardin BO (1965) "Dynamic vs. static shear modulus for dry sand", *Materials Research and Standards*, American Society for Testing and Materials, 232-235.

Humphrey D and Manion W (1992) "Properties of tire chips for lightweight fill", *Grouting, Soil Improvement, and Geosynthetics*, 2:1344-1355

Ladd RC (1978) "Preparing test specimens using under-compaction", *Geotechnical Testing Journal*, 1(1):16-23

Lee J.H Salgado R Bernal A and Lovell CW (1999) "Shredded tires and rubber-sand as lightweight backfill", *Journal of Geotechnical and Geoenvironmental Engineering*, 125(2):132-141

Masad E Taha R Ho C and Papagiannakis T (1996) "Engineering properties of tire/soil mixtures as a lightweight fill material", *Geotechnical Testing Journal*, GTJODJ, 19(3):297-304

Menq FY (2003) "Dynamic Properties of Sandy and Gravelly Soils", Ph.D. Thesis, University of Texas at Austin

Pamukcu S and Akbulut S (2006) "Thermoelastic enhancement of damping of sand using synthetic ground rubber", *Journal of Geotechnical and Geoenvironmental Engineering*, ASCE, 132(4):501-510

Saxena SK Reddy KR (1989) "Dynamic moduli and damping ratios for Monterey No.0 sand by resonant column tests", *Soils and Foundations*, Japanese Society of Soil Mechanics and Foundation Engineering, 29(2):37-51

Seed HB Wong RT Idriss IM and Tokimatsu K (1986) "Moduli and damping factors for dynamic analysis of cohesionless soils", *Journal of Geotechnical Engineering*, ASCE, 112(11):1016-1103

Zhang J Andrus RD and Juang CH (2005) "Normalized shear modulus and material damping ratio relationships", *Journal of Geotechnical and Geoenvironmental Engineering*, ASCE, 131(4):453-464

Zornberg JG Carbal AR and Viratjandr C (2004) "Behaviour of tire shred - sand mixtures", *Canadian Geotechnical Journal*, 41:227-241



### GEOSYNTHETICS AS MITIGATION MEASURE FOR SEISMIC HAZARD ON GEOSTRUCTURES

Varvara ZANIA<sup>15</sup>, Ioanna TZAVARA<sup>16</sup>, Yiannis TSOMPANAKIS<sup>17</sup>, and Prodromos N. PSARROPOULOS<sup>18</sup>

### ABSTRACT

Seismic distress on engineering geostuctures can be attributed to: (a) the propagation of seismic waves and the subsequent dynamic response, which is commonly referred as strong motion effects, and (b) the permanent deformations developed during an abrupt fault rupture. Under this perspective, the devastating effect of earthquakes on geostuctures, like highway or railway embankments, earth dams and waste landfills, may be categorized to slope failure of the soil/waste mass and to excessive permanent deformations of the structure. It is evident that the socio-economical and environmental consequences associated with a potential failure of the aforementioned geostuctures

<sup>15</sup> PhD Candidate, Technical University of Crete, Greece, zaniab@tee.gr

<sup>16</sup> PhD Candidate, Technical University of Crete, Greece, itzavara@yahoo.gr

<sup>17</sup> Asst. Professor, Technical University of Crete, Greece, jt@science.tuc.gr

<sup>18</sup> Lecturer, Hellenic Air Force Academy, Athens, Greece, prod@central.ntua.gr

are undesirable. For this reason, taking advantage of the reinforcing effect of the geosynthetics, the aforementioned hazards may be reduced or even avoided. The current study aims to demonstrate the ability of the geosynthetics to be used as mitigation measures against the earthquake effects on geostructures. Therefore, the potential failure modes are initially identified, regarding both fault rupture propagation and strong motion effects. Subsequently, parametric finite-element analyses are conducted, and the impact of the most important parameters on the examined issues is estimated. In accordance, several reinforcement scenarios are examined and analyzed following the same procedures. The efficiency of the application of geosynthetics for the prevention of slope instabilities and the reduction of the anticipated stress levels on the geostructures is assessed. Results indicate that the use of geosynthetics for seismic hazard mitigation is very efficient and may provide a reliable method for the seismic design of large-scale geostructures.

Keywords: geosynthetics, permanent deformations, fault rupture, slope stability.

## INTRODUCTION

Geosynthetics have been widely used over the last decades, mainly due to the numerous functions that they have been efficiently applied which are reinforcement, drainage, filtration, containment, and separation. Moreover, the applications of geosynthetics involve various fields of engineering practice, such as geotechnical, transportation, hydraulic, and geoenvironmental. The development of these applications is still ongoing, not only on the evaluation of the performance, but also on the expansion of application areas of these engineering materials (Koerner, 2000). The design of earth structures like soil embankments, earth dams, and waste landfills may include also the use of geosynthetics aiming at base reinforcement, waterproofing, and containment, respectively. However, it is evident that the use of geosynthetic reinforcement in the prevention or the reduction of the potentially developed seismic distress within the aforementioned geostructures would also be valuable.

Seismic distress of geostructures is provided as a result of any of the two main types of earthquake loading. The first component of seismic distress is related to the strong ground motion provided by the waves propagating from the seismic source, while the second one is related to permanent ground deformation due to abrupt fault dislocation. Permanent ground deformation may also result from liquefaction, lateral spreading or foundation settlement, but the investigation of these types of ground failure is beyond the scope of the present study.

The hazard of earth structures associated with an abrupt fault dislocation is the development of permanent ground deformation that may threaten the integrity of the geostructure or its components. However, the fault rupture propagation through soil deposits has been shown to be affected by the fault type, its dip angle, the magnitude of the fault displacement, and the properties of the overlying soil layer. Several researchers have investigated these issues by conducting small-scale sandbox experiments or by performing numerical analyses which employed the finite element or finite difference method. In addition field observations have provided valuable insights into the developed failure patterns. More specifically, studies based on field observations report that strike-slip faults propagate almost vertically producing a relatively narrow zone of deformation (Bray et al., 1994a). Furthermore, the angle of fault rupture propagation reduces near the ground surface in the case of reverse faults, while the opposite holds for normal faults resulting to even vertical surface exposure (Lade et al., 1984). Normal faults are also characterized by a secondary failure surface, which is commonly developed in the case of a small dip angle, and emerges as a graben.

These observations are consistent with the results of small-scale sandbox experiments conducted by Cole and Lade (1984). Moreover, Cole and Lade (1984) have shown that the relative amount of fault dislocation (relatively to the height of the soil layer) required for a reverse fault to reach the ground surface is larger than the corresponding of a normal fault. Recently numerical methods have been also utilized for the investigation of the deformations developed by fault propagation through soil layers. The finite element method (Bray et al., 1994b, Lin et al., 2006, Anastasopoulos et al., 2007 and Zania et al., 2008b) and the finite difference method (Papadimitriou et al., 2007) have been employed, and valuable aspects of the problem have been addressed. Bray et al. (1994b), after verifying their numerical methodology by small scale experiments, have shown that reverse fault propagation through clayey soil is related to bending of the upthrown block over the downthrown. According to Lin et al. (2006) the most important parameters affecting the propagation of a reverse fault through sandy soil are the Young's modulus and the dilation angle.

In accordance to the observations of Cole and Lade (1984), Anastasopoulos et al. (2007) have concluded that the magnitude of fault dislocation for the rupture to reach surface increases in case of loose sand compared to dense sand, and in case of reverse fault compared to normal fault. Moreover, Papadimitriou et al. (2007) have shown that in clayey soils the magnitude of fault dislocation for the rupture to reach surface is lower than the corresponding of sandy soils. Zania et al. (2008b) have examined the behavior of earth embankments subjected to displacements induced by both normal and reverse faults, and observed that for low dip angles a secondary failure surface develops due to normal fault propagation and the developed permanent deformation may be greater when the fault tip is located under the slopes of the geostructure.

The dynamic loading hazards of the aforementioned geostructures, which are related to wave propagation, are mainly associated with the development of excessive dynamic shear stresses, which can initiate slope instability of the soil or waste mass. A catastrophic failure has not been observed, however, in the 2001 Bhuz, India earthquake several medium and minor earth dams were damaged as a result of slope instability (EERI, 2001). Additionally, failure patterns implying the development of seismic slope displacements in waste landfills were reported after the 1994 Northridge earthquake (Matasovic et al., 1998). Moreover, geosynthetics are placed at soil embankments with reinforced foundation and waste landfills with geomembrane barrier in order to achieve stability and prevention of environmental pollution respectively. Nevertheless, the geosynthetics form discrete boundaries along which low shear strength is attained. More specifically, Fishman and Pal (1994) have shown that the shear strength of the clay to smooth geomembrane interface is less than clay alone in all cases examined, while Koerner et al. (1986) report that soil - geosynthetic interfaces exhibit at most 50-88% of the shear strength of the intact clay soil.

Therefore, an additional hazard is the accumulation of seismic displacements (slippage) along the aforementioned interfaces. However, both hazards are considered during the seismic slope stability assessment, which is conducted in the current practice by the employment of the pseudostatic and the permanent deformation methods. The latter is based on the well-known Newmark's sliding block model (1965), hence lately one of its major assumptions, which is the contribution of the flexibility of the sliding mass, has concentrated the research interest. The calculation of the seismic displacements taking simultaneously into account the inertia response (coupled) of simple SDOF models has shown that the two step procedure (decoupled) may be conservative (Kramer and Smith, 1997 and Rathje and Bray, 2000). The comparison of the two failure modes for waste landfills following a decoupled procedure (Zania et

al., 2008a) has shown that circular slope failure is in general more critical, except when the shear strength of waste material is higher and the response of the geostructure is close to resonance.

The most common approach used to limit the hazards of fault rupture propagation is the avoidance of the region of surface exposure of the fault. However, the location of large-scale geostructures is mandated by several engineering or socio-economical factors, and therefore the prevention of their construction in the vicinity of an active fault may be unfeasible. Under this perspective, there have been proposed alternative approaches like (a) the use of ductile compacted or reinforced fill to distribute the fault movements, and (b) designing the facility to be capable to undergo some amount of ground deformation without collapse or significant damage (Bray, 2001). Moreover, the use of geosynthetics has been proposed for earthquake hazard mitigation of buildings, by suggesting their application as foundation isolation. More specifically, Yegian et al. (1999) carried out shaking table tests of model buildings and have shown that, due to the low shear strength geosynthetic interface seismic displacements develop and the transmitted acceleration levels appear to be reduced.

The aim of the current study is to illustrate the potentially beneficial role of the geosynthetics in mitigating the earthquake hazard on geostructures arising from both fault rupture and seismic wave loading. For this purpose, initially finite element analyses are performed in order to investigate the ability of the geosynthetics to reduce the permanent deformation of the geostructure, examining also the effect of several important parameters, like the interface properties, the material properties of the geosynthetics, and the mechanical properties of the underlying soil layer. Moreover, the potential of the geosynthetics to prevent the development of slope instability taking advantage of their reinforcing effect is examined. For this purpose, the pseudostatic method is employed and specifically the limit equilibrium method, while the required geosynthetic force is estimated for two different slope heights, a wide range of slope inclination, various angles of internal friction, and several cases of applied acceleration. Figure 1 presents a schematic illustration of the two investigated applications of geosynthetics as mitigation measures against earthquake hazards.

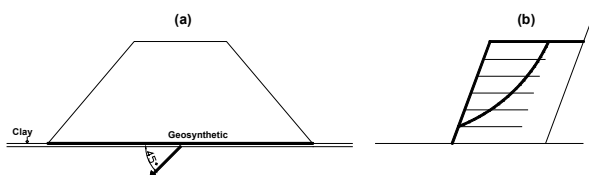


Figure 1. Schematic illustration of the examined cases of the application of geosynthetics as mitigation measures for (a) fault rupture and (b) slope instability in geostructures

## MITIGATING FAULT RUPTURE

### Methodology - Modelling

The finite element modelling was conducted with the ABAQUS (2004) software. The models developed for the investigation of mitigation measures in the current study are based in the corresponding of a former study (Zania et al., 2008b) aiming to provide a direct estimation of the impact of the geosynthetics. Therefore the height and the deck of the embankment analysed are equal to 20m and 40m respectively, and it is characterized by smooth slope inclination 1:3 (V: H). The discretization was performed with quadrilateral plane strain elements with size 0.5m, a mesh which is considered dense enough to reproduce accurate results. The finite element mesh is shown in Figure 2. Along the foundation of the embankment a geosynthetic

layer was placed, which was discretized with truss elements since the geosynthetics are considered to attain only axial stiffness. A clay layer 1m in height was considered to be constructed as an underlying foundation layer. The material properties are shown in Table 1. Initially, the interface was not considered to be able to develop sliding and the geosynthetic material behaviour was set to be linear elastic with Young's modulus equal to 300MPa. The fault tip was considered at the axis of symmetry of the model, while the imposed displacements were characteristic of a 45° normal fault.

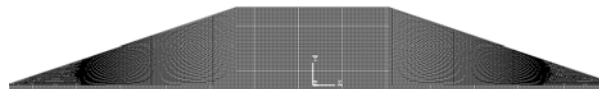


Figure 2. Finite element discretization of the examined model

Table 1. Material properties of the investigated cases

Material	Young's Modulus (MPa)	Cohesion (kPa)	Angle of friction (°)
Embankment	53.33	15	36°
medium clay	60	53	-
stiff clay	90	75	-

The results have shown that only 3.3 cm of vertical displacement are required for the fault rupture to reach the geosynthetic, while a slight increase of the vertical displacement (5cm) results to the surface exposure of the fault. However, the angle of propagation of the fault seems rather constant and equal to 60°, and the secondary failure surface propagates with angle equal to 55° to the horizontal and reaches the surface at vertical displacement 0.4m. In Figure 3 the surface deformation is shown at different base displacement levels ( $d/H = 0.5\%$ , 1%, and 1.5%) for the models with and without geosynthetic. It is obvious that the application of the geosynthetic at the base of the embankment has reduced the permanent deformations, through the developed tensile stresses. The region of high developed axial stress is rather narrow and it was observed in a distance of 1.5-2m from the fault tip (both sides), while the maximum axial stress for base vertical displacement equal to 0.7m was 120MPa, which is regarded as excessive tensile stress. Note that only geosynthetics intended for reinforcement (geogrids) are characterized by greater values of ultimate tensile strength and therefore are appropriate for this application.

### Effect of clay layer properties

The effect of the mechanical properties of the foundation clay layer is also examined, by analyzing the already described model for stiffer clay. For this purpose the clay was considered to be characterized by a Mohr-Coulomb failure envelope (stiff clay in Table 1). The required fault dislocation for the fault to reach the geosynthetic is reduced to 2.8cm, while for the surface outcrop is 4.9cm. However, neither the direction of propagation of the two failure surfaces nor the displacement for the surface exposure of the secondary failure surface, are affected by the clay stiffness. The magnitude of the permanent ground deformation at the surface is slightly affected by the stiffness of the clay layer. Conversely, the maximum axial stress developed along the geosynthetic is generally increased compared to the clay of medium stiffness, implying that the increase of the stiffness of the foundation layer has a negative impact on the mitigation of fault rupture propagation (see Figure 4).

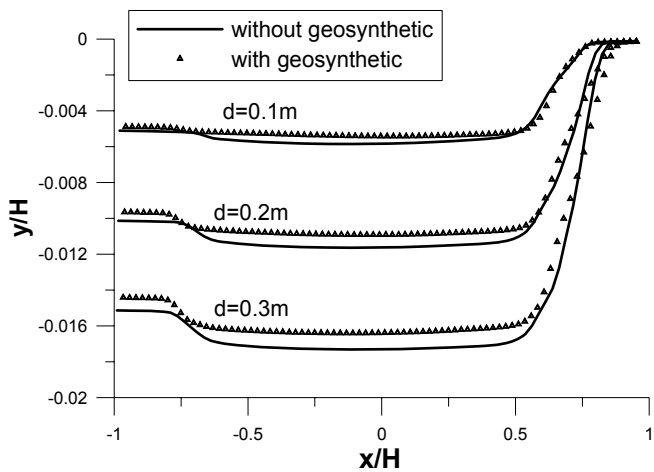


Figure 3. Impact of the geosynthetic on the magnitude of the developed surface deformation during the dislocation of a 45° normal fault

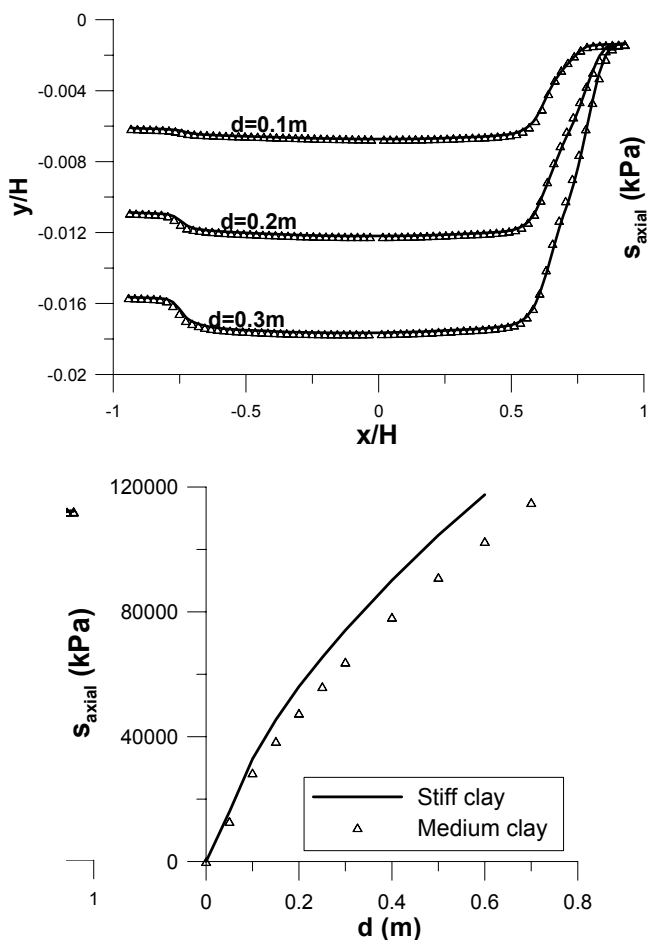


Figure 4. Impact of the stiffness of the clay layer on the magnitude of the developed surface deformation and on the maximum tensile stresses of the geosynthetic during the dislocation of a 45° normal fault

*Effect of geosynthetic properties*

The impact of the mechanical properties of the geosynthetic was investigated for two cases: (a) increase of the Young's modulus (600MPa), and (b) consideration of elasto - plastic behavior with yield stress ( $\sigma_y$ ) equal to 16MPa. The latter resembles to the mechanical properties of an HDPE geomembrane. The fault rupture propagation procedure is not affected by the increase in the elasticity modulus of the geosynthetic, since the dislocation required for the fault to reach the geosynthetic and the surface, the displacement

for the outcrop of the secondary failure surface and the direction of the propagation of the primary and secondary failure surface have not been altered. Regarding the distress of the geosynthetic, it is expected that the tensile stresses are increased. More specifically, the fault dislocation is a problem of imposed displacements and therefore the developed strains are initially expected to be comparable for each case and the tensile stresses increased for the geosynthetic of the higher Young's modulus. Moreover, as the soil continuously deforms the plastic strains accumulate under the yield stress and the axial strains of the stiffer geosynthetic are lower, though the tensile axial stresses receive higher values (Figure 5). In contrast, the surface deformation is affected in a minor extent.

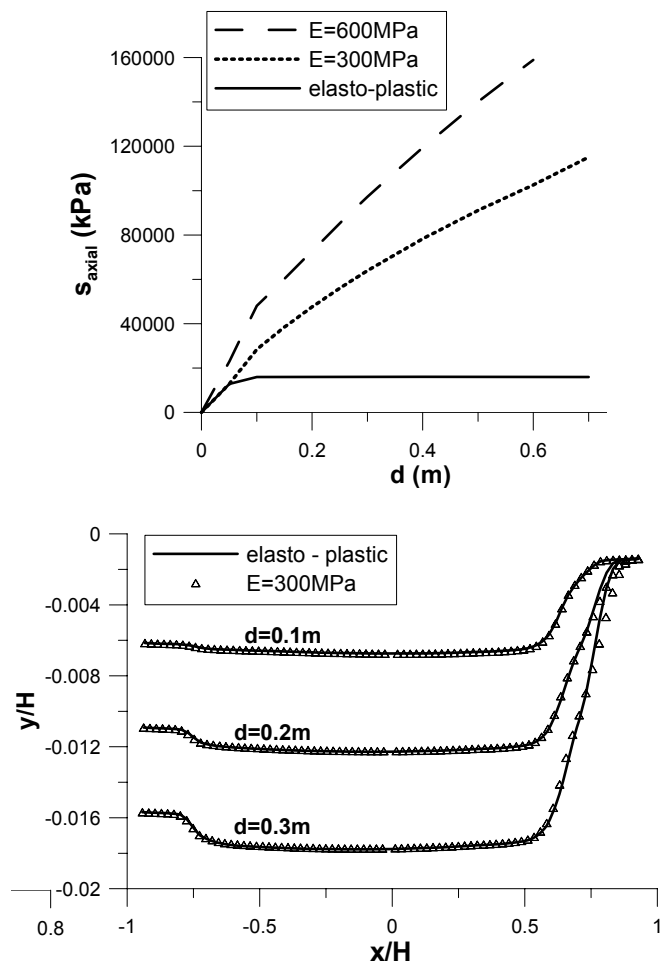


Figure 5. Impact of the mechanical properties of the geosynthetic on the magnitude of the developed surface deformation and the maximum tensile stresses of the geosynthetic during the dislocation of a 45° normal fault

Accordingly, the effect of the consideration of the elasto-plastic stress-strain behaviour of the geosynthetic is examined. The fault rupture propagation procedure does not seem to be affected by the stress-strain relationship of the material. The yield stress is developed for fault displacement equal to 5.6cm. Moreover, the axial tensile strains increase continuously receiving greater values than the corresponding of the elastic behaviour. The maximum axial strain is equal to 100% at maximum fault displacement almost equal to 0.7m, since geomembranes attain a value of strain at break of the order of 500% the performance of the material is considered satisfactory. Regarding the surface displacements, Figure 5 shows that a minor increase of the deformations is observed when considering geomembrane's material nonlinear behavior.

As already mentioned the inclusion of geosynthetics provides a low shear strength interface along which slip displacements are possibly being developed. The effect of this phenomenon was also investigated. For this purpose two new models were developed considering Coulomb type friction: (a) along the upper interface, which is characterized by angle of friction equal to  $9^\circ$  and (b) along both upper and lower interfaces of the geosynthetic, which are characterized by the angle of friction of  $9^\circ$  and  $12^\circ$  respectively. The models were on purpose selected to exhibit the lowest angle of friction along the upper interface, aiming to investigate the ability of the decoupling the base displacement from the geostructure through the slippage. The double interface has affected the fault rupture propagation process only in the magnitude of the base displacement required for the secondary failure surface to develop (0.5m). Initially, slip displacements develop along the upper interface at the hanging wall side, where an increase of the shear stress is followed by decrease of the normal stress. However, as the displacement increases (0.15m) slippage takes place at the lower interface as well, at the footing wall side and the increase of the slip displacements at the upper interface is limited. This may be attributed to the axial stresses which develop along the geosynthetic, which reduce the transmitted shear stresses and therefore the lower interface becomes the critical one. As the fault displacement becomes greater than 0.3m sliding is observed to increase along the upper interface especially at the projection of the fault tip. Finally, at base vertical displacement equal to 1m the slip displacements of the upper interface are about 0.2m, while along the lower interface the corresponding value is almost double.

Figure 6 shows the surface deformation obtained from the second model compared to the corresponding from the non sliding interface. It is evident that the beneficial contribution of double sliding in the reduction of the permanent deformation is increased at higher base fault displacement levels. A similar reduction of the surface deformation was not observed for the single sliding interface model. Moreover, the aforementioned double sliding evolution results also to lower axial stresses at the geosynthetic. Figure 6 presents the maximum tensile stresses along the geosynthetic for all the three examined cases, i.e. (a) non sliding interfaces, (b) upper sliding interface, and (c) double sliding. It is obvious that in the case of single upper sliding interface, the developed axial stresses are the highest. Conversely, double sliding has also resulted in decrease of the distress of the geosynthetic.

**MITIGATING SLOPE INSTABILITY**

**Methodology**

The investigation of the use of geosynthetics in reinforced soil slopes of geostructures aiming to prevent the development of a potential instability is performed by employing the pseudostatic method. The pseudostatic method is a direct extension of the static slope stability analysis, considering also the seismic loading as horizontal and vertical inertia forces, which are equal to the seismic coefficient multiplied by the weight of the sliding mass. In the current study the limit equilibrium method and more specifically the simplified Bishop method (1954) was modified and applied in a fortran code developed by the authors, in order to calculate the required geosynthetic force. More specifically, after the estimation of the unreinforced factor of safety of the slope, the total reinforcement tension per unit width of slope ( $T_S$ ) required to obtain the required factor of safety ( $FS_R$ ) was calculated according to the following equation (FHWA, 2001):

$$T_S = (FS_R - FS_U) \frac{M_D}{R} \quad (1)$$

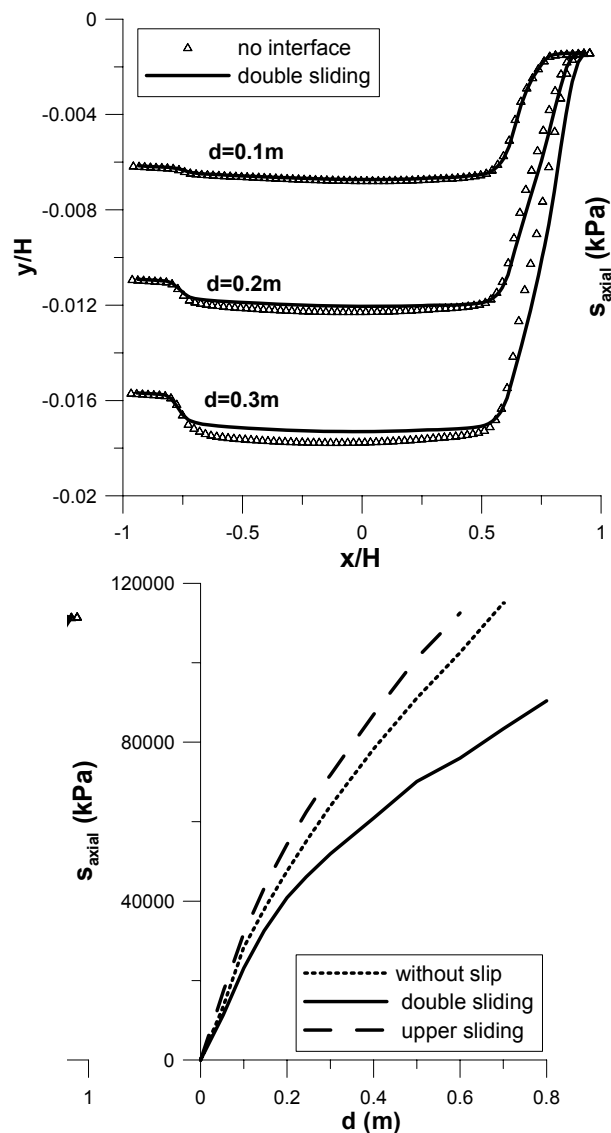


Figure 6. Impact of the interface properties of the geosynthetic on the magnitude of the developed surface deformation and the maximum tensile stresses of the geosynthetic during the dislocation of a  $45^\circ$  normal fault

where  $FS_R$  the factor of safety of the reinforced slope,  $FS_U$  the factor of safety of the unreinforced slope,  $M_D$  the destabilizing moment and  $R$  the radius of the circle.

The procedure described was conducted for several circles and the maximum calculated value of the total reinforcement tension was determined. Moreover, according to the seismic norms (EC8, 2003) the required factor of safety of a soil slope is considered to be equal to unity. Therefore, the above equation which is based on the assumption that the reinforcing moment is added on the resisting moments, yields the same results as if the reinforcing moment was subtracted from the driving moments. Additionally, the moment arm of the reinforcement forces was assumed to be equal to the radius of the circle, meaning the forces were considered to act tangentially to the circle, as proposed (FHWA, 2001) for continuous extensible reinforcement, i.e. geotextiles or geogrids. Initially a slope 6m high was analysed, considering slope inclination varying between 45 and 70 degrees and several values were selected for angle of friction of the soil within the range of 30 - 45 degrees. In Figure 7 the resulting total reinforcing tension is shown for two cases: (a) no applied acceleration, and (b) horizontal seismic coefficient equal to 0.16. The first case is only presented for completeness, since the static factor of safety of reinforced slopes is at least equal to 1.3 (FHWA, 2001). It is evident that the increase of the slope inclination, and the

decrease of the angle of friction result to increase of the required reinforcement tension. In addition, the application of the seismic coefficient has increased substantially (almost 100%) the required reinforcement tension.

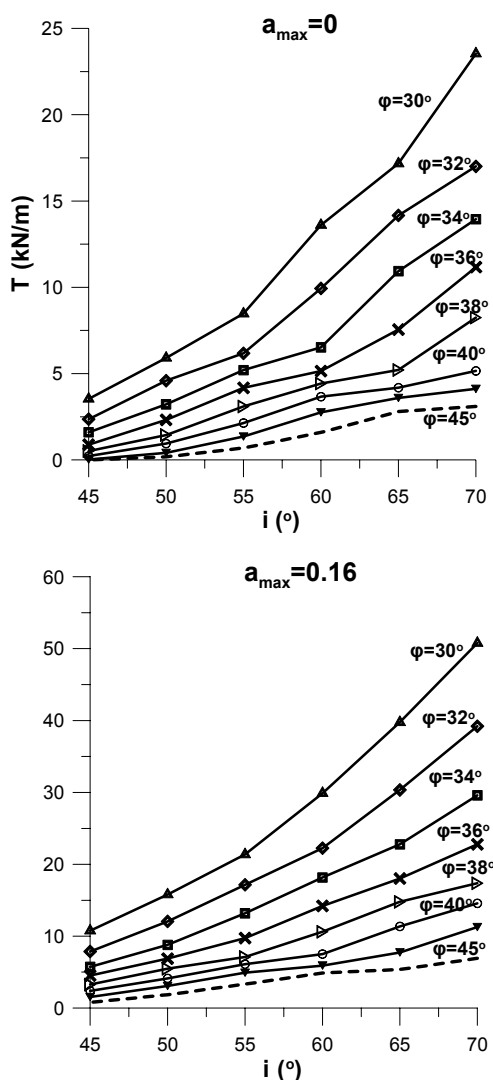


Figure 7. Variation of the total reinforcement tension for several slope inclinations and angles of internal friction. The results correspond to a slope with 6m height subjected to  $a_{max}=0$  and to  $a_{max}=0.16$

### Parametric evaluation

The effect of several parameters was investigated by an extended parametric study. Two values of seismic coefficient were selected to highlight the impact of the level of the applied acceleration and the results are presented in Figure 8. The maximum reinforcement tension increased by almost 50% as the seismic coefficient increased from 0.24 to 0.36.

Moreover, the impact of the vertical component of the seismic coefficient was estimated. The vertical seismic coefficient was considered equal to 50% of the horizontal component as suggested by seismic codes (EC8, 2003). By observing Figure 9 it is obvious that the total reinforcing tension is increased compared to the corresponding one shown in Figure 8, which does not account for the effect of the vertical seismic coefficient on slope stability. Finally, an additional parameter was examined, i.e. the height of the reinforced slope. The results shown in Figure 10 correspond to slope height equal to 15m. It can be observed that the reinforcement tension is substantially increased, by receiving values almost five times the corresponding of the slope with height equal to 6m.

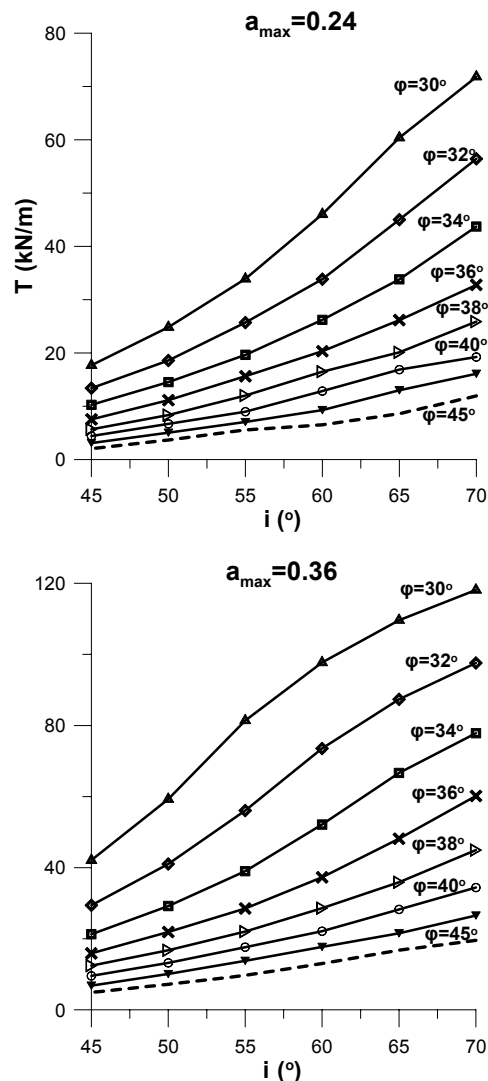


Figure 8. Variation of the total reinforcement tension for several slope inclinations and angles of internal friction. The results correspond to a slope with 6m height subjected to  $a_{max}=0.24$  and to  $a_{max}=0.36$

### CONCLUSIONS

The potential use of the geosynthetics in mitigating the earthquake hazard on a typical geostructure arising from both fault rupture and seismic wave loading was investigated in the current study. For this purpose, initially finite element analyses were performed and the ability of the geosynthetics to reduce the permanent deformation developed at the geostructure, due to abrupt fault displacement was verified. More specifically, it was shown that the reinforcing effect of the geosynthetics result to a reduction of the surface deformation, which is further enhanced by the development of slip interfaces at both sides of the geosynthetic. However, this is achieved by the application of smooth geomembranes which are characterized by low shear strength along their surface. It has been presented that geomembranes perform successfully during the fault rupture propagation, without reaching their breakage strain even at high values of base fault dislocation. In contrast, the use of stiff geosynthetics and/or stiff soil foundation materials was proven to be detrimental for the distress on the geosynthetics, while their contribution to ground deformation reduction was negligible.

Moreover, the application of the geosynthetics as reinforcement to prevent the development of seismically induced slope instability was investigated. The pseudostatic method was employed following also relevant design guidelines for

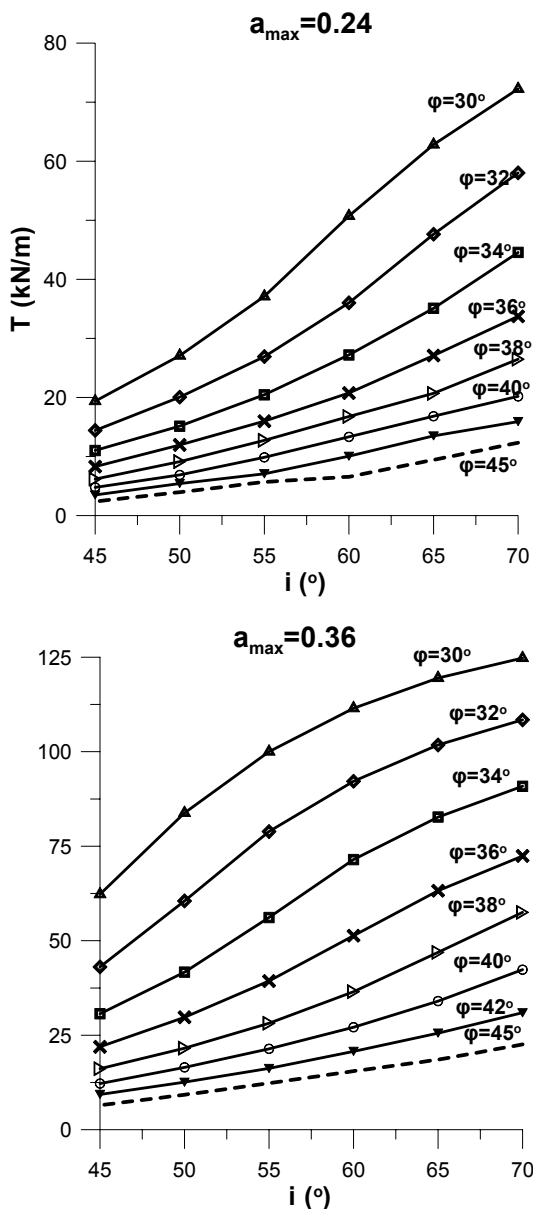


Figure 9. Variation of the total reinforcement tension for several slope inclinations and angles of internal friction. The results correspond to a slope with 6m height subjected to  $a_{max}=0.24$  and to  $a_{max}=0.36$  and vertical acceleration equal to 50% of the  $a_{max}$

reinforced slopes. The investigation of most of the involved parameters has shown that:

- the increase of the slope inclination results to an increase of the required reinforcement tension for stability,
- the increase of the angle of internal friction decreases the total reinforcing tension,
- the increase of the seismic coefficient from 0.16 and 0.24 to 0.36 resulted to a 100% and 50% increase of the required reinforcement tension,
- the vertical acceleration does not affect considerably the magnitude of the required reinforcement,
- the increase of the height of the slope is the most crucial factor, since it provides the greatest reinforcement efficiency.

Conclusively, the current investigation has shown that the geosynthetics may be efficiently applied as mitigation measures to reduce the anticipated permanent deformation

arising from a fault dislocation and to prevent the development of seismic slope instability in large-scale embankments.

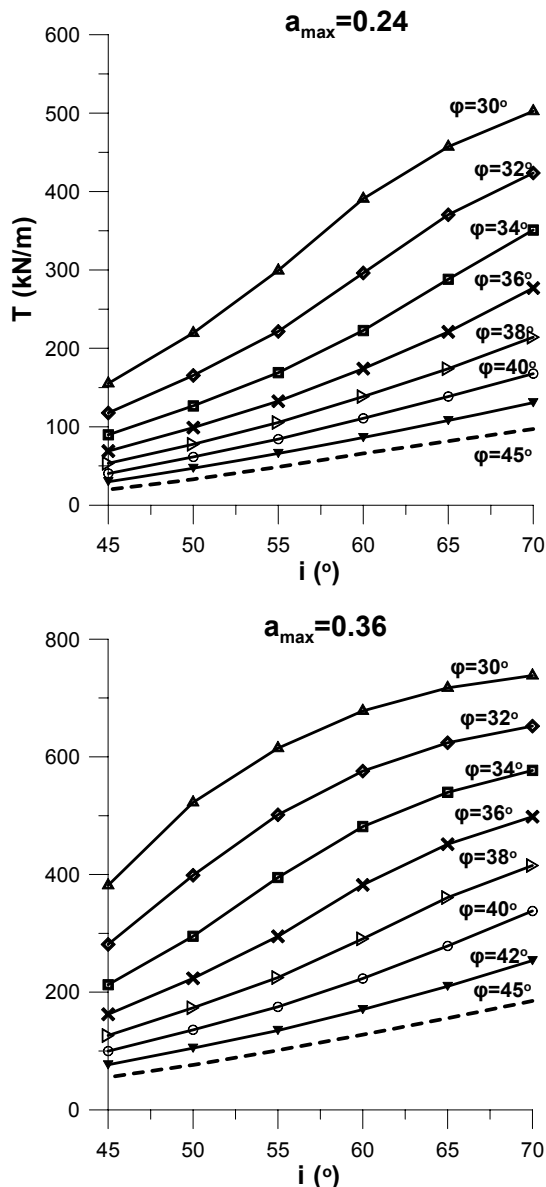


Figure 10. Variation of the total reinforcement tension for several slope inclinations and angles of internal friction. The results correspond to a slope with 15m height subjected to  $a_{max}=0.24$  and to  $a_{max}=0.36$  and vertical acceleration equal to 50% of the  $a_{max}$

#### Acknowledgement

Financial support from a basic research fund from the Research Committee of the Technical University of Crete is gratefully acknowledged.

#### REFERENCES

ABAQUS (2004) *Analysis User's Manual Version 6.4*, ABAQUS Inc, USA

Anastasopoulos I, Gazetas G, Bransby MF, Davies MCR and El Nahas A (2007) "Fault rupture propagation through sand: Finite-element analysis and validation through centrifuge experiments", *Journal of Geotechnical and Geoenvironmental Engineering*, 133(8): 943-958

Bishop AW (1954) "The use of the slip circle in the stability analysis of slopes", *Geotechnique*, 5(1): 7 -17

- Bray JD (2001) "Developing mitigation measures for the hazards associated with earthquake surface fault rupture", *Workshop on Seismic Fault-Induced Failures – Possible Remedies for Damage to Urban Facilities*, University of Tokyo Press, 55-79
- Bray JD, Seed RB, Cluff LS, and Seed HB (1994a) "Earthquake fault rupture propagation through soil", *Journal of Geotechnical Engineering*, 120 (3): 543-561
- Bray JD, Seed RB, and Seed HB (1994b) "Analysis of earthquake fault rupture propagation through cohesive soil", *Journal of Geotechnical Engineering*, 120 (3): 562-580
- Cole DA, and Lade PV (1984) "Influence zones in alluvium over dip-slip faults", *Journal of Geotechnical Engineering*, 110 (5): 599-615
- Earthquake Engineering Research Institute (2001) Bhui, India Republic, January 26, 2001. Earthquake Reconnaissance Report, (EERI)
- Eurocode 8 (2003) Design of structures for earthquake resistance, Part 5: Foundations, retaining structures and geotechnical aspects, CEN-ENV, European Committee for Standardization, Brussels
- Federal Highway Administration (2001) Mechanically stabilized earth walls and reinforced soil slopes design and construction guidelines, FHWA, National Highway Institute, Office of Bridge Technology
- Fishman KL and Pal S (1994) "Further study of geomembrane/cohesive soil interface shear behavior", *Geotextiles and Geomembranes*, 13 (9): 571-590
- Koerner RM (2000) "Emerging and future developments of selected geosynthetic applications", *Journal of Geotechnical and Geoenvironmental Engineering*, 126(4): 291-306
- Koerner RM, Martin JP and Koerner GR (1986) "Shear strength parameters between geomembranes and cohesive soils", *Geotextiles and Geomembranes* 4: 21-30
- Kramer SL, and Smith MW (1997) "Modified Newmark model for seismic displacements of compliant slopes", *Journal of Geotechnical and Geoenvironmental Engineering*, 123(7): 635-644
- Lade PV, Cole DA, and Cummings D (1984), "Multiple failure surfaces over dip-slip faults", *Journal of Geotechnical Engineering*, 110 (5): 616-627
- Lin M-L, Chung C-F, and Jeng F-S (2006) "Deformation of overburden soil induced by thrust fault slip," *Engineering Geology*, 88: 70-89
- Matasovic N, Kavazanjian EJ, and Anderson R (1998) "Performance of solid waste landfills in earthquakes," *Earthquake Spectra* 14(2): 319-334
- Newmark NM (1965) "Effect of earthquakes on dams and embankments", *Geotechnique* 15(2): 139-160
- Papadimitriou A, Loukidis D, Bouckovalas G, and Karamitros D (2007) "Zone of excessive ground surface distortion due to dip-slip fault rupture", *Proceedings of the 4th International Conference on Earthquake Geotechnical Engineering*, Thessaloniki, Greece, June 25-28
- Rathje EM, and Bray JD (2000) "Nonlinear coupled seismic sliding analysis of earth structures", *Journal of Geotechnical and Geoenvironmental Engineering*, 126(11): 1002-1013
- Yegian MK, Kadakal U, and Catan M (1999) "Geosynthetic for Earthquake Hazard Mitigation", *Geosynthetics '99*, Boston, Mass., April
- Zania V, Tsompanakis Y, Psarropoulos PN, Papadimitriou AG (2008a) "Failure mechanisms of landfills under dynamic loading", *Proceedings of ASCE Geotechnical Earthquake Engineering and Soil Dynamics IV Conference*, Sacramento, May 18-22
- Zania V, Tsompanakis Y, and Psarropoulos PN (2008b) "Fault rupture and kinematic distress of earth filled embankments", *Proceedings of 14th World Conference on Earthquake Engineering*, Beijing, China, October 12-17

# ΤΙΜΗΤΙΚΕΣ ΔΙΑΚΡΙΣΕΙΣ ΕΛΛΗΝΩΝ ΓΕΩΤΕΧΝΙΚΩΝ

To Institution of Civil Engineers τίμησε τον **Π. Ντακούλα**, Αναπληρωτή Καθηγητή του Πανεπιστημίου Θεσσαλίας, και τον **Γ. Γκαζέτα**, Καθηγητή του Εθνικού Μετσοβίου Πολυτεχνείου, μέλη της ΕΕΕΕΓΜ, με το βραβείο **HSIEH AWARD 2009** για το καλύτερο άρθρο σε θέματα δυναμικής του εδάφους και των κατασκευών στα περιοδικά του. Το άρθρο έχει τίτλο «**Insight into seismic earth and water pressures against caisson quay walls**» και δημοσιεύθηκε στο επιστημονικό περιοδικό **Geotechnique** το 2008.

Dakoulas, P. & Gazetas, G. (2008). *Geotechnique* 58, No. 2, 95–111 [doi: 10.1680/geot.2008.58.2.95]

## Insight into seismic earth and water pressures against caisson quay walls

P. DAKOULAS\* and G. GAZETAS†

Motivated by the need to explain the large displacement and rotation that numerous caisson-type quay walls suffered in the port of Kobe during the devastating 1995 earthquake, a detailed numerical analysis is presented for the response of such a wall from Rokko Island. Utilising the Pastor–Zienkiewicz elasto-plastic constitutive model, an effective stress dynamic analysis is performed using as input the accelerogram recorded 32 m below the ground surface in the nearby Port Island. The evolution during shaking of lateral displacements, plastic strains and pore water pressures sheds some light on the complex interplay of several simultaneously occurring phenomena: the development of oscillatory inertia forces on the wall, in phase or out of phase with the backfill soil and water pressures; the simple-shear seismic deformation of the soil and the ensuing initial development of positive excess pore water pressures in the backfill and the foundation soil; the extensional deformation developing in the ‘active wedge’ behind the wall, with the ensuing generation of negative excess pore water pressures; and the continuous dissipation and redistribution of water pressures. The conventional generalised Mononobe–Okabe theory is also reviewed, and extensive comparisons are made with the numerically computed effective and water pressures against the wall. Finally, a surprising role of the relative density of rubble behind the wall is highlighted.

**KEYWORDS:** case history; earth pressure; earthquakes; liquefaction; numerical modelling; retaining walls

\* Department of Civil Engineering, University of Thessaly, Volos, Greece.

† School of Civil Engineering, National Technical University, Athens, Greece.

Επίσης, οι συγγραφείς έχουν προσκληθεί από το Institution of Civil Engineers / Society for Earthquakes and Civil Engineering Dynamics (SECED) να παρουσιάσουν το εν λόγω ερευνητικό τους έργο στο Λονδίνο.

**Subject: T K Hsieh Prize**

**Dear Professors Dakoulas and Gazetas**

On behalf of the SECED committee I would like to congratulate you, once more, on your recent award of the T K Hsieh prize.

SECED would be delighted to host a lecture on your winning paper which appeared in *Geotechnique* (**March 2008 issue**)

*“Insight into seismic earth and water pressures against caisson quay walls”*

at the Institution of Civil Engineers in London. The paper was very well received by the Geotechnics and Earthquake Engineering communities in London. Therefore, we are convinced that such a lecture would be of great interest to both academics and practising engineers in the UK. The timing of the lecture can be arranged at your convenience (i.e. you might wish to combine it with any other activities you might have in London).

Regards

Stavroula Kontoe

Society for Earthquakes and Civil Engineering Dynamics,  
Institution of Civil Engineers Associated Society, United Kingdom



Ο Καθηγητής της Σχολής Πολιτικών Μηχανικών του Εθνικού Μετσοβίου Πολυτεχνείου και μέλος της ΕΕΕΕΓΜ **Παύλος Μαρίνος** επελέγη από τη Γεωλογική Εταιρία της Αμερικής (GSA) από κοινού με την Ένωση Τεχνικών Γεωλόγων της ίδιας χώρας (AEG), ως ο «**2010 Richard Jahns Distinguished Lecturer**». Ο θεσμός χρονολογείται από το 1988 και για πρώτη φορά προκρίνεται μη Αμερικανός επιστήμων. Επιλέγεται κάθε χρόνο επιστήμων ο οποίος μέσω της «εξαιρετικής του έρευνας έχει συμβάλει στην προαγωγή της Τεχνικής Γεωλογίας και που τα αποτελέσματα της έρευνας αυτής είναι επίκαιρα». Ο επιλεγείς παρουσιάζει σειρά διαλέξεων κυρίως στα πιο σημαντικά Πανεπιστήμια (Σχολές Γεωλογίας, Πολιτικού Μηχανικού και Μεταλλειολόγων Μηχανικών) στις περισσότερες πολιτείες των Ηνωμένων Πολιτειών και σε Ιδρύματα του Καναδά. Προγραμματίζονται περί τις 60 διαλέξεις που θα πραγματοποιηθούν το πρώτο εξάμηνο του 2010.

# ΠΡΟΣΕΧΕΙΣ ΓΕΩΤΕΧΝΙΚΕΣ ΕΚΔΗΛΩΣΕΙΣ

Για τις παλαιότερες καταχωρήσεις περισσότερες πληροφορίες μπορούν να αναζητηθούν στα προηγούμενα τεύχη του «περιοδικού» και στις παρατιθέμενες ιστοσελίδες.

Stuva Tagung'09 – Stuva Conference'09 "Tunnels – Key to Sustainable Mobility", 1-3 December 2009, CCH Hamburg, Germany, [www.stuva.de/STUVA-Conference-09.tagung.0.html?&L=1](http://www.stuva.de/STUVA-Conference-09.tagung.0.html?&L=1)

International Symposium on Geotechnical Engineering, Ground Improvement, and Geosynthetics for Sustainable Mitigation and Adaptation to Climate Change including Global Warming, 3 to 4 December 2009, Bangkok, Thailand, [www.set.ait.ac.th/acsig/conference](http://www.set.ait.ac.th/acsig/conference)

International Symposium on Ground Improvement Technologies and Case Histories (ISGI09), 9 to 11 December 2009, Singapore, [ISGI09@nus.edu.sg](mailto:ISGI09@nus.edu.sg)

Conference on Improving the Seismic Performance of Existing Buildings and Other Structures, 9 – 11 December 2009, San Francisco, USA, [www.atc-sei.org](http://www.atc-sei.org)

13<sup>th</sup> International Conference on Structural & Geotechnical Engineering, Cairo, Egypt, 27-29 December 2009, [www.icsg2009.com](http://www.icsg2009.com)

GeoFlorida - Advances in Analysis, Modeling & Design, February 20-24, 2010, West Palm Beach, Florida, USA [content.asce.org/conferences/geoflorida2010/index.html](http://content.asce.org/conferences/geoflorida2010/index.html)

CAVING 2010 Second International Symposium on Block and Sublevel Caving, 20 – 22 April 2010, Perth, Australia, [www.caving2010.com](http://www.caving2010.com)

CPT'10 2<sup>nd</sup> International Symposium on Cone Penetration Testing, May 9 - 11, 2010, Huntington Beach, California, USA.

The Seventeenth South Asian Geotechnical Conference, Taipei, Taiwan, May 10 – 13, 2010, [www.17seagc.tw](http://www.17seagc.tw)

ITA – AITES 1010 World Tunnel Congress and 36<sup>th</sup> General Assembly "TUNNEL VISION TOWARDS 2020", Vancouver, Canada, May 14 - 20, 2010, [www.wtc2010.org](http://www.wtc2010.org)

12<sup>o</sup> Διεθνές Συνέδριο της Ελληνικής Γεωλογικής Εταιρείας, Πάτρα, 19 - 22 Μαΐου 2010, [www.synedra.gr](http://www.synedra.gr)

78th ICOLD Annual Meeting & International Symposium "DAMS AND SUSTAINABLE WATER RESOURCES DEVELOPMENT", 23 – 26 May 2010, Hanoi, Vietnam, [www.vncold.vn/icold2010](http://www.vncold.vn/icold2010)

IX International Conference on Geosynthetics, Guarujá, Brazil, 23 – 27 May 2010 - [www.igsbrasil.org.br/icg2010](http://www.igsbrasil.org.br/icg2010)

Fifth International Conference on Recent Advances in Geotechnical Earthquake Engineering and Soil Dynamics and Symposium in Honor of Professor I. M. Idriss, May 24 – 29, 2010, San Diego, California, USA, [5geoeqconf2010.mst.edu](http://5geoeqconf2010.mst.edu)

11<sup>th</sup> International Conference "Geotechnical Challenges in Urban Regeneration", 26<sup>th</sup> – 28<sup>th</sup> May 2010, ExCel London, [www.geotechnicalconference.com/page.cfm/Link=20](http://www.geotechnicalconference.com/page.cfm/Link=20)

Tenerife 2010 Cities on Volcanos, 3rd International Workshop on Rock Mechanics and Geo-engineering in Volcanic Environments, Canary Islands, 31st of May and 1st of June 2010, [www.citiesonvolcanoes6.com](http://www.citiesonvolcanoes6.com)

BRATISLAVA 2010 14<sup>th</sup> Danube-European Conference on Geotechnical Engineering, Bratislava, Slovakia, 2<sup>nd</sup> – 4<sup>th</sup> June 2010, [www.decge2010.sk](http://www.decge2010.sk)

NUMGE 2010 7th European Conference on Numerical Methods in Geotechnical Engineering June 2 - 4, 2010, Trondheim, Norway, [www.ivt.ntnu.no/numge2010](http://www.ivt.ntnu.no/numge2010)

2010 MOSCOW - International Geotechnical Conference GEOTECHNICAL CHALLENGES IN MEGACITIES, 7 – 10 June 2010, Moscow, Russia [www.GeoMos2010.ru](http://www.GeoMos2010.ru)

International Conference Underground Construction Prague 2010 Transport and City Tunnels, 14 – 16 June 2010, Prague, Czech Republic, [www.ita-aites.cz](http://www.ita-aites.cz)

Rock Mechanics in Civil and Environmental Engineering, European Rock Mechanics Symposium (EUROCK 2010) ISRM Regional Symposium on Rock Mechanics, Lausanne, Switzerland, 15 – 18 June 2010, [lmr.epfl.ch](http://lmr.epfl.ch)

7th International Conference on Physical Modelling in Geotechnics, Zurich, Switzerland, 28 June - 1 July 2010, [www.icpmg2010.ch](http://www.icpmg2010.ch)

ER2010 Earth Retention Conference 3, August 1 – 4 2010, Bellevue, Washington, USA, [content.asce.org/conferences/er2010](http://content.asce.org/conferences/er2010)

Isap Nagoya 2010 - The 11<sup>th</sup> International Conference on Asphalt Pavements, August 1 to 6, 2010, Nagoya, Japan, [www.isap-nagoya2010.jp](http://www.isap-nagoya2010.jp)

ISRS V The 5<sup>th</sup> International Symposium on In-Situ Rock Stress, August 25-28, 2010 Beijing, China, [www.rockstress2010.org](http://www.rockstress2010.org)

Pipelines Conference 2010, August 28 - September 1, 2010, Keystone Resort & Conference Center, Keystone, (Dillon) Colorado, [content.asce.org/conferences/pipelines2010/call.html](http://content.asce.org/conferences/pipelines2010/call.html)

14th European Conference on Earthquake Engineering, Ohrid, FYROM, August 30 – September 3 2010, [www.14ecee.mk](http://www.14ecee.mk)

Geologically Active 11th IAEG Congress, 5 – 10 September 2010, Auckland, New Zealand, [www.iaeg2010.com](http://www.iaeg2010.com)

GBR-C 2k10 - 3rd International Symposium on Geosynthetic Clay Liners, 15 - 16 September 2010, Würzburg, Germany



**1<sup>st</sup> International Conference on  
Information Technology in Geo-Engineering  
16-17 September 2010, Tongji University, Shanghai  
[geotec.tongji.edu.cn/ICITG2010](http://geotec.tongji.edu.cn/ICITG2010)**

1st International Conference on Information Technology in Geo-Engineering (ICITG-Shanghai 2010) will be held on 16-17 Sep, 2010, in Tongji University in Shanghai, China.

It will be held under the auspices of both the JTC2 Committee, the International Society of Soil Mechanics and Geotechnical Engineering (ISSMGE) and Chinese researchers of Geotechnical Engineering.

Information technology has changed every aspect of our lives, and has experienced increasing applications in Geo-Engineering. It has played more and more important role in the investigation, design, construction and maintenance of Geo-Engineering. In addition, innovative information technology concepts, strategies and equipments keep emerging and have been applied to Geo-Engineering to improve efficiency and ensure safety. The conference aims to provide a showcase for scientists, developers and engineers to review recent developments and advancements of information technology in Geo-Engineering, and offer a forum to discuss and debate future directions. In addition, it will invite several well-known researchers to give keynote lectures on these topics.

Main Topics:

- Information Management System
- Data Standardization
- Simulation and Visualization
- Virtual Reality and Augmented Reality
- Artificial Intelligence Techniques
- Novel Computational Techniques
- Data Acquisitions and Monitoring
- Database and Data Mining
- High-performance computing
- Geo-Modeling
- Geo-Informatics
- Numerical Methods for Geo-Engineering
- Integration of Geo-model and Numerical Model
- Applications of IT

For more information, please contact:

Prof. Hehua Zhu  
Department of Geotechnical Engineering, Tongji University  
1239 Siping Rd., Shanghai 200092, China  
Tel: +86-21-65985014/5220  
Fax: +86-21-65985140  
E-mail: [zhuhehua@tongji.edu.cn](mailto:zhuhehua@tongji.edu.cn)

Prof. David Toll  
School of Engineering, University of Durham, Durham, DH1 3LE, UK  
Tel: (+44/0) 191 334 2388  
Fax: (+44/0) 191 334 2390  
Email: [d.g.toll@durham.ac.uk](mailto:d.g.toll@durham.ac.uk)

Associate Prof. Xiaojun Li  
Department of Geotechnical Engineering, Tongji University  
1239 Siping Rd., Shanghai 200092, China  
Tel: +86-21-65985174  
Fax: +86-21-65985140  
E-mail: [lixiaojun@tongji.edu.cn](mailto:lixiaojun@tongji.edu.cn)



II International Congress on Dam Maintenance and Rehabilitation, 28th-30th September 2010, Zaragoza, Spain  
[www.damrehabilitationcongress2010.com](http://www.damrehabilitationcongress2010.com)

International Symposium on Geomechanics and Geotechnics: From Micro to Macro 10 - 12 October 2010, Shanghai, China, [geotec.tongji.edu.cn/is-shanghai2010](http://geotec.tongji.edu.cn/is-shanghai2010)

11<sup>th</sup> International Symposium on Concrete Roads, Seville (Spain) 13th - 15th October 2010, [www.2010pavimentosdehormigon.org](http://www.2010pavimentosdehormigon.org)

ARMS - 6 ISRM International Symposium 2010 and 6<sup>th</sup> Asian Rock Mechanics Symposium "Advances in Rock Engineering", New Delhi, India, 23 - 27 October 2010, [www.cbip.org](http://www.cbip.org)

2nd International Conference on Geotechnical Engineering - ICGE 2010 Innovative Geotechnical Engineering, October 2010, Hammamet, Tunisia

ICSE-5 5<sup>th</sup> International Conference on Scour and Erosion, 7 - 10 November 2010, San Fransisco, USA, [www.icse-5.org](http://www.icse-5.org)

ISFOG 2010 2<sup>nd</sup> International Symposium on Frontiers in Offshore Geotechnics, 8 - 10 November 2010, Perth, Western Australia, [w3.cofs.uwa.edu.au/ISFOG2010](http://w3.cofs.uwa.edu.au/ISFOG2010)

6ICEG 2010 - Sixth International Congress on Environmental Geotechnics, November 8 - 12, 2010, New Delhi, India [www.6iceg.org](http://www.6iceg.org)

5<sup>th</sup> International Conference on Earthquake Geotechnical Engineering, Santiago, Chile, 17 - 20 January 2011, [www.5icege.cl](http://www.5icege.cl)

International Conference on Tunnelling and Trenchless Technology, 1-3 March 2011, Kuala Lumpur (Malaysia), [www.iem.org.my/external/tunnel/index.htm](http://www.iem.org.my/external/tunnel/index.htm)



## **GEO-FRONTIERS 2011**

13-16 March | Dallas, Texas USA | Sheraton Dallas Hotel

**Advances in Geotechnical Engineering**  
[www.geofrontiers11.com](http://www.geofrontiers11.com)

The objective of Geo-Frontiers 2011 is to share new developments in geotechnical engineering technologies. Attendees will be exposed to the latest state of the art and practice as applied to geotechnical engineering.

For information contact:

Barbara Connett, Technical Program  
Direct: + 1 651 225 6914  
[biconnett@ifai.com](mailto:biconnett@ifai.com)



WTC2011 Helsinki, AITES-ITA 2011 World Tunnel Congress and 37th General Assembly, 21-25 May 2011, Helsinki, Finland, [www.ril.fi/web/index.php?id=641](http://www.ril.fi/web/index.php?id=641)

XIV Asian Regional Conference Soil Mechanics and Geotechnical Engineering, Hong Kong, China, 23 - 28 May 2011



## IS - SEOUL 2011

### Fifth International Symposium on Deformation Characteristics of Geomaterials

Wednesday-Friday, Aug. 31-Sep. 3, 2011 Seoul, Korea

[www.isseoul2011.org](http://www.isseoul2011.org)

**IS-Seoul 2011** provides a unique forum to discuss the knowledge of the complex deformation response in geomaterials. IS-Seoul 2011 is prepared under the success of previous symposia: IS-Hokkaido 1994, IS-Torino 1999, IS-Lyon 2003, and IS-Atlanta 2008. This symposium focuses on the understanding of the deformation properties of geomaterials before failure, and especially on pointing out the small strain shear modulus as a fundamental characteristic of geomaterials.

The IS-Seoul 2011 will be an ideal place where you can exchange your ideas with colleagues via the discussions in the session, and the conference papers. The IS-Seoul 2011 will host the first Bishop Lecture sponsored by the International Society of Soil Mechanics and Geotechnical Engineering (TC29) and provide an opportunity to publish peer-reviewed journal papers in "Soils and Foundations". A one-day short course will be held in combination with IS-Seoul 2011 on Tuesday, August 30, 2011.

Goals of the Symposium:

- Research and developments in advanced laboratory geotechnical testing, including apparatus, techniques, data acquisition and interpretation.
- Applications of advanced laboratory and field testing to integrated site characterization and ground modelling.
- Demonstrating the value of practical engineering applications. This involves reporting collaborative studies on laboratory and field testing, sampling, theoretical and numerical analysis, project engineering and full scale observation.

Themes

I. Experimental Investigations from very small strains to beyond failure

- 1) Advances in laboratory and field methods
- 2) Data interpretation and geotechnical imaging
- 3) Multi scale problems in geomechanics (micro-to-macro strain)
- 4) Advanced sampling
- 5) Behaviour at geotechnical interfaces

II. Behaviour, characterisation and modelling of various geomaterials

- 6) Physical and numerical modelling
- 7) Anisotropy and localization
- 8) Time dependent responses (ageing, viscous and cycling effects)

- 9) Special characteristics of particular geomaterials:
  - Unsaturated soils,
  - Cemented and stabilized soils,
  - Frozen soils including hydrates,
  - Mixtures (soils with inclusions)

III. Practical prediction and interpretation of ground response: field observation and case histories

- 10) Integrated site characterization
- 11) Performance evaluation of geotechnical structures
- 12) New field methods of ground deformation measurement

Contact:

Professor Dong-Soo Kim  
KAIST Department of Civil and Environmental Engineering  
335, Gwahangno, Yuseong-gu, Daejeon, 305-701, Korea  
Email: [mailto:dskim@kaist.ac.kr](mailto:mailto:dskim@kaist.ac.kr)  
Tel: +82-42-350-5659  
Fax: +82-42-350-7200



## 6th International Symposium on Sprayed Concrete

12-15 September 2011, Tromsø, Norway  
[www.sprayedconcrete.no](http://www.sprayedconcrete.no)

WELCOME TO NORWAY AND TROMSØ

The Norwegian Concrete Society has been a leading participant regarding the use of wet-mix sprayed concrete for many years. It is therefore with great pleasure that we announce the Sixth International Symposium on the MODERN USE OF WET-MIX SPRAYED CONCRETE FOR UNDERGROUND SUPPORT. This conference will be located in Tromsø, in the north of Norway.

We sincerely hope that many of our international colleagues will again take the opportunity to present papers, exchange experiences and discuss the latest developments in wet-mix sprayed concrete.

The main symposium themes will be design, construction and durability of wet-mix sprayed concrete in underground structures. In view of the latest incidences in Norway regarding failure in the rock support system in a highway tunnel, the support philosophy has been heavily debated in Norway. The Norwegian Concrete Association is currently revising the Publication No 7, Sprayed Concrete for Rock Support – Technical Specification, Guidelines and Test Methods. This publication will be debated during the symposium.

Wet-mix sprayed concrete technology has been further developed to a much higher level since the first symposium in 1993, with the latest developments in chemical additives, application equipment and fibers. It will continue to change, and the sixth International Symposium in Tromsø will ensure that delegates are kept abreast of the new developments in the use of this material.

**Tromsø – the gateway to the Arctic.** The city of Tromsø; the Gateway to the Arctic, with the most Northern Lights in the world, 2 months of Midnight Sun, a lively, colourful downtown rich in Arctic history, surrounded by the drama of the Lyngen Alps, blue fjords and hundreds of islands, is a surprise a mere 2000 km from the North Pole.

Tromsø is the largest city in the Nordic countries north of the Arctic Circle and is home to the world's northernmost university, brewery and cathedral. The city lives on education, research, administration, fishing exports and satellite technology. The centre of the north has 64492 residents and the Municipality of Tromsø covers an area of 2558 km<sup>2</sup>. Around 50,000 live in the centre of Tromsø, while the remainder is scattered throughout the whole municipality.

We are looking forward to see you at the symposium in Tromsø in the autumn of 2011.

The Symposium will focus on wet mix fibre reinforced sprayed concrete for underground support.

There will be four main sessions consisting of invited and submitted papers, followed by discussions.

#### **Support design**

- \* Geological conditions
- \* Load capacity
- \* Rock mass classification
- \* Squeezing and swelling rock
- \* Water leakage
- \* Frost action
- \* Fire performance
- \* Rock burst and spalling
- \* Design methods and criteria
- \* Case histories

#### **Durability**

- \* Environmental exposure
- \* Early and long term capacity
- \* Sprayed concrete mix design
- \* Saline water
- \* Alkali aggregate reaction
- \* Frost
- \* Deformations, loading
- \* Critical parameters
- \* Service Life prediction
- \* Case histories of performance

#### **Codes and specifications**

- \* Health and safety
- \* Design of reinforcement
- \* Concrete materials
- \* Admixtures for sprayed concrete
- \* Use of fibres, ductility
- \* Quality Assurance
- \* Nozzle man certification
- \* Testing and documentation
- \* Fire protection with sprayable system and sprayed concrete

#### **Construction / mining**

- \* Spraying equipment
- \* Use of fibres and admixtures
- \* Spraying technique
- \* Water and frost protection
- \* Case histories

#### **CONTACT INFORMATION**

Mrs. Siri Engen  
The Norwegian Society of Chartered Technical and Scientific Professionals (Tekna)  
P.O.Box 2312, Solli  
N-0201 OSLO, NORWAY  
Fax: +47 22 94 75 01  
E-mail: [siri.engen@tekna.no](mailto:siri.engen@tekna.no)

XV European Conference on Soil Mechanics and Geotechnical Engineering, 12 – 15 September 2011, Athens, Greece, [www.athens2011ecsmge.org](http://www.athens2011ecsmge.org)

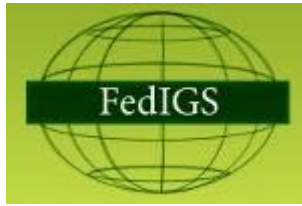
24<sup>th</sup> WORLD ROAD CONGRESS, 25 – 30 September 2011, Mexico City, Mexico

XIV Panamerican Conference on Soil Mechanics and Geotechnical Engineering (October) & V PanAmerican Conference on Learning and Teaching of Geotechnical Engineering & 64th Canadian Geotechnical Conference, Toronto, Ontario, Canada, 2 - 6 October 2011

Beijing 2011, 12<sup>th</sup> International Congress on Rock Mechanics, 16 – 21 October 2011, Beijing, China, [www.isrm2011.com](http://www.isrm2011.com)



# ΝΕΑ ΑΠΟ ΤΙΣ ΔΙΕΘΝΕΙΣ ΓΕΩΤΕΧΝΙΚΕΣ ΕΝΩΣΕΙΣ



**FEDERATION OF  
INTERNATIONAL GEOENGINEERING SOCIETIES**  
[www.issmge.org](http://www.issmge.org)

The website of the Federation of International Geoengineering Societies ([www.fedigs.org](http://www.fedigs.org)) is now online and regularly updated with information on the FedIGS's activities.

FedIGS was founded by the three learned Societies ISSMGE, ISRM, IAEG, on the principle that each of the participating associations/societies, whenever joining FedIGS, will retain its identity and autonomy.

The role of the Federation is to carry out functions for the international geo-engineering community that could not be carried out with the same effectiveness and efficiency by the Members individually.

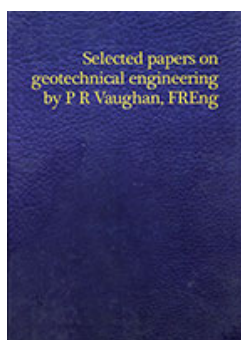
# ΝΕΕΣ ΕΚΔΟΣΕΙΣ ΣΤΙΣ ΓΕΩΤΕΧΝΙΚΕΣ ΕΠΙΣΤΗΜΕΣ

## Rapid Load Testing on Piles

Paul Holscher and Frits A. van Tol

To obtain data about the stiffness and bearing capacity of a foundation pile, the Rapid Load Test could be an effective and economic alternative for a static load test. In order to judge this, the influence of rate effects in clay and pore water pressures in sand should first be understood. This book presents the latest developments in the research that is carried out to unravel these effects. It contains current contributions by world wide leading academics. Moreover the editors summarize the empirical field data and discuss advanced centrifuge modeling. This indispensable information source on the progress in Rapid Load Testing is intended for researchers and professionals working on the load testing of foundation piles.

(CRC Press, Taylor & Francis Group, December 2008)



## Selected Papers on Geotechnical Engineering by P R Vaughan, FREng

Peter R Vaughan

This book brings together twenty of the most important papers by the late Professor Peter Rolfe Vaughan on geotechnical engineering. Selected by Peter's closest colleagues at Imperial College and the Geotechnical Consulting Group, these papers were reproduced along with the obituary published in Géotechnique, a full listing of his bibliography, some photographs and personal reflections by David Hight, David Potts, Nebojša Kovacevic and Finlay Jardine on working with Peter.

These papers illustrate Peter's academic work and his considerable impact on civil engineering practice. Many of the papers were awarded distinguished prizes and some are drawn from sources that are now hard to access. This volume will be valuable to researchers, practitioners and all those who studied or worked with Peter.

(Thomas Telford, Ltd, 2009)



## Offshore Geotechnical Engineering

E.T. Richard Dean

With activity in the engineering of offshore structures increasing around the world, Offshore geotechnical engineering offers a timely in-

Offshore  
geotechnical  
engineering  
Principles and practice  
E. T. R. Dean

roduction to many of the core design and assessment skills required of those working in the sector, in accordance with the latest codes and standards.

All major aspects of the subject are covered in depth, including offshore site investigation, surveys, soil mechanics, jackups, jacket platforms, gravity platforms, pipelines, artificial islands, wind turbine support structures, and deepwater solutions. The author provides extensive practical guidance on the assessment of geohazards and site-specific soils data, and on how this is applied to the design, installation, maintenance, and eventual de-commissioning of offshore structures and their foundations.

Through the use of real examples and case studies, the reader is provided with the knowledge to:

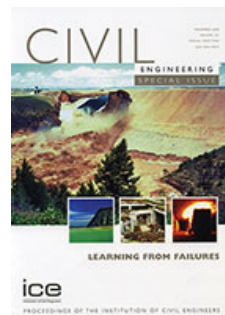
- identify the principal geotechnical issues for offshore developments
- prepare for common challenges of offshore geotechnical engineering
- design a programme of offshore investigations
- carry out and manage design calculations

The first book to offer this information in a single place, Offshore geotechnical engineering is a comprehensive resource that will appeal to a broad spectrum of sectors – as a structured basic training for those entering the field, a comprehensive introductory text for students and lecturers, and a highly useful reference for those already working in offshore geotechnical engineering.

## Contents

- Disclaimers
- Preface
- Dedication
- Acknowledgements
- Contents
- Abbreviations & Notation
- Codes of Practice
- Useful websites
- Introduction
- Offshore surveys and site investigations
- Soil mechanics
- Jackup Platforms
- Jacket Platforms
- Gravity Platforms
- Pipelines, flowlines, cables and risers
- Artificial islands
- Deep and ultra-deep water
- Renewable energy
- References

(Thomas Telford Ltd, 27 November 2009)



## Learning from Failures: A Civil Engineering Special Issue

This special issue of the highly respected Civil Engineering journal from the Proceedings of the Institution of Civil Engineers looks to study and learn from the catastrophes,

collapses and failures that fascinate and horrify the civil engineering community.

(Thomas Telford, Ltd, 2009)



### **Seismic Risk Assessment and Retrofitting**

With Special Emphasis on Existing Low Rise Structures  
Series: Geotechnical, Geological, and Earthquake Engineering, Vol. 10

**Ilki, A., Karadogan, F., Pala, S. & Yuksel, E. (Editors)**

Many more people are coming to live in earthquake-prone areas, especially urban ones. Many such areas contain low-rise, low-cost housing, while little money is available to retrofit the buildings to avoid total collapse and thus potentially save lives. The lack of money, especially in developing countries, is exacerbated by difficulties with administration, implementation and public awareness.

The future of modern earthquake engineering will come to be dominated by new kinds of measuring technologies, new materials developed especially for low-rise, low-cost buildings, simpler and thus lower cost options for retrofitting, cost cutting and raising public awareness.

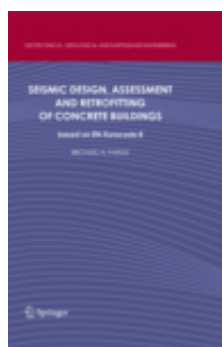
The book covers all the areas involved in this complex issue, from the prevention of total building collapse, through improvement techniques, to legal, financial, taxation and social issues.

The contributors have all made valuable contributions in their own particular fields; all of them are or have been closely involved with the issues that can arise in seismic zones in any country. The recent research results published here offer invaluable pointers to practicing engineers and administrators, as well as other scientists whose work involves saving the lives and property of the many millions of people who live and work in hazardous buildings.

#### **Written for:**

Researchers and scientists in applied geoscience (geology; geophysics; physical geography), engineering (civil, system analysis, municipal) and architecture; consulting engineers and other professionals dealing with risk assessment, construction, civil protection planning and emergency, urban planning, insurance

(Springer, 2009)



### **Seismic Design, Assessment and Retrofitting of Concrete Buildings**

based on EN-Eurocode 8  
Series: Geotechnical, Geological, and Earthquake Engineering, Vol. 8

**Fardis, Michael N.**

Reflecting the historic first European

seismic code, this professional book focuses on seismic design, assessment and retrofitting of concrete buildings, with thorough reference to, and application of, EN-Eurocode 8. Following the publication of EN-Eurocode 8 in 2004-05, 30 countries are now introducing this European standard for seismic design, for application in parallel with existing national standards (till March 2010) and exclusively after that. Eurocode 8 is also expected to influence standards in countries outside Europe, or at the least, to be applied there for important facilities. Owing to the increasing awareness of the threat posed by existing buildings substandard and deficient buildings and the lack of national or international standards for assessment and retrofitting, its impact in that field is expected to be major.

Written by the lead person in the development of the EN-Eurocode 8, the present handbook explains the principles and rationale of seismic design according to modern codes and provides thorough guidance for the conceptual seismic design of concrete buildings and their foundations. It examines the experimental behaviour of concrete members under cyclic loading and modelling for design and analysis purposes; it develops the essentials of linear or nonlinear seismic analysis for the purposes of design, assessment and retrofitting (especially using Eurocode 8); and gives detailed guidance for modelling concrete buildings at the member and at the system level. Moreover, readers gain access to overviews of provisions of Eurocode 8, plus an understanding for them on the basis of the simple models of the element behaviour presented in the book.

Also examined are the modern trends in performance- and displacement-based seismic assessment of existing buildings, comparing the relevant provisions of Eurocode 8 with those of new US prestandards, and details of the most common and popular seismic retrofitting techniques for concrete buildings and guidance for retrofitting strategies at the system level. Comprehensive walk-through examples of detailed design elucidate the application of Eurocode 8 to common situations in practical design. Examples and case studies of seismic assessment and retrofitting of a few real buildings are also presented.

#### *From the reviews:*

"This is a massive book that has no equal in the published literature, as far as the reviewer knows. It is dense and comprehensive and leaves nothing to chance. It is certainly taxing on the reader and the potential user, but without it, use of Eurocode 8 will be that much more difficult. In short, this is a must-read book for researchers and practitioners in Europe, and of use to readers outside of Europe too. This book will remain an indispensable backup to Eurocode 8 and its existing Designers' Guide to EN 1998-1 and EN 1998-5 (published in 2005), for many years to come. Congratulations to the author for a very well planned scope and contents, and for a flawless execution of the plan". *AMR S. ELNASHAI*

"The book is an impressive source of information to understand the response of reinforced concrete buildings under seismic loads with the ultimate goal of presenting and explaining the state of the art of seismic design. Underlying the contents of the book is the in-depth knowledge of the author in this field and in particular his extremely important contribution to the development of the European Design Standard EN 1998 - Eurocode 8: Design of structures for earthquake resistance. However, although Eurocode 8 is at the core of the book, many comparisons are made to other design practices, namely from the US and from Japan, thus enriching the contents and interest of the book". *EDUARDO C. CARVALHO*

(Springer, 2009)

## Bridginess

More of the Civil Engineering Life

Brian Brenner, et.



### **Bridginess: More of the Civil Engineering Life**

**Brian R. Brenner**

If you've ever been asked to calculate the live load for a herd of elephants...

If you've ever built a sand castle to study soil mechanics...

If you've ever had to choose between your date and your favorite bridge...

...Brian Brenner has written the book for you. *Bridginess: More of the Civil Engineering Life* finds Brenner turning his pen and his signature wit to the subjects of urban sprawl, airport infrastructure planning, and, of course, bridges. After reading this collection, you will know bridges from more angles than a through truss. You will think twice before placing a salad on the roof of your car. And you will know just what makes a truly great college response letter. These essays range from humorous to informative, autobiographical to historical. They encompass the full range of Brenner's talent as a writer, as well as an engineer. With his charming and fluid style, Brenner makes civil engineering funny, interesting, and at times, even glamorous.

Brian Brenner, P.E., is a vice president and structural engineer with Fay, Spofford and Thorndike in Burlington, Massachusetts. Brian's work includes bridge design projects throughout New England and the New York metropolitan area. Brian also contributes as a professor of the practice at Tufts University, where he teaches the bridge and concrete design classes and advises students on several research projects. In 2008, Brian received the Fischer Award, given to the Tufts Engineering School Professor of the Year.

(ASCE Press, 2009)



### **DID TIME BEGIN? WILL TIME END?**

**Maybe the Big Bang Never Occurred**

**Paul H Frampton** (University of North Carolina, USA)

Although everyone is familiar with the concept of time in everyday life and has probably given thought to the question of how time began, recent scientific developments in this field have not been accessible in a simple understandable form. This book is important as it presents to readers current ideas about the role of time in theoretical cosmology.

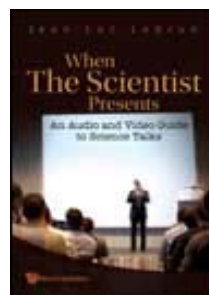
Recent observational discoveries, especially that the expansion rate of the universe is accelerating, have revolutionized the understanding of the energy content of the universe. This development leads to new possibilities for the beginning and end of cosmological time. This book emphasizes the notion of entropy and describes how it is theoretically possible that the universe may end in a finite time or that time can cycle and never end.

Provided here is twenty-first century scientific knowledge, written by one of the world's most eminent theoretical physicists, that will better enable the public to discuss further the fascinating idea of time. It is ideally suited also for young people considering a career in scientific research.

#### **Contents:**

- Why do Many Other Scientists Believe Time Began at a Big Bang?
- Smoothness of the Universe
- Structure in the Universe
- Dark Matter and Dark Energy
- Composition of the Universe's Energy
- Possible Futures of the Universe
- Advantages of Cyclic Cosmology
- Summary of Answers to the Questions: Did Time Begin? Will Time End?

(World Scientific, September 2009)



### **WHEN THE SCIENTIST PRESENTS**

**Jean-Luc Lebrun** (Trainer of researchers and scientists from A\*STAR Research Institutes, Singapore & Former Director, Apple-ISS Research Centre, Singapore)

This book looks at the presenting scientist from a novel angle: the presenter-host. When scientists give a talk, the audience ("guests") expects the title of the talk to determine presentation content, they require understandable slides, and they demand visible and audible scientific authority. To each expectation corresponds a set of skills: personal (voice, host qualities, time control), technical (presentation tools and slide design), and scientific (Q&A, slide content).

The author takes an original human factor view of the presentation delivery, in which the audience is easily distracted, rapidly forgetful, and increasingly impatient. Thus, insightful pointers are given on how to deliver the talk, how to craft the slides, and how to prevent the computer from rendering the presenting host-scientist into a "ghost". In addition, the book goes in-depth over the treatment of questions by examining the motives and style of the questioners, and advising on how best to answer to each type of questioner.

The book comes with a DVD for audio and video examples, and includes essential PowerPoint and Keynote techniques that a presenter cannot live without.

#### **Contents:**

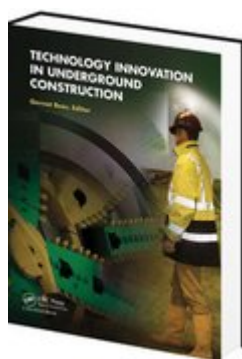
- **Content Selection:**
  - Paper and Oral Presentation: The Difference
  - Content Filtering Criteria
- **Audience Expectations:**
  - General Audience Expectations
  - Scientific Audience Expectations
- **The Slides:**
  - Five Slide Types, Five Roles
  - Slide Design

• **The Presenter:**

- The Master of Tools
- Scientist and Perfect Host
- The Grabbing Voice
- The Answerable Scientist

**Readership:** Students, graduates, postgraduates, and professionals seeking help in improving their scientific presentation skills.

(World Scientific, August 2009)



**Technology Innovation in Underground Construction**

**Gernot Beer (Editor) Institute for Structural Analysis, Graz University of Technology, Austria**

The results of the biggest research initiative on underground construction were presented recently at a two-day workshop and final event in an underground cultural facility Dom-im-Berg in Graz, Austria. The project lasted 4 years and involved 41 partners (clients, industry, SMEs, manufacturers, research institutions, Universities) from 11 countries of the European Union. The budget (financed 50% by the EC) was 26 Million Euros.

A book has been published "Technology Innovation in Underground Construction" which present highlights of the achievements of the projects. The chapters in the book have been grouped according to the main headings design, processes, equipments, materials and maintenance/repair with the last chapter describing some innovative exploratory technology.

Richly-illustrated reference guide presenting innovative techniques focused on reducing time, cost and risk in the construction and maintenance of underground facilities:

A primary focus in the technological development in underground engineering is to ease the practical execution and to reduce time, cost and risk in the construction and maintenance of underground facilities such as tunnels and caverns. This can be realized by new design tools for designers, by instant data access for engineers, by virtual prototyping and training for manufacturers, by robotic devices for maintenance and repair for operators and many more advances.

This volume presents the latest technological innovations in underground design, construction, and operation and comprehensively discusses novelties in ground improvement, simulation, process integration, safety, monitoring, environmental impact, equipment, boring and cutting, personnel training, materials, robotics and more. The novelties presented are the result of a big research project focussed on advancing underground engineering, in which many players in the discipline have been involved.

Written in an accessible style and with a focus on applied engineering, this book is aimed at a readership of engineers, consultants, contractors, operators, researchers, manufacturers, suppliers and clients in the underground engineering business. It may moreover be used as educa-

tional material for advanced courses in tunnelling and underground construction.

Readers of the ita@news can receive 20% discount by entering reduction code **616KE** upon checkout at **crcpress website** (<http://www.crcpress.com/product/isbn/9780415551052>). Offer valid until 31 December 2009

(CRC PRESS, October 16, 2009)

# ΗΛΕΚΤΡΟΝΙΚΑ ΠΕΡΙΟΔΙΚΑ



[www.geoengineer.org](http://www.geoengineer.org)

Κυκλοφόρησε το Τεύχος #59 του Newsletter του Geoengineer.org (Νοέμβριος 2009) με πολλές χρήσιμες πληροφορίες για όλα τα θέματα της γεωτεχνικής μηχανικής. Υπενθυμίζεται ότι το Newsletter εκδίδεται από τον συνάδελφο και μέλος της ΕΕΕΕΓΜ Δημήτρη Ζέκκο ([secretariat@geoengineer.org](mailto:secretariat@geoengineer.org)).



**INTERNATIONAL TUNNELLING AND  
UNDERGROUND SPACE ASSOCIATION**

[ita@news](mailto:ita@news) n°31

[www.ita-aites.org/cms/index.php?id=487](http://www.ita-aites.org/cms/index.php?id=487)

Κυκλοφόρησε το Τεύχος Νο. 31 – Οκτώβριος 2009 των ita@news της International Tunnelling Association.



[www.geosyntheticssociety.org/newsletters.htm#Nov09](http://www.geosyntheticssociety.org/newsletters.htm#Nov09)

Κυκλοφόρησε το τεύχος Αρ.3 του Τόμου 25, Νοέμβριος 2009 των Νέων της International Geosynthetic Society.

## **ΕΕΕΕΓΜ**

Τομέας Γεωτεχνικής  
ΣΧΟΛΗ ΠΟΛΙΤΙΚΩΝ ΜΗΧΑΝΙΚΩΝ  
ΕΘΝΙΚΟΥ ΜΕΤΣΟΒΙΟΥ ΠΟΛΥΤΕΧΝΕΙΟΥ  
Πολυτεχνειούπολη Ζωγράφου  
15780 ΖΩΓΡΑΦΟΥ

Τηλ. 210.7723434  
Τοτ. 210.7723428  
Ηλ-Δι. [secretariat@hssmge.gr](mailto:secretariat@hssmge.gr) ,  
[geotech@central.ntua.gr](mailto:geotech@central.ntua.gr)  
Ιστοσελίδα [www.hssmge.org](http://www.hssmge.org) (υπό κατασκευή)

«ΤΑ ΝΕΑ ΤΗΣ ΕΕΕΕΓΜ» Εκδότης: Χρήστος Τσατσάνιφος, τηλ. 210.6929484, τοτ. 210.6928137, ηλ-δι. [pangaea@otenet.gr](mailto:pangaea@otenet.gr)

«ΤΑ ΝΕΑ ΤΗΣ ΕΕΕΕΓΜ» «αναρτώνται» και στην ιστοσελίδα [www.hssmge.gr](http://www.hssmge.gr)